



UNIVERSITÀ DEGLI STUDI DI MILANO
FACOLTÀ DI SCIENZE AGRARIE E ALIMENTARI

SCUOLA DI DOTTORATO
Terra, ambiente e biodiversità

Dipartimento di Scienze Agrarie e Ambientali - Produzione, Territorio, Agroenergia

Corso di dottorato in Ecologia Agraria - XXVIII° ciclo

TESI DI DOTTORATO DI RICERCA

Analysis of agro-ecosystems exploiting optical satellite data time series
the case study of Camargue region, France

Dottorando:
GIACINTO MANFRON
R10360

Coordinatore del corso di dottorato:

Prof. GRAZIANO ZOCCHI

Docente guida:

Prof. ROBERTO CONFALONIERI

Ricercatore di supporto:

Dott. MIRCO BOSCHETTI

Dott. SYLVESTRE DELMOTTE

A.A.
2014-2015

Al sorriso di Linda e Jacopo,

all'amicizia di Marta e Paolo

Table of contents

| | | |
|-----|---|----|
| 1 | Introduction..... | 1 |
| 1.1 | Agriculture monitoring in a changing world..... | 1 |
| 1.2 | Role of remote sensing in providing information on crop status and dynamics | 2 |
| 1.3 | Satellite remote sensing | 3 |
| 1.4 | Research framework: the SCENARICE project..... | 6 |
| 1.5 | Introduction to the study area: the French Camargue..... | 7 |
| 1.6 | Scope of the thesis..... | 10 |
| 1.7 | Executive summary..... | 10 |
| 2 | Exploiting satellite time series for agricultural systems monitoring | 12 |
| 2.1 | Analyses of seasonal crop dynamics exploiting time series of satellite data..... | 12 |
| 2.2 | Application examples | 27 |
| 2.3 | Operational crop monitoring systems exploiting satellite time series data | 33 |
| 2.4 | Conclusions..... | 36 |
| 3 | Inter-annual variability of winter wheat sowing dates through satellite time series analysis: 2003-2013 estimation in Camargue, France..... | 38 |
| 3.1 | Introduction..... | 38 |
| 3.2 | Material and Methods..... | 41 |
| 3.3 | Results | 52 |
| 3.4 | Discussion and conclusions | 62 |
| 3.5 | Annex 1: smoothing process | 64 |
| 4 | Analysis of crop changes through satellite time series for the definition of farm typologies in Camargue, France..... | 65 |
| 4.1 | Introduction..... | 65 |
| 4.2 | Study area..... | 67 |
| 4.3 | Material and Methods..... | 68 |
| 4.4 | Results | 78 |
| 4.5 | Discussion | 84 |

| | | |
|-----|---|----|
| 5 | Improving satellite time series resolution with data fusion techniques. Advantages for crop monitoring..... | 87 |
| 5.1 | Introduction..... | 87 |
| 5.2 | Study area and Materials..... | 88 |
| 5.3 | Methods..... | 88 |
| 5.4 | Results | 90 |
| 5.5 | Discussions and conclusion | 95 |
| 6 | Summary and final Conclusions..... | 96 |

List of figures

| | |
|--|----|
| Figure 0-1 - The study area of the <i>Parc naturel régional de Camargue</i> (PNRC). Agricultural land use map of the park with reference to 2006. | 9 |
| Figure 1-1- Spectral reflectance characteristics of green leaves (from: www.markelowitz.com/Hyperspectral.html) | 14 |
| Figure 1-2 – Simple schematization of vegetation index time series production process. (A) Multispectral wavebands datasets of an optical satellite image. (B) Image vegetation index evaluation. (C) Final time series, retrieved after the processing of a set of satellite images. The lower-right graph represents a single pixel time series..... | 18 |
| Figure 1-3 – Raw EVI data time series concerning rice (blue) and its interpolation as example of smoothing procedure. | 20 |
| Figure 1-4 - Phenology metrics extracted from a seasonal VI curve. MIN - beginning of the season, SoS – onset of the season, MAX – VI maximum value during the season, EoS – onset of the senescence, Length – time between SoS and EoS points, Amplitude – VI value difference between MAX and SoS. | 26 |
| Figure 1-5 - Linear regression between the seasonally (from sowing to harvest) integrated absorbed PAR and dry matter at harvest (g·m ⁻²) of nine commercial winter wheat plots. From Atzberger (1997). | 32 |
| Figure 1-6 - Representative logos of Operational crop monitoring systems services. Left to right: Famine Early Warning System (FEWS-NET), Global Information Early Warning System (GIEWS), Monitoring Agricultural Resources (MARS) unit, Global Monitoring of Food Security (GMFS) program and China Crop Watch System (CCWS) program | 36 |
| Figure 2-1 – Main cultivated areas in the study site of the <i>Parc naturel régional de Camargue</i> (PNRC). Figure 1-A: Study area at Landsat high spatial resolution (Landsat-8, DOY.163, RGB-543). Figure 1-B: Study area at MODIS moderate spatial resolution (MODIS MYD13Q1, DOY.161, EVI grey scale). Figure 1-C: Land use map of Camargue 2006 (<i>Occupation du sol 2006 du PNR de Camargue</i>). Figure 1-D: Land use map of Camargue 2011 (<i>Occupation du sol 2011 du PNR de Camargue</i>). The borders of the study area are represented in dark blue lines. Rice, winter wheat and other crops are reported in green, light blue and orange respectively in figure 1-C and 1-D. In figure 1-C and 1-D, water bodies, non-agricultural areas and areas of not interest are coloured respectively in black, white and grey. | 42 |
| Figure 2-3 - Flow chart representing the key methodological steps and the data used during this work. | 43 |
| Figure 2-4 - Comparison between winter wheat agronomic cycle and the EVI time series (red line) extracted for a winter wheat cultivated area | 46 |
| Figure 2-5 – Identification of WIN _{end(2)} as function of DOY (MIN _{EVI}) values. | 49 |
| Figure 2-6 - Visual interpretation process of randomly selected MODIS pixel. Pixels were overlapped to RGB Landsat high resolution images and labelled as “winter wheat” (blue pixels) or “other crops” (yellow pixels). Landsat-7 images are in RGB false colour composite (bands: 4-3-2) representation..... | 51 |

| | |
|--|----|
| Figure 2-7 – Three farms in Camargue for which it was available a field survey database for the year 2011, 2012 and 2013. Farm 1: Mejanas, farm2: Megias, farm 3: Arnaudo. The 2013 land use informations are displayed..... | 52 |
| Figure 2-8 - Example of typical EVI temporal trend for principal crop categories in Camargue: winter wheat (A), CORN (B), RICE (C), SORGHO (D), SUNFLOWER (E), ALFALFA (F), VITICULTURE (G), HORTICULTURE (H) and MEADOW (I). | 54 |
| Figure 2-9 – Example of winter wheat mapping results obtained for the year 2006. (A) 2006 winter wheat detection map, the estimated wheat cultivated areas are shown in red. (B) 2006 winter wheat sowing date estimations map, the color ramp (red to green) indicates sowing estimations occurrences. (C) Zoom of the detection map. (D) Zoom on the sowing date estimations map. Figure C and D report in white color winter wheat polygons of the 2006 land use map of the Camargue region. | 56 |
| Figure 2-10 - Comparison between winter wheat sowing dates and crop sowing estimations for three farms during the year 2011, 2012 and 2013, n=142 comparisons. (A) Scatter plot among observed and estimated data, with 8-days and 16-days interval of confidence. In grey colours are reported the comparison's frequency. (B) Distribution of validation residual errors according to the MODIS time composite. (C) Distribution of residual errors according to the observed sowing date. | 58 |
| Figure 2-11 - Inter-annual variability of crop sowing estimation for winter wheat in Camargue. Frequency histograms of the estimation values from the year 2003 to 2013. In the lower-right corner: pairwise correlations between estimations years. | 59 |
| Figure 2-12 – Comparison between winter wheat sowing date estimations and rain meteorological data for the period 2003-2013 in Camargue..... | 61 |
| Figure 2-13 – Main steps during the preprocessing of the EVI time series. (A) EVI raw, (B) spike detection and removal, (C) small drops detection and gap filling, (D) weighted SAV-GOL smoothing, (E) local minima and maxima individuation..... | 64 |
| Figure 3-1 - The Camargue study area. In red colour: PNRC boundaries. In green colour: arable land surface, according 2011 PNRC land use dataset. In the zoom on the upper-right corner it is possible to appreciate farm limits and single fields boundaries..... | 68 |
| Figure 3-2 – Flow chart representing the data involved in the work and the main methodological steps identified to retrieve main farm management typologies in Camargue. | 69 |
| Figure 3-3 – Time series of MODIS 250m EVI index for winter and summer crops for the period DOY 177, before the harvest seasons, to DOY 365 of the harvesting (reference) season. The red (181 pixels) and green (3446 pixels) series represent the winter and summer crop respectively..... | 71 |
| Figure 3-4 - Time series of summer crops (green color, fig. 4A and 4B) and winter crops (red color, fig. 4C and 4D) in different pixel purity conditions (high homogeneity, fig. 4A and 4C and mixture condition on fig. 4B and 4D). Green colored fields represent single fields for which land use datasets attributed summer crop | |

| | |
|--|----|
| cultivations presence and red colored fields related where it was for winter crop presence. The white grid represents the MODIS 250m pixel resolution for which time series was retrieved. | 75 |
| Figure 3-5 - Homogeneously cultivated areas (HCA) winter and summer crop estimations. A) - Farms limit (white color; ID 1605 and ID 221) and fields border (yellow color); B) identification of all the HCA inside the farm (blue colored areas) and MODIS 250m pixel grid (white lines); C) Time series based estimations of winter (red) and summer (green) crop; D) The final estimation representation at HCA level for each farm. | 76 |
| Figure 3-6 - Production of the reference dataset by visual interpretation of homogeneous cultivated areas (HCA). Landsat-7 images are in RGB false color composite (4-3-2) representation: spring and summer acquisition is reported in left and right panel respectively..... | 77 |
| Figure 3-7 – Farm trajectories for two farms in Camargue, farm ID.221 (upper panel) and farm ID.1605 (lower panel). Green lines represent temporal trajectories of those farm portion dedicated to summer crop while red lines represent winter crop ones. Grey circles indicate the portion of farm for which no estimations were produced..... | 80 |
| Figure 3-8 – Schematic representation of a three levels hierarchical clusterization process. The clustering produced six groups identified by the letter from A to F; the number of farms in each cluster is also reported..... | 81 |
| Figure 3-9 - Trajectories of winter and summer cultivation presence for six farms clusters in Camargue. Each graph reports in the x-axis the time line from year 2003 to 2013 and in the y-axis the percentage of farm area occupied by summer (Green lines) and winter crop (Red lines). Grey circles highlight the portion of farm for which no estimations were produced..... | 82 |
| Figure 3-10 – Spatial distribution of six clusters representing different farm land use managements for the study area of Camargue. | 83 |
| Figure 4-1 – The study area of the <i>Parc naturel régional de Camargue</i> (PNRC). On the left, <i>SPOT-4 TAKE-5 image at 20m resolution (NDVI RGB DOY 74:124:139)</i> . On the right, <i>MODIS MOD09A1 image product at 500m resolution (RGB true colour.)</i> | 88 |
| Figure 4-2 – Schematic representation of the data fusion approach proposed by Bisquert et al. (2015)..... | 90 |
| Figure 4-3 – Accuracy assessment of the fusion method. Resulting output image (A) compared to the corresponding reference one (B). (C) Scatter plot between the resulting fused datasets (Predictions) and the testing dataset images (Target). (D) Example of a pixel temporal profile for the input (blue HR image and read LR image) and resulting output “fused dataset” (green)..... | 91 |
| Figure 4-4 – Comparison between the spatial and temporal resolution in three dataset: S4T5 dataset (A, A1), MODIS dataset (B, B1), dataset resulting after “fata fusion” (C, C1)..... | 92 |
| Figure 4-1 –Fusion of SPOT 4 Take 5 NDVI and NWI2 time series for the three main cultivations in Camargue: rice, winter wheat and alfalfa in left, central and right panel respectively. Left panels (A and C; E | |

and G; I and K) shows the original S4T5 data while right panels (B and D; F and H; J and L) the dataset obtained by the fusion process. 94

List of tables

| | |
|--|----|
| Table 2-1 – (from Gilabert et al., 2010 in Maselli et al.,2010. Modified) Summary of some representative VIs, chronologically ordered. Notation: ρ_{blue} , ρ_{green} , ρ_{red} , ρ_{mir} refer to reflectance in blue, green, red, near infrared, short wave infrared and middle infrared bands, respectively; a and b are the slope and intercept of the soil line; and L, X, Y, and Z are different soil correction factors. (I): intrinsic indices, (S) associated with the soil line indices, (H) hyperspectral indices | 15 |
| Table 3-1 – Average crop calendar for the main cultivated crop in Camargue..... | 42 |
| Table 3-2 – Summary of the Landsat images dataset | 50 |
| Table 3-3 – Comparison between Landsat visual interpretation based reference dataset and estimations based on MODIS EVI time series analyses. UA = user accuracy, PA = producer accuracy, CE = commission error, OE = omission error, OA = overall accuracy, K = Cohen’s k coefficient..... | 57 |
| Table 4-1 – List of the selected Landsat images for the validation process..... | 74 |
| Table 4-2 – Description of the accuracy metrics evaluated from the confusion matrix..... | 77 |
| Table 4-3 - Error matrices between reference and estimated data for 400 homogeneous cultivated spatial units. Validation results are reported individually for each year (2003, 2006, 2009, and 2012) and also all together. Results are reported as sums of areas (in hectares). UA: user accuracy, PA: producer accuracy, CE: commission error, OE: omission error, OA: overall accuracy and K: Cohen’s coefficient..... | 79 |
| Table 5-1 – Statistical assessment of the fusion images database. IDW: Inverse Distance Weight approach statistics by setting the parameter “p” to values 1, 2 and 3. # HR/LR: pairs of Images to be fused. P: power parameter. R: correlation between data fusion images and testing dataset. RMSE: Root Mean Square Error. Accuracy: average of the residual values (see Eq.3). | 91 |

Acknowledgments

My gratitude and appreciation first and most of all goes to Dr. Mirco Boschetti and Dr. Sylvestre Delmotte without whom this endeavor would have been impossible. Their guidance helped me a lot through all the time of the research and writing of this thesis. My sincere thanks also to Prof. Roberto Confalonieri, my tutor, for his support and supervision.

Deepest gratitude is also due to all the CNR IREA colleagues, especially to Dr. Pietro Alessandro Brivio who contributed to the revision of this thesis and was always available to give me advices.

I'm proud to thank my officemates, Francesco, Alberto, Ramin and Gigi. My sincere thanks for all the helps you provided me during these years. Thanks for the jokes, the laughs and all the moments spent together inside and outside the office. Many thanks also to my colleagues Paolo Villa, Giacomo Fontanelli, Daniela Stroppiana, Lorenzo Busetto and Gloria Bordogna. For the help they provided and for all the stimulating discussion made together around satellites and agriculture.

I would like to show my gratitude to all the colleagues of INRA-Montpellier. Thanks again Sylvestre, for every skype call, every hint and suggestion you provided me during this period. I deeply appreciated the work you've done on my regard. My sincere thanks also for the help received from Laure Hossard, and the precious suggestions that Jean Marc Barbier, Jean Claude Couderc and Santiago Lopez Ridaura gave me in these years. I thank you all for the successful collaboration.

Thanks also to the fellow friends of Cassandra-UNIMI, in particular Simone Bregaglio, Tommaso Stella, Giovanni Cappelli, Valentina Pagani e Francesca Orlando, with whom I shared and I will share this experience.

Thanks to my parents Rosetta & Marcello to my cugnà Luca and my sister Ilenia who kindly supported me and finally to my nephew Linda and Jacopo to whom I'm happy to dedicate this effort.

In addition, I would like to thank my friends Paolo, Marta and Stefano, and all whose names are missing here for their push, support and understanding.

Abstract

The research activities presented in this manuscript were conducted in the frame of the international project SCENARICE, whose aim is to demonstrate the contribution of different technical and scientific competences, to assess current characteristics of analyzed cropping systems and to define sustainable future agricultural scenarios. Dynamic simulation crop models are used to evaluate the efficiency of current cropping systems and to predict their performances as consequence of climate change scenarios. In this context, a lack of information regarding the intra- and inter-annual variability of crop practices was highlighted for crops such as winter wheat, for the study area of Camargue. Moreover, a description of possible future cropping systems adaptation strategies was needed to formulate short term scenario farming system assessment. To perform this analysis it is fundamental to identify the different farm typologies representing the study area.

Since it was required to take into account inter-annual variability of crop practices and farm diversities to build farm typologies, representative data of the study region in both time and space were needed.

To address this issue, in this work long term time series of satellite data (2003-2013) were exploited with the specific aims to: (i) provide winter wheat sowing dates estimations variability on a long term period (11 years) to contribute in base line scenario definition and (ii) reconstruct farms land use changes through the analysis of time series of satellite data to provide helpful information for farm typologies definition.

Two main research activities were carried out to address the defined objectives. Firstly a rule-based methodology was developed to automatically identify winter wheat cultivated areas in order to retrieve crop sowing occurrences in the satellite time series. Detection criteria were derived on the basis of agronomic expert knowledge and by interpretation of high confidence temporal signature. The distinction of winter wheat from other crops was based on the individuation of the crop heading and establishment periods and considering the length of the crop cycle. The detection of winter wheat cultivated areas showed that 56% of the target in the study area was correctly detected with low commissions (11%). Once winter wheat area was detected, additional rules were designed to identify sowing dates. The method was able to capture the seasonal variability of sowing dates with errors of ± 8 and ± 16 days in 45% and 65% of cases respectively. Extending the analysis to the 11 years period it was observed that in Camargue the most frequent sowing period was about October 31th (± 4 days of uncertainty). The 2004 and 2006 seasons showed early sowings (late September) the 2003 and 2008 seasons were slightly delayed at the beginning of November. Sowing dates were not correlated to the seasonal rainfall events; this led us to formulate the hypothesis that sowing dates could be much more influenced by the harvest date of the preceding crop and soil moisture, which are related to rains but also to the date of last irrigations and to the wind.

The second activity was related to define farm typologies. Temporal trajectories of winter and summer crops cultivated areas were estimated at farm scale level based on satellite data time series in the 2003-

2013 periods. The validation demonstrated that the method was able to produce maps with high overall accuracy (OA 92%) and very low commission errors (3% for summer crops and 7% for winter crops). Omission errors were very low for summer crops (3%) and higher but within an acceptable level for winter crops (31%). Temporal trajectories of annual winter and summer crop land use at farm level were assumed as indicators of farm management (e.g. intensive monoculture farm or diversified crop producer). Trajectories were analysed through a hierarchical clustering procedure to identify farm management typologies. We were able to identify six typologies out of 140 farm samples, covering 75% of the arable land in the study area. A semantic interpretation of the farm types, allowed formulating hypothesis to describe farming systems. The size of the farms seemed to be an explanatory variable of the intensive or extensive farm management.

The two main activities presented in this thesis highlighted the importance of time series spatial and temporal resolution for crop monitoring purposes. Currently, only heterogeneous remotely sensed data in terms of spatial and temporal resolutions are available for agricultural monitoring. Forthcoming sensors (i.e. ESA Sentinel-II A/B) will offer the chance to exploit coexisting high spatial and temporal resolutions for the first time.

A preliminary application of an innovative methodology for the fusion of heterogeneous spatio-temporal resolution remotely sensed datasets was provided in the final section of the thesis with the aim to (i) produce high spatio-temporal resolution time series and (ii) verify the quality and the usefulness of the generated time series for monitoring the main European cultivated crops. The experiment positively demonstrated the contribution of data fusion techniques for the production of time series at high space-time resolution for crop monitoring purposes. The application of data fusion techniques in the main methodologies presented in this work appears to be beneficial.

To conclude this thesis framework, satellite remotely sensed data properly analyzed has shown to be a reliable tool to study large-scale crop cultivations and to retrieve spatially and temporally distributed information of cropping systems. Remote sensing time series analyses lead to highlight patterns of intra- and inter-annual dynamics of agro-practices and were also useful to define farm typologies based on multi-temporal land use trajectories. Results contribute in enriching the studies and the characterization of the Camargue study area, in particular providing information such as sowing dates that are not available at present for the considered study area and represent a step forward in respect to the actual (static) available crop calendar informations. Moreover, the achieved results provide supplementary information layers for summarize and classify the diversity of the farm in the study area and to characterize farming systems.

Riassunto

Le ricerche presentate in questo elaborato si inseriscono nell'ambito del progetto internazionale SCENARICE, il cui scopo è quello formulare tramite un approccio multi-disciplinare scenari di medio e lungo termine circa la sostenibilità di sistemi agricoli a scala regionale considerando possibili ricadute di impatto ambientale, sulla produttività agricola, su quella economica e sociale. Nell'ambito del progetto modelli agronomici per la stima della crescita colturale sono utilizzati per valutare la produttività dei sistemi agricoli e prevedere gli effetti dei cambiamenti climatici nel breve e lungo termine. In particolare, per ciò che concerne l'area di studio del parco regionale della Camargue (Sud della Francia), informazioni importanti per la modellistica come la variabilità delle pratiche agricole non risultano ad oggi presenti per colture di frumento duro (seconda coltura più rappresentativa dopo il riso) ed è inoltre presente un forte interesse circa le possibili (future) strategie di adattamento nella gestione delle aziende agricole in risposta a fattori come cambiamenti climatici, variazioni dei livelli di sussidio e volatilità dei prezzi di mercato. Considerata pertanto la necessità di rappresentare questa variabilità, distribuita nello spazio e nel tempo, la scelta di analizzare serie temporali di dati telerilevati da satellite è stata adottata per raggiungere i seguenti obiettivi: (i) stimare la variabilità delle epoche di semina di frumento duro nel lungo periodo per contrire alla definizione di "scenari base" per la modellistica agronomica e (ii) caratterizzare le tipologie di gestione colturale delle aziende agricole in Camargue analizzando la dinamica di cambiamento degli investimenti colturali nel lungo periodo.

Per raggiungere il primo obiettivo è stato sviluppato un algoritmo basato su regole per l'analisi di serie temporali. L'algoritmo è in grado di individuare in modo automatico le aree coltivate a frumento duro e in queste di stimare l'epoca di semina. Le regole di identificazione sono basate sulla conoscenza agronomica e sull'interpretazione di serie temporali ad alta attendibilità per il frumento e si basano sull'identificazione dei periodi di inizio crescita e massimo sviluppo vegetativo e sulla lunghezza del ciclo colturale. A seguito dell'identificazione, ulteriori regole sono implementate per identificare l'epoca di semina. In fase di validazione, l'algoritmo è stato in grado di identificare automaticamente il 56% delle aree coltivate a frumento duro producendo pochi errori di commissione (11%). La variabilità stagionale delle epoche di semina è stata stimata producendo errori di ± 8 e ± 16 giorni rispettivamente nel 45% e 65% dei casi.

Il metodo è stato esteso per il periodo 2003-2013 evidenziato nella data del 31 Ottobre (± 4 giorni) il periodo con più alta frequenza di stima delle semine. Le stagioni 2004 e 2006 hanno evidenziato semine anticipate rispetto alla media (fine Settembre) mentre per le stagioni 2003 e 2008 le stime sono state di poco posticipate (inizio Novembre). Le stime prodotte non sono risultate correlate all'andamento stagionale delle piogge. Questo ha portato a formulare l'ipotesi che le semine di frumento duri per l'area studio siano maggiormente influenzate da fattori quali le epoche di raccolta delle colture antecedenti la

coltura di frumento e l'umidità del suolo, quest'ultima a sua volta legata all'ultimo evento stagionale di irrigazione e all'intensità/frequenza del vento nella stagione.

Con riferimento al secondo obiettivo di tesi è stato sviluppato un metodo di stima della presenza di colture estive (CEst) e colture invernali (CInv) a scala di azienda agricola, tramite analisi di serie temporali di dati satellitari. Il metodo è in grado di stimare le due categorie di colture con accuratezza globale pari al 92% ed un basso errore di commissione (3% per CEst e 7% per CInv). Gli errori di commissione si sono rivelati bassi (3%) per le CEst e più alti (31%) ma di valore accettabile per la stima delle CInv. Il metodo è stato applicato nel periodo 2003-2013 per derivare le traiettorie di investimento colturale nelle aziende agricole della Camargue. Le traiettorie sono state assunte come indicatori della tipologia di gestione aziendali (aziende omosuccessive, aziende che diversificano/rotano le colture) e sono state sottoposte a clusterizzazione gerarchica multilivello al fine di identificare macro-tipologie di gestione (ripartizione) colturale nelle aziende agricole. Sei macro-tipologie sono state isolate in riferimento ad un campione di 140 aziende agricole rappresentanti il 75% della superficie agricola dell'area studio. L'interpretazione a livello semantico di queste tipologie ha portato a formulare una serie di ipotesi per descrivere la dinamica temporale delle rispettive traiettorie. La dimensione aziendale sembra spiegare il comportamento più o meno intensivo della gestione colturale aziendale. Il monitoraggio delle dinamiche d'uso del suolo agricolo da serie temporali di dati telerilevati è un approccio innovativo per l'analisi della gestione colturale delle aziende agricole e a differenza di approcci già consolidati, permette di formulare ipotesi di evoluzione a breve termine sulle strategie di gestione delle aziende agricole.

Nella parte conclusiva del lavoro vengono riportati i risultati preliminari dell'applicazione di una innovativa metodologia per la fusione (*data fusion*) di immagini satellitari. Questa metodologia permette di ottenere serie temporali a risoluzione spazio-temporale migliore rispetto a quella che caratterizza le immagini di input. L'applicazione del metodo ha evidenziato il contributo positivo di queste tecniche per il monitoraggio delle colture agricole. Ulteriori applicazioni di questa metodologia appaiono potenzialmente utili per migliorare l'accuratezza di individuazione delle colture e della stima della variabilità di pratiche agricole.

In conclusione, il telerilevamento si è rivelato uno strumento idoneo per fornire informazioni utili a (i) evidenziare pattern interannuali nella dinamica delle colture e (ii) definire "tipologie gestionali" per le aziende agricole presenti nell'area studio. I risultati ottenuti sono ritenuti fondamentali per completare lo studio e la caratterizzazione della Camargue fornendo informazioni (ad oggi mancanti) sulle epoche di semina del frumento sull'intera area di studio e utili per la definizione di scenari di base. Le informazioni prodotte sulla gestione colturale negli ultimi 11 anni per 140 aziende aggiungono ulteriori dati da integrarsi a quelli disponibili per la caratterizzazione delle aziende agricole.

Sviluppi futuri prevedono l'uso di tecniche innovative per il miglioramento della risoluzione spaziale e temporale delle immagini (diminuzione delle fonti di rumore nelle serie temporali) applicando tecniche di "data fusion" tra dati a diversa granularità spazio temporale.

1 Introduction

1.1 Agriculture monitoring in a changing world

Agro-ecosystems are sites or integrated regions of agricultural production (i.e. a farm), whereby continual human intervention is needed for the maintenance of an equilibrium created by man himself with the aim of maximizing the food and fiber production provided by a few domesticated plant and animal species. In these systems, the equilibrium is maintained through a continuous energy input flow (in form of fertilizers, agro-chemical products or gasoline used during tillage operations) that makes stable a balance designed to create optimal conditions for the growth of the cultivated plants and the animals raised (Taffetani et al., 2011).

Sustainable agricultural management is of fundamental importance not only to guarantee productivity of current farmlands, but also to conserve the natural environment. Since the beginning of the so called “green revolution” in the 1950s (Borlaug N.E, 2007), the management of agro-ecosystems strongly changed in order to address a world growing demand of food and energy. A direct consequence of the intensification of crop growing systems and the exploitation of natural resources is the severe deterioration of the ecological status of many agro-ecosystems.

Referring to the principle of “Sustainable intensification” (Pretty J., 2008), makes it possible to appreciate the role of survey activities in agricultural areas in leading crop management strategies through a rationale use of the natural resources (water, soil) and a rational use of the primary production input factors (fertilizer, oil etc.) as means to maximize (crop) production and minimize environmental impact.

Studying and providing information about crop cultivated areas during the cropping season, will play a key-role to cope with the challenging future scenario of the agricultural development (Atzberger, 2013). The global trend in this context will be characterized by an increasing world population, that is estimated to reach 9 billion people by 2050 (Godfray et al., 2010) and as a consequence, the per capita demand for crops will increase or even double, as was Tilman’s prospect of the period 2005-2050 (Tilman et al., 2011). These future trends will take place in a context of climate change: it is expected that temperature and precipitation patterns will change in the next decades, with more frequent extreme meteorological conditions (Godfray et al., 2010; Field et al., 2014).

It is easy to imagine that the global agriculture will face a strong change in the next decades to deal with the next food demand. These changes will necessary lead to processes of agricultural extensification and intensification. Extensifications, by discovering additional land for crop production. Intensifications by reaching for example higher yields or by improving agronomical practices.

Some authors shown that a significant increase in primary production could be reached focusing on strategies such us: reducing the yield gaps of under-productive agricultural lands, increasing cropping efficiency, shifting diets and reducing waste. They estimate that together these strategies could double food production, while reducing the environmental impacts of agriculture (Foley et al., 2011).

Achieving this goal is difficult, as agriculture must cope with climate change and also compete with other land uses that conflict with food production (e.g., biofuel production, urban expansion, etc.). Rising temperatures, changing in precipitation regimes, increasing of atmospheric carbon dioxide levels, will strongly drive and impact future productions. These changes will be positive in some agricultural systems and regions, and negative in others, and these effects will vary through time (Parry et al., 2004).

In this context, monitoring the evolution of agricultural activities is necessary and essential to perform near real time assessment of agricultural systems in a changing world. Considering the main future perspectives of agricultural crop productions, updated information about the status of crops, the crop quality condition and the season characteristics will be of great importance to support early warning decision support systems, to support food security initiatives and also to provide decision makers with feedback on their policies and investments. Future transitions have to be monitored closely at a temporal and spatial scale.

The added value of depicting agro-ecosystems changes in crop monitoring activities is proportional to the temporal dimension in provide this information kind. As pointed out by the Food and Agriculture Organization (FAO, 2011), the need for timeliness is a major factor underlying agricultural statistics and associated monitoring systems. Information is worth little if it becomes available too late.

1.2 Role of remote sensing in providing information on crop status and dynamics

Many scientific approaches are commonly used in agronomy and in the other environmental sciences to derive information on agro-ecosystems. For example cropping system can be analyzed (i) acquiring direct measurements (e.g. Leaf Area Index - LAI, canopy temperature, soil moisture etc.), (ii) exploiting agro-ecological indicators (defined as variable that provide information about other variables that are difficult to access - Gras et al, 1989), (iii) using crop growth models (e.g. the Water Account Rice Model - Confalonieri et al., 2009; Crop-Syst - Stockle et al., 2003 or the WORld FOod STudies model - van Diepen et al., 1989) or iv) making farm interviews or consulting census data.

These approaches have different advantages and drawbacks and they should be used in an integrated and complementary way.

- Direct measurements of crop biophysical parameters represent extremely precise data, but it is not always feasible task, they represent an expensive and time consuming approach to adopt at large scale.

- Agro-ecological indicators are usually represented by scores or numbers that varies between zero to ten, or zero to one. They're ready to use, quick and cheap but cannot explain crop processes during the season, they can provide a "judgment" or an "opinion" on the investigated aspects.
- One of the main features of a crop growth models is the ability (after a suitable calibration) to explain in time the dynamics of a crop system, it can be also an important instrument to assess future cropping system scenarios and to compare different scenarios. Models are also cheap and often easy to use.
- Satellites observation can provide spatial and temporal information on the variability and state of crop canopies (Kumar and Monteith, 1981; Moulin et al., 1998). The large spatial coverage and high temporal revisit frequency of satellite images makes them particularly useful for near real-time information collection at the regional scale (Rembold, 2013). Remote sensing tool represents a suitable way to analyze crop cultivated areas on large scale (Justice et al., 1985).

This research work focus on the retrieval of information about crop cultivated areas at farm and regional scale, exploiting the analysis of long time series of satellite data (the following section will provide a short introduction to satellite remote sensing).

The reasons that lead to test remote sensing contribution for agro-ecosystem monitoring are in agreement with the (above cited) sentences that describes some of the main advantages of this approach. Moreover, nowadays another great advantage of remote sensing data is the possibility of having free of charge data and direct access to data archives that have been collected since 70's (Landsat data) or since 2000 (Moderate Resolution Imaging Spectroradiometer – MODIS data).

1.3 Satellite remote sensing

In general, remote sensing refers to the activities of recording/observing/perceiving (sensing) objects or events at a faraway (remote) perspective. In remote sensing discipline, sensors are not in direct contact with the objects which are observed.

<http://www.crisp.nus.edu.sg/~research/tutorial/earth.htm> The information flow needs a physical carrier to travel from the objects to the sensors through an intervening medium. The electromagnetic radiation is normally used as an information carrier in remote sensing. The output of a remote sensing system in Earth Observation field is usually a digital image representing the scene being observed. Further steps of image processing, analysis and interpretation are generally required in order to extract useful information from the satellite images. According to this, the human visual system could be considered as an example of a remote sensing system.

<http://www.crisp.nus.edu.sg/~research/tutorial/airbrn.htm>In a more restricted sense, satellite remote sensing refers to the technology of acquiring information about the earth's surface (land and ocean) by using sensors onboard on satellites platforms. These are then equipped with sensors looking down to the earth. They are like "eyes" in the "sky" that constantly observe the earth surface. In Optical Remote Sensing, optical sensors detect solar radiation reflected or scattered from the earth, forming images resembling photographs taken by a camera high up in space. The wavelength region usually extends from the visible and near infrared (commonly abbreviated as VNIR) to the short-wave infrared (SWIR).

Different targets such as vegetation, water, soil, buildings and roads reflect visible and infrared light in different ways. They have different colors and brightness when seen under the sun. The interpretation of optical images, require the knowledge of the spectral reflectance signatures of the various materials (natural or man-made) covering the surface of the Earth.

Remote sensing images are normally in the form of digital images (raster image made of digital numbers – DN). In order to extract useful information from satellite acquisitions, image processing techniques are employed to allow the image interpretation. There are many image analysis techniques available and the methods used depend on the requirements of the specific problem concerned. In many cases algorithms are used to underline different or specific thematic classes into the image. The resulting product is a thematic map of the study area. This thematic map can be combined with other databases of the test area for further analysis and utilizations.

1.3.1 Remote sensing time series for the analysis of agricultural systems

Remote sensing is the science of obtaining and interpreting information from a distance, using sensors that are not in physical contact with the object to be observed. It therefore includes a variety of techniques, tools and resources that improve interpretive skills perceive by eye and human brain, providing the viewer information about objects at a distance and the environment which surrounds them (P.A. Brivio, 2006). The main focus of remote sensing is to detect, quantify and analyze electromagnetic energy, because of the strong correlations between the physical nature of land surface bodies and its electromagnetic spectral behavior.

Many remote sensing applications are devoted to the agricultural sector. Satellite images can contribute in supporting agriculture by offering information on the spatial and temporal variation of important canopy state variables (i.e. LAI, Chlorophyll content, evaporative fraction - EF, Fraction of Absorbed Photosynthetically Active Radiation - fAPAR) which would be very difficult to obtain otherwise. Remote sensing could also be used for investigating seasonal crop phenology (i.e. Start of growing season, green-up occurrence, crop heading, crop senescence, crop length) and for the identification of crop practices (Sowing period, flooding period and irrigation, harvest). Satellite images could furthermore provide reliable

information in support of crop growth models for yield estimation assessment and agricultural future scenario comparison and evaluation (Moulin et al., 1998).

1.3.2 Contribution of satellite images time series analysis

High temporal and spatial resolution of satellite images are key factors for capturing seasonal crop dynamics. Recently, the use of high temporal resolution satellite data has been emerging as a promising tool for studying crop cultivated areas allowing an approach based on the exploitation of time series satellite data. These works were mainly done with low-resolution optical sensors such as the Advanced Very High Resolution Radiometer (AVHRR), the Moderate Resolution Imaging Spectro-radiometer (MODIS) or the vegetation sensor on board of the *Satellite Pour l'Observation de la Terre*, Satellite for observation of Earth (SPOT).

Existing approaches aimed to detect phenological events through the analysis of time series satellite data were described in a recent contribution of You et al. (2013). According to the authors, these studies mainly follow two methodological steps: the production of reliable satellite remote sensing vegetative index (VI) time series and the handling of the time series in order to determine the timing of specific phenological events.

Developing the time series involves the construction of VI time series on the base of available satellite images and the data filtering to reduce the impact of atmospheric condition. The filtering procedure is needed mainly due to cloud contamination occurrence on the measured reflectance (noise reducing). In this step the primary methodologies involve the use of various filters, such as the application of Savitzky-Golay filtering (Savitzky and Golay, 1964) or Fourier filter (Azzali et al., 2000; Atkinson et al. 2012), or involve the fitting of various functions such as asymmetric Gaussian functions (Hird et al., 2009; Huemann et al., 2007) or logistic functions (Zhang et al., 2003, 2004).

After smoothed time series are constructed, many phenology detection methods can be applied. Here, the time series are analyzed to detect specific phenological events such as the start, end, and length of the growing season (SoS, EoS, and LoS). The most common methods for this step include threshold methods, curvature change-rate methods, harmonic analysis, moving average methods, and maximum slope and inflection point methods. Among these, the rule based and threshold approaches methods are the most common one. Detailed information about these methodological steps will be presented in chapter 1.

Remote sensing can significantly contribute in agricultural crop monitoring and crop assessments. Time series analysis approach is widely used in remote sensing to estimate phenological key stage occurrences and crop practices timings. This approach can also contribute to perform inter-annual variability analysis of crop seasonal features. The spatial and temporal resolution of satellite images are very important features, they significantly contribute on the accuracy of the produced estimations.

1.4 Research framework: the SCENARICE project

This thesis project has been hosted at the Italian National Research Council (CNR) at the Institute for the Electromagnetic Sense of the Environment (IREA) and carried out within an international French-Italian Rice Science and Technology (FIRST) project Initiative, founded by Agropolis Foundation (<http://www.agropolis-fondation.fr/>) and Fondazione Cariplo (<http://www.fondazionecariplo.it/>). This initiative aims at developing and supporting scientific research in the agro-food sector. The Name of the project is SCENARICE standing for “Scenario integrated assessment for sustainable rice production systems: Exploring plausible, probable and possible futures for sustainable rice production systems”. One of the main characteristics of SCENARICE project is the integration of different scientific disciplines, which have in common the specialization on agricultural monitoring, in particular on rice cropping systems. In this project, each partner contributes in the definition of future agricultural scenarios taking into consideration different aspects such as environmental conditions/constraints, climate change, policy changes and technical innovations. The SCENARICE framework is also based on a participatory approach with stakeholder and farmers to develop and assess the different scenarios.

Strategic objective of the SCENARICE project is to identify and analyze more sustainable Rice Production Systems (RPS) using a methodological framework based on the technological expertise of each partner: rice growth/development/production simulation models, geomatics, remote sensing and GIS techniques, agent-based and bio-economic models. Particular attention is being dedicated to the analysis of the interactions of socio-economic and environmental drivers of change with the farming systems for the evaluation of scenarios of future RPS. Expected results of the project, in addition to the creation of an integrated set of tools and techniques, will be the definition of sustainable RPS scenarios and the comparative analysis of these for each case studies: The Camargue region in Southern France, the Lomellina region in North-West Italy, the Makeny region in Sierra Leone and finally the Ambohibary region in Madagascar.

Within the SCENARICE project, the general scope of the thesis is the development and testing of methods based on remote sensing to provide information at farm and regional scale on the crop cultivated areas of South-East France. The case study is the Camargue region, with particular attention to the *Parc Naturel Régional de Camargue*. This area is situated at the mouth of the Rhone River and it is an important ecological and agricultural region, especially for the cultivation of Rice and Wheat. A more complete description of the study area can be appreciated in Figure 1-1.

This thesis project contributes to the development of the SCENARICE project in Camargue by studying winter wheat sowing dates variability and farm typologies definition with the purpose to investigate the inter-annual variability of agronomic practices and to study long term farm management behavior. In the research project the Moderate Resolution Images Spectroradiometer (MODIS) images were analyzed together with ancillary information datasets represented by crop survey data at farm level and agricultural land use maps at regional scale. This work is based on the improvement of a recently proposed remote

sensed based methodology for mapping and monitoring rice crop fields (Boschetti et al., 2009; Manfron et al., 2012a; Manfron et al., 2012b) with the aim to extend its capability analysis on the monitoring of other cultivated crops (i.e. winter wheat).

1.5 Introduction to the study area: the French Camargue

The Camargue region (Figure 1-1) is a Mediterranean area located in southern France along the Rhône River mouth. It is a delta shaped region that spreads over about 180.000 ha between the Mediterranean Sea (South) and the two main arms of the Rhône River, the eastern arm being called the *Grand Rhône* and the western arm the *Petit Rhône*. This region has a strong ecological and agronomic identity and is protected and preserved by different levels of public authorities. For agricultural issues the most important authority is the Regional Natural Park of Camargue (*Parc naturel régional de Camargue PNRC*) which cover most of the land between the two branches of the Rhône river (*Grande Camargue*) and other small areas outside this.

Agriculture is a predominant activity in this area and has a key role in term of natural area conservation and environmental impact of the region. The agricultural activities take place in almost the 25÷30% of the PNRC area (from 29.000 to 33.000 ha). Among the main cultivated crop in Camargue, rice and durum wheat account for almost 85% of the crop cultivated areas, with prevalence of rice on durum wheat (roughly 2/3 and 1/3). Irrigated rice cultivation plays a key role in maintaining low soil salinity levels of fields and durum wheat cultivation is an important winter-spring dry crop used in rotation after rice to avoid mono-cropping weed stress and yield decreasing. Crop shifts of rice and winter wheat account usually a four year period. According to Mouret (Mouret et al., 2004), these two crops have an ambivalent ecological impact because they contribute to preserve the surrounding ecosystem and, when they are cropped intensively, they can threaten the ecological equilibrium of this protected area. The secondary cultivated crops in Camargue are represented from alfalfa, sunflowers, maize, soybean, lentils, peas and sorghum. These crops are mainly cultivated in farms with animals, as rotation crops after rice in rice organic farms and in seasons where rice represent a less profitable crop (low subsidies levels) together with an increasing of wheat cultivated surface. Farms in Camargue are characterized by a strong fragmentation of field plots. Farmers usually manage nearby fields homogeneously, maintaining the same crop types and crop-practices (e.g. fertilization, irrigation, sowing dates, crop rotation) during the agricultural seasons in order to simplify their work. This management is particularly related to crop irrigation and water management optimizations.

There are about 300 farms in Camargue and almost 200 of these are rice producers. The farm surfaces vary from 50 to over than 1000 ha with average total extension of 300 ha which account 160 ha of arable land.

The climatic condition of the Camargue region is represented by dry summers, rainy autumns and warm winters. Particular climatic feature is the significant presence of a dry wind coming from the north (Mistral) that blows frequently creating a micro-climate of low air humidity. This peculiarity tends to decrease the

incidence of pests and diseases on crop cultivations and increases the annual evapotranspiration level of the region (1200-1400 mm per year). The average rainfall of Camargue accounts only 600 mm per year. Rains are mainly concentrated in autumn, influencing winter crops management activities, especially the date of sowing.

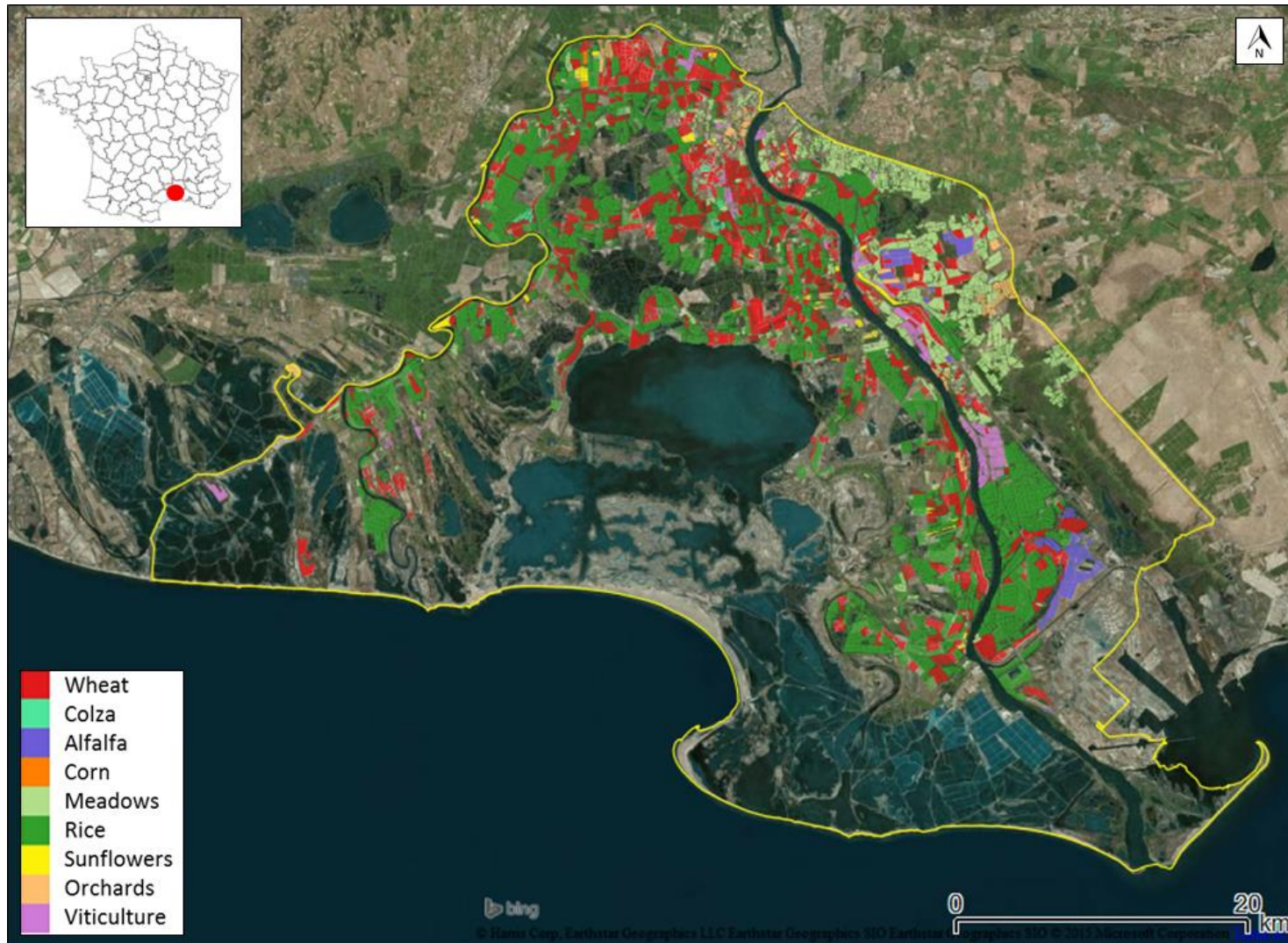


Figure 1-1 - The study area of the *Parc naturel régional de Camargue* (PNRC). Agricultural land use map of the park with reference to 2006.

1.6 Scope of the thesis

This thesis was developed within an international project frame, where dynamic simulation crop models were used to predict the consequences of climate change scenarios on the cropping systems performances in Camargue.

Concerning this study area partners highlighted a lack in information regarding the intra and inter-annual variability of farmer practices of crop management (i.e. sowing date). More in detail, it has been noticed that such information (data) are well known for what concern rice cropping systems, that are the most represented in the Camargue study area and for which crop practices are homogeneous in space and time. Concerning instead, cultivations like winter wheat (the second crop more representative in the study area), seasonal variability in crop practices are greater and a description of this variability in space and time is actually missing and could be of great interest for its use in cropping system models. The origin of this variability in crop practices is mainly due to the occurrence of several crop preparative works falling in the autumn period, seasonal period where rainy events are more concentrated.

Another important effort that lead these researches within the SCENARICE project, were represented by considering possible future cropping systems adaptation strategies at farm level. This level usually is not always explicitly considerate, despite decisions regarding production, management and in particular adaptation strategies are made at this level (Reidsma et al., 2015). Farm level decisions are not only influenced by climate. Technological development, policy and the market largely influence agricultural decision making. Their influence has been larger than climate change (Chiotti and Johnston 1995, Hermans et al 2010).

Given the specific requirements of SCENARICE project and the overlap of the project needs with the thesis research framework, the following objectives have been defined:

1. To provide winter wheat sowing dates estimation on a long term period, in order to identify the inter- and intra-annual variability of the crop practice and produce information useful to build baseline and future crop modelers scenarios in the study area of Camargue;
2. To monitor Camargue's farms land use through the analysis of time series of satellite data, with the final aim to provide helpful information for farm characterization definition (farm typing).

1.7 Executive summary

The following dissertation considers two different applications of satellite time series analysis for agricultural information retrieval on the estimation and analyses of agro-practices for a long time period in Camargue.

Chapter 1 presents a bibliographic review focused on applications of remote sensing time series analysis for the estimation of agricultural crop practices and for the identification of farm typologies by mean the monitoring of crop land use.

Chapter 2 and 3 presents the main research contributions carried out during the program. Chapter 2 presents a regional scale application of time series analyses for the estimation of intra- and inter- annual variability of winter wheat sowing practices and chapter 3 analyzes the contribution of remote sensing time series on characterize farming system land use trajectories.

Chapter 4 shows a preliminary application of an innovative methodology for the fusion of heterogeneous spatio-temporal resolution remote sensed datasets, and its potential in agricultural monitoring purposes application.

The final chapter, chapter 5, recaps the presented activities and critically examines the researches carried out during the PhD program concluding this manuscript.

2

Exploiting satellite time series for agricultural systems monitoring

This chapter illustrates the usefulness of retrieving from Earth Observation data information on cropping systems. Particular attention will be dedicated to the time series analyses approach that represent the methodology applied in all the researches introduced in the manuscript. During the first section will be provided a short review of existing methods exploited to produce and analyse satellite time series. Such informations are described in three main steps concerning: spectral indices retrieval (1.1), noise removal (1.2) and time series information retrieving (1.3). Examples of applications in which time series analysis contributed to crop monitoring are shown in section 2. Sections 2.1 and 2.2 are related to chapter 2 and chapter 3 respectively and provide a short review on time series analyses applications devoted to agro-practices estimations and farm typologies definition. Section 2.3 discuss about the combined use of the information derived from time series with crop simulation modelling with the aim to improve models predictive performances on agroecosystems. Existing operational agricultural monitoring systems, taking advantage of satellite data are presented in the last section (section 3) the meaning of this is section, is only to provide the reader an overview on the most important information services that operatively provide added value information on agricultural systems, exploiting satellite data informations.

2.1 Analyses of seasonal crop dynamics exploiting time series of satellite data

Phenology is the study of periodic events in the life cycle of living species. In the case of plants, understanding the timing of critical events of plant growth is relevant for various activities related to crop management, such as irrigation scheduling, fertilizer management, evaluating crop productivity, and analysing seasonal ecosystem carbon dioxide (CO₂) exchanges (Sakamoto et al., 2005). The accurate monitoring of phenology represents can also contribute to farm practices management since it allows assessing if the most critical stages of growth occur during periods of favourable (or not) weather conditions (Curnel et al., 2007).

In recent years, for the analyses of crop phenology and agronomic practices (crop management events) the use of Earth observation satellites with high frequency revisit time has been largely explored. In particular, the analysis of time series of satellites spectral measurements allow to describe vegetation seasonal dynamics, for a better monitoring and understanding of the biophysical changes in the vegetation cover and phenology in different ecosystems over large areas (Bradley and Mustard 2008). Agricultural monitoring applications of remote sensed time series embrace a wide range of species (cereals, forages, energy crops etc.). This methodology can be applied for monitoring at different spatial scale, from regional

(Huang et al., 2009; Shihua et al., 2014) to national (Xiao et al., 2005) and continental scale (Justice et al., 1989).

Many research efforts have been directed towards the assessment of satellite time series in order to retrieve seasonal information about the main crop cultivations. As an example, wheat cropped areas were analysed in the works of Huang et al., (2009), Meng et al., (2009) or Linin Lu et al., (2014), where time series were used to identify the seasonal occurrence of wheat crop phenological-related parameters for crop models. In other contributions such as the one of Xiao et al., (2005), Boschetti et al., (2009) or Shihua et al., (2014), time series analysis were helpful to monitor paddy rice cultivated areas and to spatially represent these information on thematic maps. Also maize, that together with wheat and rice represent the three main worldwide cultivations, has been successfully monitored through the time series approach retrieving information on maize phenological growth stages in Iowa, Illinois and Nebraska (USA “corn belt” region) (Yu et al., 2012; Shen et al., 2013).

The determinations of phenology from remotely sensed time series can be done with a number of different approaches. Taking into consideration the contributions of Beck et al., (2006), Curnel et al., (2008), De Beurs et al., (2010), You et al., (2013) and Zhang et al. (2013), that specifically focus on this topic, it is possible to put in evidence three main methodological steps usually applied in the approach of satellite time series analysis:

1. Calculation of time series of spectral indices;
2. Time series data cleaning;
3. Identification of crop seasonal stages;

In the next sections (1.2, 1.2 and 1.3) the above steps are presented. A detailed description of the aforementioned representative methodological steps are provided giving examples on the main techniques currently available in literature, discussing their pros and cons and introducing the strategies chosen for the researches presented in chapter 2 and 3.

2.1.1 Time series of spectral indices for enhancing crop vegetation behavior

One of the main strategy adopted to derive information on land surface biophysical parameters (such as LAI, fAPAR etc.) from remotely sensed data is based on the evaluation of spectral indices specifically designed for studying vegetation, called Vegetation Indices (VIs).

A VI is a variable derived from the spectral reflectance of two or more reflectance wavebands which can be related to the value of a biophysical parameter (Gilabert et al., 2010). Another advantage in the employment of VIs is that it allows reduce and synthetize multi-band information of the optical satellite image (Gilabert et al., 2010).

VI represents a common empirical strategy used in satellite remote sensing to extract land surface information from Earth Observation Systems data. They can provide empirical relationships with some

optical characteristics of the surface minimizing the sensitivity to external influences (atmosphere, sensor view angle, sun angle, etc.) and internal variations (canopy background, litter, etc.) (Huete et al., 1988, 1989).

VIs combine reflectance measurements from different wavebands in the solar region, the ones most useful for vegetation monitoring take into account the red (R) and near infrared (NIR) wavelengths regions, because green vegetation strongly absorbs solar radiation in the visible region and strongly reflects solar radiation in the NIR region. These bands can enhance the vegetation presence from the measured signal and help to produce indicators sensitive to the vegetation photosynthetic activities and canopy structural variations (Gao et al., 2000).

Figure 2-1 shows the spectral reflectance features of green leaves. This figure explains the typical regions of reflectance and absorption for vegetation and the reason why NIR and R bands are the most often used to design VIs. Among the reflective spectra three main domains control the leaf reflectance: the first is the visible domain (0.4 μm \div 0.7 μm), characterized by low reflectance due to pigments absorption (chlorophyll a and b, carotenes and xanthophyll). Here the absorptions in the blue and red regions induce a reflectance peak at the green region, this determine the normal green appearance of healthy vegetation. The second domain is along the NIR region (0.7 μm \div 1.3 μm), the absorption here is very low (hence reflectance is high) due to the radiation scattering caused by the leaf mesophyll structures that determines high reflectance and transmittance of the incoming NIR radiations. The third domain is in the middle infrared region (1.3 μm \div 2.5 μm) and is mainly driven from the leaf water content. Reflectance decrease with the increase of water content, the main water absorption picks are situated at 1.4, 1.9 and 2.7 μm . The region between the first and the second domains is called “red-edge” region.

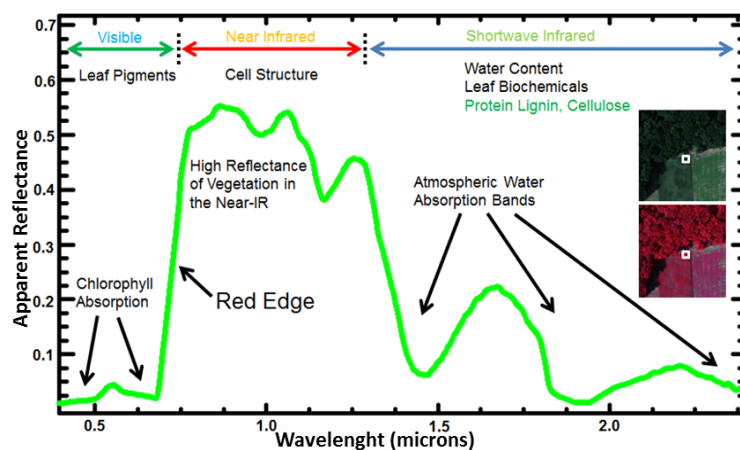


Figure 2-1- Spectral reflectance characteristics of green leaves (from: www.markelowitz.com/Hyperspectral.html)

Many different VI are exploited in literature and according to their main features they can be subdivided into three main broad categories (Boschetti M., 2011): intrinsic indices, associated with the soil line indices and atmospheric resistant indices (Table 2-1). The intrinsic indices (I), for example Ratio Vegetation Index (RVI, Jordan et al. 1969) or Normalized difference Vegetation Index (NDVI, Rouse et al. 1977), are

characterized by simple combinations of reflectance bands sensed on the surfaces. The association with the line of the soil indices (S), as Perpendicular Vegetation Index (PVI, Richardson et al. 1987) or Enhanced Vegetation Index (EVI), express values which are less influenced by the effect of reflectance of the soil and finally the *atmospheric resistant* indices (A), are designed to attenuate the effects of atmospheric contaminations, for example Atmospherically Resistant Vegetation Index (ARVI, Kaufman and Tanré, 1992). Table 2-1 reports a list of the most common used indices to monitor vegetation. A more detailed description of Normalized Difference Vegetation Index (NDVI) and Enhanced Vegetation Index (EVI) index is then provided: NDVI because it is one of the most commonly used in literature for vegetation monitoring from time series analyses and the second because it was used for the applicative chapters (chp.2 and chp.3) of my work.

Table 2-1 – (from Gilabert et al., 2010 in Maselli et al.,2010. Modified) Summary of some representative VIs, chronologically ordered. Notation: ρ_{blue} , ρ_{green} , ρ_{red} , ρ_{mir} refer to reflectance in blue, green, red, near infrared, short wave infrared and middle infrared bands, respectively; a and b are the slope and intercept of the soil line; and L, X, Y, and Z are different soil correction factors. (I): intrinsic indices, (S) associated with the soil line indices, (H) hyperspectral indices

| Name | Equation | reference | Approach |
|--|--|--|----------|
| Ratio vegetation index | $RVI = \frac{\rho_{nir}}{\rho_{red}}$ | Jordan (1969) Pearson & Miller (1972) | (I) |
| Transformed vegetation index | $TVI = \sqrt{\frac{\rho_{nir}}{\rho_{red}} + 0.5}$ | Rouse et al., (1974) | (I) |
| Normalized difference vegetation index | $NDVI = \frac{\rho_{nir} - \rho_{red}}{\rho_{nir} + \rho_{red}}$ | Rouse et al., (1974) | (I) |
| Modified NDVI | $MNDVI = \frac{\rho_{nir} - \rho_{mir}}{\rho_{nir} + \rho_{mir}}$ | Jürgens (1997) | (I) |
| Square root of RVI | $SRRVI = \sqrt{\frac{\rho_{nir}}{\rho_{red}}}$ | Nalepka et al., (1977) | (I) |
| Difference vegetation index | $DVI = \rho_{nir} - \rho_{red}$ | Tucker (1979) | (I) |
| Global environmental vegetation index | $GEMI = \eta(1 - 0.25\eta) \frac{\rho_{red} - 0.125}{1 - \rho_{red}}$ $\eta = \frac{2(\rho_{nir}^2 - \rho_{red}^2) + 1.5\rho_{nir} + 0.5\rho_{red}}{\rho_{nir} + \rho_{red} + 0.5}$ | Pinty & Verstraete (1992) Verstraete & Pinty (1996) | (I) |

| | | | |
|---|--|--|-----|
| Non-linear vegetation index | $NLI = \frac{\rho_{nir}^2 - \rho_{red}}{\rho_{nir}^2 + \rho_{red}}$ | Goel & Qi (1994) | (I) |
| Re-normalized difference vegetation index | $RDVI = \frac{\rho_{nir} - \rho_{red}}{(\rho_{nir} + \rho_{red})^{1/2}}$ | Roujean & Breon (1995) | (I) |
| Green vegetation index | $VI_{green} = \frac{\rho_{green} - \rho_{red}}{\rho_{green} + \rho_{red}}$ | Gitelson <i>et al.</i> (2002) | (I) |
| Soil adjusted vegetation index | $SAVI = \frac{\rho_{nir} - \rho_{red}}{\rho_{nir} + \rho_{red} + L} (1+L)$ | Huete (1988) | (S) |
| Perpendicular vegetation index | $PVI = \frac{\rho_{nir} - a\rho_{red} - b}{\sqrt{1+a^2}}$ | Richardson & Wiegand (1977) | (S) |
| Soil adjusted ratio vegetation index | $SAVI_2 = \frac{\rho_{nir}}{\rho_{red} + b/a}$ | Major <i>et al.</i> (1998) | (S) |
| Weighted difference vegetation index | $WDVI = \rho_{nir} - a\rho_{red}$ | Clevers (1988) | (S) |
| Transformed SAVI | $TSAVI = \frac{a(\rho_{nir} - a\rho_{red} - b)}{a\rho_{nir} + \rho_{red} - ab + X(1+a^2)}$ | Baret & Guyot (1991) | (S) |
| Modified SAVI | $MSAVI = \frac{2\rho_{nir} + 1 - \sqrt{(2\rho_{nir} + 1)^2 - 8(\rho_{nir} - \rho_{red})}}{2}$ | Qi <i>et al.</i> (1994) | (S) |
| Enhanced vegetation index | $EVI = G \left(\frac{\rho_{nir} - \rho_{red}}{\rho_{nir} + C_1\rho_{red} - C_2\rho_{blue} + L} \right)$ $L = 1; C_1 = 6; C_2 = 7.5; G = 2.5$ being C_1 and C_2 the coefficients for the aerosol resistance term, and G the gain factor. | van Leeuwen <i>et al.</i> (1999) Huete <i>et al.</i> (2002) | (S) |
| Optimized SAVI | $OSAVI = \frac{\rho_{nir} - \rho_{red}}{\rho_{nir} + \rho_{red} + Y}$ | Rondeaux <i>et al.</i> (1996) | (S) |

| | | | |
|---|--|-------------------------------|-------|
| Generalized SAVI | $GESAVI = \frac{\rho_{nir} - a\rho_{red} - b}{\rho_{red} + Z}$ | Gilbert <i>et al.</i> (2002) | (S) |
| Soil and atmospherically resistant vegetation index | $SARVI = \frac{(\rho_{nir}^* - \rho_{rb}^*)(1+L)}{\rho_{nir}^* + \rho_{rb}^* + L}$ | Kaufman & Tanré (1992) | (S/A) |
| Visible Atmospherically resistant Index | $VARI_{green} = \frac{\rho_{green} - \rho_{red}}{\rho_{green} + \rho_{red} - \rho_{blue}}$ | Gitelson <i>et al.</i> (2002) | (A) |
| Atmospherically resistant vegetation index | $ARVI = \frac{\rho_{nir}^* - \rho_{rb}^*}{\rho_{nir}^* + \rho_{rb}^*}$ $\rho_{rb}^* = \rho_{red}^* - \gamma(\rho_{blue}^* - \rho_{red}^*)$ <p>ρ^* is a reflectance value with prior correction for molecular scattering and ozone absorption</p> | Kaufman & Tanré (1992) | (A) |
| Green ARVI | $GARI = \frac{\rho_{nir} - [\rho_{green} - (\rho_{blue} - \rho_{red})]}{\rho_{nir} + [\rho_{green} - (\rho_{blue} - \rho_{red})]}$ | Gitelson <i>et al.</i> (1996) | (A) |

Once a VI is extracted from a single multispectral satellite image, it could then be expanded into a satellite VI time series (You *et al.*, 2013). Satellites can acquire multispectral images of the same portion of the Earth surface with a pre-defined revisiting time; depending on the geometry parameters of its orbit (e.g. MODIS sensor can acquire one the same portion of the Earth one a day). This is the reason why we have regular image acquisitions for the study areas. In particular if a series of multispectral images are available for the same place, the VI can be calculated from all of them obtaining maps that describe the temporal behavior of the VI. This aspect in remote sensing is called multi-temporal analysis or time series analysis and it is particularly important for vegetation dynamics monitoring.

In Figure 2-2 there is a schematization regarding how VI time series are made. Multispectral satellite images are made by a series of images (Fig. 2A) each one representing the reflectance value of a specific band. In the example, three are acquired in the visible and two in the infrared domains. Available data are combined according to specific formulas to calculate the VI (in the example the NDVI index), hence producing a new image with pixel VI values (Figure 2B). This operation is reiterated on each available satellite dates (i.e. for the MODIS 8-day composite a total of 46 VI images per year can be retrieved). Once layer stacking of the VI images is done, it is possible to visualize and analyze the VI for a pixel of the area (Figure 2C).

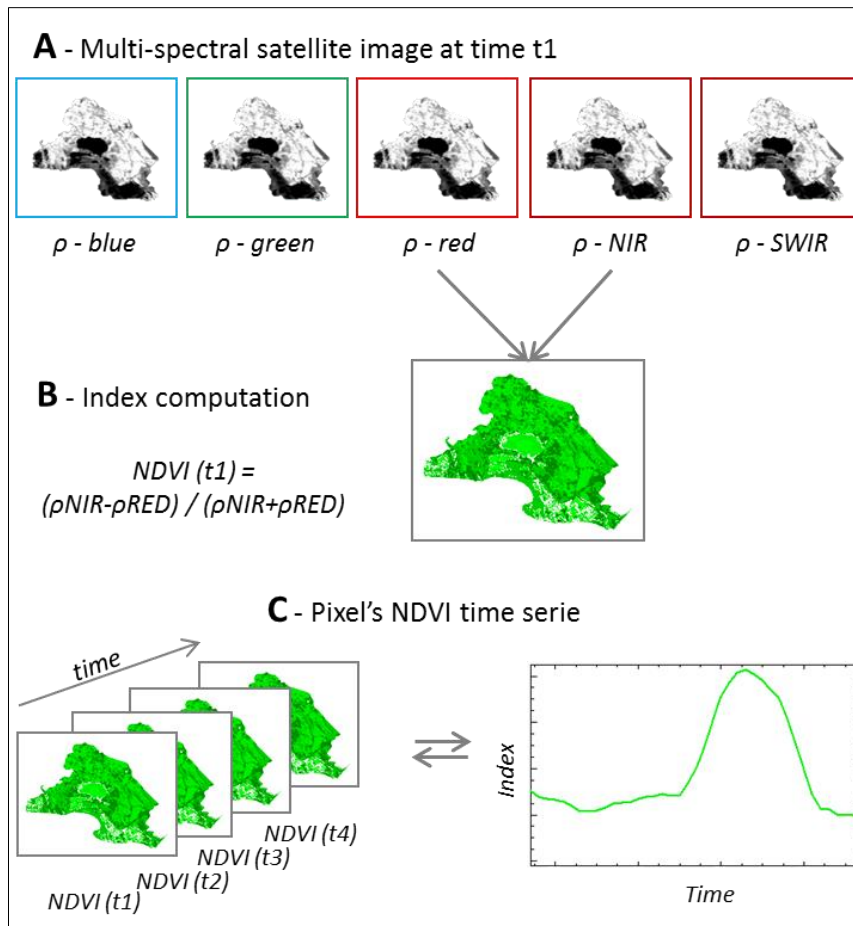


Figure 2-2 – Simple schematization of vegetation index time series production process. (A) Multispectral wavebands datasets of an optical satellite image. (B) Image vegetation index evaluation. (C) Final time series, retrieved after the processing of a set of satellite images. The lower-right graph represents a single pixel time series.

Normalized Difference Vegetation Index

NDVI is calculated from the red and near-infrared light reflected by vegetation (see row 3 of table 1). Healthy vegetation absorbs most of the visible light and reflects a large portion of near-infrared energy (Figure 2-1). On the contrary vegetation in stress condition absorbs less visible and more near-infrared light. This index was exploited as a proxy of net primary production and other plant biophysical variables over varying biome types (Lenney et al., 1997), to identify different ecoregions (Ramsey et al., 1995), to make map of land cover and to monitor phenological phases of the earth vegetation (Huete and Liu, 1994). Time series of NDVI are valuable for many Earth science fields (Atzberger et al. 2014). Moreover, as the NDVI is normalized, it reduces the effect of sensor calibration degradation (Wardlow et al., 2007). This index is often used for the composition of temporal-series and remote sensing applications for the monitoring of vegetation covers (Lunetta et al., 2006; Wardlow et al., 2007; Nutini et al., 2012). Since it is evaluated from a normalized difference, NDVI values for a given image pixel always result in a number that ranges from minus one (-1) to plus one (+1). In presence of clouds, snow cover and free-standing water surfaces the index takes very low or even negative values, because infrared reflectance is higher than red reflectance. NDVI values are slightly higher than zero on soil and between 0.4 and 0.7 for vegetated area. Only very dense vegetation reaches values greater than 0.8.

This index is simple and easy to be implemented and it performs effectively when the canopy cover is intermediate (among LAI values from 1.0 to 2.5). NDVI uses only two spectral bands that are monitored by almost all the satellite's sensors designed for the Earth observation.

Some limitations have been noticed for NDVI index. First it saturates over dense canopy (Huete et al., 2002) and secondly it is sensitive to atmospheric conditions. Moreover, when the canopy is very sparse the soil background spectral properties can affect the *NDVI* value (Xiao et al., 2003).

Enhanced Vegetation Index

At the beginning of the 2000s, when satellite data provided by MODIS sensors were made available, MODIS Land Discipline Group designed a new vegetation index to be used with MODIS data: the Enhanced Vegetation Index (EVI). With reference to formula presented in table 1, the EVI is a modified NDVI *index* with a soil adjustment factor "*L*" and two coefficients C_1 and C_2 which describe the use of blue band in correction of red band for atmospheric aerosol scattering. The coefficients, C_1 , C_2 , and L , were empirically determined as 6.0, 7.5, and 2.0, respectively. This algorithm has an improved sensitivity to high biomass presence and improved vegetation monitoring through a de-coupling of the canopy background signal and a reduction in atmospheric influences (Huete and Justice, 1999). The range of values of the EVI is -1 to 1, where healthy vegetation generally falls between values of 0.20 to 0.80. EVI can be linearly correlated with leaf area index, and has a higher sensitivity to biomass presence compared to NDVI (Huete et al., 2002).

Despite both NDVI and EVI indices are commonly used for vegetation studying and vegetation time series analysis, the EVI index was chosen for the present work because it was originally designed to improve the performance of NDVI index, especially for MODIS data. In particular this index once evaluated from MODIS multispectral images demonstrated to show a minor susceptibility on cloud contamination noises and a higher sensitivity at medium-high canopy LAI values compared with NDVI index (Huete et al., 2002; Wardlow et al., 2007).

2.1.2 Time series data cleaning

Several pre-processing operations are applied to optical satellite acquisitions in order to reduce the noise components in the acquired radiometric signal due to several factors such as sensor resolution and calibration (Vermote et al., 1995), digital quantization errors (Viovy et al., 1992), orbital and sensor degradation (Kaufmann R.K., 2000) and ground and atmospheric conditions (Tanré et al., 1992). An example of noise removal operation is proposed in Figure 2-3, where it is shown the EVI time series of a satellite image pixel before (blue) and after (red) a data cleaning procedure.

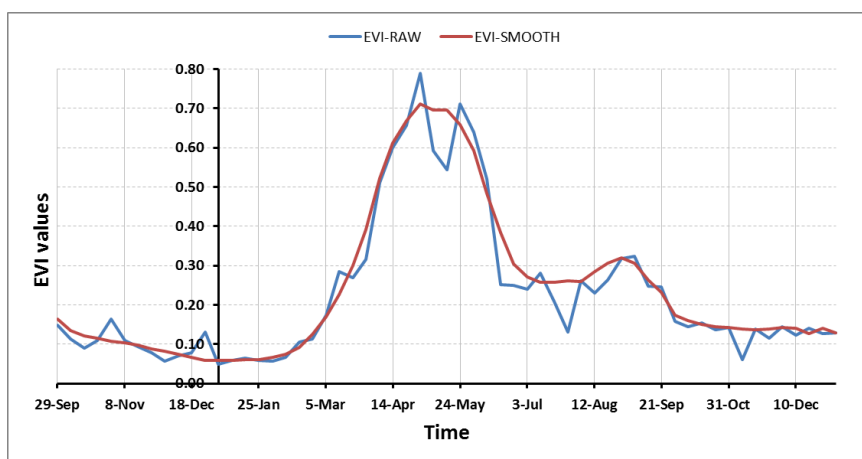


Figure 2-3 – Raw EVI data time series concerning rice (blue) and its interpolation as example of smoothing procedure.

A common methodology applied to reduce these noise components is the creation of “composite images” of satellite data by considering the best acquisition values over a specified time period. One of the possible techniques used is called Maximum Compositing Value (MCV), (Holben, 1986) and the resulted satellite images are defined as a “composite products”. MCV products are usually produced for a week, ten days (decade), or 16-days periods.

A consequence of the application of this methodology is the degradation of the acquisition temporal resolution. For example MODIS sensors have a daily acquisition (365 acquisitions per year) but the derived MODIS MOD13Q1 composite product is provided with an 8-day temporal resolution (46 composite images per year). Despite the fact that the MCV approach concretely increase data quality, image compositing procedure is not sufficient to get a definitive clean “cloud-free like” dataset to perform VI time series analysis throughout the growing season.

Such residual noise is mainly due to remaining sources of errors (cloud cover, atmospheric contamination, snow, or shadow) that alterate (generally decrease) the evaluated VI values. False highs, although much less frequent (Viovy et al., 1992), can also occur at high solar or scan angles (in which case the numerator and denominator in the VI ratio are both near zero) or because of transmission errors, such as line drop-out (Viovy et al., 1992). To minimize the problem of false highs, the downloadable products are generally based on low-angle observations wherever possible.

Most of the remaining errors in the satellite composite images tend to decrease VI values. These unusual structures of error are less trustworthy in respect to the high one and this break the assumptions of use many standard statistical approaches to remove them (Pettorelli et al., 2005).

MODIS derived vegetation indices data are generally well-documented and their quality has already been controlled through the pre-processing, what decrease the risk to face many of the above-mentioned problems (Smith et al., 1997; Tucker et al., 2005; James et al., 1994; Gutman 1999).

Despite these quality checks, VI time series may be difficult or even impossible to analyse with an automated procedure without further noise filtering. It is therefore necessary to reconstruct the time series as it would be without atmospheric disturbance. Such reconstruction must be done pixel by pixel.

Different smoothing methods are proposed in literature to filter out the rate of noise from optical satellite time series (i.e. Curnel and Oger, 2007; De Beurs et al., 2010; Atzberger et al., 2013). It is not appropriate to define a performance ranking among these methodologies because their efficiency depends on specific application, however, according to Combal & Bartholomè, (2010) it is possible to highlight useful criteria to select the most appropriate one:

- I. capacity to eliminate false drops and (eventual) false upper spikes;
- II. capacity to identify and keep reliable signals;
- III. capacity to reconstruct the time series behavior in order to identify key phenological stage;
- IV. capacity to be usable in near-real time (i.e. forward values should not be needed);
- V. capacity to be usable in any environmental condition since a large number of time profile types can be found increasing the study area scale;
- VI. simplicity of the algorithm.

Some of the most commonly applied techniques for the analyses of crop cultivated areas are described below:

i. Curve-fitting methods:

The curve-fitting method, initially develop by van Dijk et al. (1985), aims at fitting a polynomial or Fourier function (Olsson and Eklundh, 1994; Azzali et al., 2000; Atkinson et al. 2012) to the NDVI time series. An advantage of this method is that the trajectory can be predicted and the time series can be summarized by

several parameters linked to the function. Shortcomings of the medium-order polynomials are that they're too inflexible to recreate an entire seasonal NDVI pattern, and can smooth the data too much; Fourier analysis instead fails to characterize each annual NDVI trajectory separately. It can generate spurious oscillations in the NDVI time series (Van Dijk et al., 1985). Curve fitting methodologies generally aren't able to well accommodate the false low and high error structure, and are therefore heavily affected by false lows or high.

ii. Step-wise logistic regression method:

This method was initially developed by Zhang et al. (2003). These authors proposed that the bell-shaped (similar to a Gaussian function) NDVI curves of a cultivated area can be represented using a series of piecewise logistic functions of time. Because the method treats each pixel individually without setting thresholds or empirical constants, it is globally applicable; it enables vegetation types to exhibit multiple modes of growth and senescence within a single annual cycle. As well as in the previous case, step-wise logistic regression does not accommodate the skewed error structure, and the resulting time series will therefore be heavily affected by false lows or high.

iii. Best Index Slope Extraction (BISE) method:

Initially developed by Viovy *et al.* (1992), this is a threshold driven methodology based on the slope of increasing and decreasing data values referred to as the "best index slope extraction". VI observations are judged as trustworthy or not depending on whether the rate-of-change in the NVDI is plausible.

Given a pre-defined "sliding period", a data point is only accepted if it is greater than the previous value. Time series decreases from one point to the next are only accepted if there is no regrowth within the predefined period greater than 20 percent of the difference between the preceding high and the decreased value. This threshold (usually 20%) is applied because it is assumed that changes in vegetation remain visible for a number of days, during which regrowth is slow (Fontana et al., 2008). The method is dependent on both the 20 percent threshold and the predefined "sliding period" of time (i.e. n observations). The algorithm is robust to false highs that cause implausibly rapid increases in the NDVI. The resulting profiles tend to lose some of the features of the NDVI profile and, in some cases, appear to be insensitive to the timing of NDVI increases. The sensitive point of this methodology is to correctly estimate what extent a rate of change in the VI can be considered plausible, according to the temporal resolution under consideration.

iv. Weighted least-squares linear regression:

This method was developed by Swets et al., (1999). This approach uses a sliding- combination of piecewise linear approximations to the VI time series. The window is moved one period at a time, resulting in a family of regression lines associated with each point; this family of lines is then averaged at each point and interpolated between points to provide a continuous temporal VI signal. Also, since the factors that cause

contamination usually serve to reduce VI values, the system applies a weighting factor that favours peak points over sloping or valley points. A final operation assures that all peak NDVI values are retained.

The methodology works well when successive false lows are rare, so that local “valleys” (drop in NDVI values) occur separately. When several false lows occur in sequence, they result in false local drop, which bias the estimated value downwards. Thus, this approach might not be suitable for daily data, and its applicability will depend on the frequency of cloud contamination and the strength of seasonality.

v. *Savitzky-Golay smoothing method:*

This time-domain method is based on a least squares polynomial fitting that analyse time series data using a pre-defined moving window. The method was originally designed to match the upper envelope of the time series, preserving the higher data within the series. Rather than having their properties defined in the Fourier domain, and then translated to the time-domain, Savitzky-Golay filters derive directly from a particular formulation of the data smoothing problem in the time domain (Press *et al.*, 1992). In a recent contribution, Geng *et al.* (2014), tested eight different smoothing techniques of NDVI time series over vegetated areas. Results highlighted that Savitzky-Golay techniques perform better than other for almost all the vegetation types took in consideration. Other important applications of this smoothing technique are exposed in the works of Chen *et al.*, (2004), Xiao *et al.*, (2005), Hird *et al.*, (2009) and Boschetti *et al.*, (2009).

vi. *Function fitting:*

Several studies reported the utility of the Asymmetric Gaussian and Double Logistic models over other fitting techniques and filters (Beck *et al.*, 2006; Hird & McDermid, 2009). The Asymmetric Gaussian model has been proposed within the TIMESAT toolbox by Jönsson and Eklundh (2002, 2004). This methodology exploits a Gaussian function locally adjusted over the growing and senescing parts of each season. The functions are finally merged to get a smooth transition from one season to another. This method can handle small gaps of VI data (Kandasamy *et al.*, 2013). A logistic or double logistic functions fitting methods were proposed by Zhang *et al.*, (2003, 2004) where the authors divided the EVI time series in two parts (vegetative growth and senescence) and fit the models separately.

vii. *Empirical Mode Decomposition (EMD):*

This method proposed by Huang *et al.* (1998) consists in decomposing the time series into a small number of intrinsic mode frequencies (IMFs) derived directly from the time series itself. The time series decomposition is applied using an adaptive iterative process, where the data are represented by intrinsic mode functions to which the Hilbert transform can be applied. The method requires two parameters: the threshold for convergence and the maximum number of IMFs. The first IMF, is the mostly affected by noise, and it is to remove the high frequency fluctuations (noise) at the expense of a loss in the amplitude (Demir and Erturk, 2008). The EMD method requires the time series to be continuous. To allow the application of

EMD to MODIS time series, the missing data must be previously filled by interpolation (i.e. linear) as proposed by Verger et al., (2011).

viii. Whittaker smoothing technique:

The Whittaker smoother (Whittaker, 1923) is based on the minimization of a cost function describing the balance between fidelity expressed as the quadratic difference between estimates and actual observations and roughness expressed as the quadratic difference between successive estimates. This balance is controlled by a smoothing parameter. The higher this value is, the smoother the result but at the expense of fidelity (Kandasamy et al., 2013). This methodology has been recently proposed in the works of Atzberger and Eilers (2011) and Atkinson et al. (2012) in a comparative analysis with other smoothing techniques.

Several noise factors affect optical satellite data decreasing their quality. The MCV compositing method is commonly applied to remove noise, nevertheless smoothing techniques are needed and further applied to better reconstruct time series. Different smoothing techniques have been exploited in literature, the most applied were previously described

The Savitzky-Golay (SAV-GOL) smoothing method was chosen for this research work. The SAV-GOL filter is widely adopted in remote sensing of cultivated areas and different researches show the successful application of this method in the time series of MODIS vegetation indices. This method is particularly indicated because tend to minimize overall noise meantime preserving higher vegetation-index values (Chen et al., 2004; White et al., 2006; Abílio D.C. et al., 2015). Moreover, a recent contribution of Geng et al. (2014) compared eight techniques for smoothing multi-temporal NDVI data, considering different vegetation types and sensors, and concluded that the SAV-GOL filter achieved best results in most situations.

2.1.3 Identification of crop seasonal key event

The estimation of the occurrence of key seasonal phenological stages of a crop is the final goal of the satellite time series analysis. The typical behaviour of VI time series signal, related to crop seasonal stages (Figure 2-4) allows identifying several phenological stages. Such signal can be analysed to extract information like the occurrence of key phenological events, seasonal crop metrics and indicators of some crop practices.

These informations extracted from the analysis of VI time series can have several uses. In crop monitoring sector, it allows the determination of specific agricultural stages (Sakamoto et al., 2004) and give useful information for crop management (Pan et al., 2012; Tornos et al., 2015). In other research sectors such as climate and agro-meteorological models (Boschetti et al., 2011; Boschetti et al., 2015), the knowledge of some key dates of growth stages allows a better tuning of simulations models to forecast crop productions.

Further applications also involve environmental studies (Pettorelli et al., 2005), where variations in dates of occurrence of specific growing phases or the duration of the growing cycle can be used as an early indicator of potential major changes in ecosystems induced by climate change (A. Menzel, 2002).

Different parameters related to key phenological events can be derived from VI. Before defining them it is important to further clarify what is the meaning of “phenological parameters” in remote sensing. Because of the limited ground resolution of satellite data with high revisiting frequency (i.e. in MODIS it is 250, 500 or 1000 meters), Earth observation-based methods can identify specific growth stages only in an indirect manner because the satellite data deal with mixtures of ground land covers. This marks a distinct concept from the traditional notion of a species-centric phenology (Frield et al., 2006). While in agronomy a phenological stage is defined as the timing of recurring biological events in the animal and plant world, with regard to biotic and abiotic forces and the interrelation among phases of the same or different species (Lieth, 1974; Schnelle, 1955); in remote sensing the term “land surface phenology” (LSP) is commonly used referring to the spatio-temporal development of the vegetated surface as revealed by satellite sensors. Somehow Earth observation is limited to observing the apparent phenology, not the species-specific real one. LSP metrics are primarily based on image time series of vegetation indices from optical sensors. With reference on Figure 2-4, such metrics typically individuate:

- Onset of greening, also defined as Start of Season (SoS), generally associated with the occurring of vegetation green-up period;
- Onset of senescence, or End of Season (EoS), generally related to the maturity or senescence of vegetation;
- Timing of the maximum VI value (MAX) during the growing season, representing the crop heading period and generally associated to the crop flowering period.

These metrics are also defined as “basic phenological metrics” (Curnel et al., 2007); from these basic phenological key metrics, other phenological indicators can be derived, for example the “length of the growing season”, the “time between the MAX and the SoS time series occurrences”, the “VI difference” (amplitude or delta-VI) between two basic metrics or the “VI seasonal cumulated value”. The “derived phenological metrics” (Curnel et al., 2007) are applied to compare the vegetation growing among seasons, highlighting inter-annual variability or interpreting the seasonal crop yield variability. Figure 2-4 reports an exemplification of a set of metrics derived from a generic VI time series. Similar exemplifications can be find in the contribution of Jönsson & Eklundh (2004), Chen et al., (2004), Curnel et al., (2007).

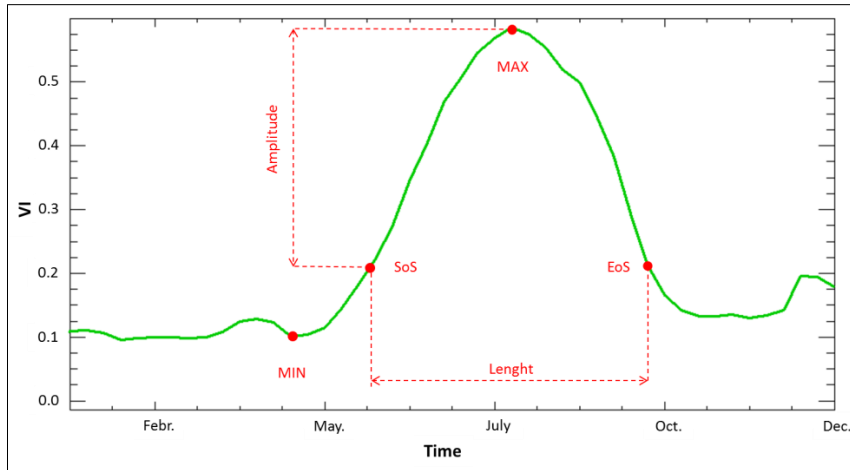


Figure 2-4 - Phenology metrics extracted from a seasonal VI curve. MIN - beginning of the season, SoS – onset of the season, MAX – VI maximum value during the season, EoS – onset of the senescence, Length – time between SoS and EoS points, Amplitude – VI value difference between MAX and SoS.

As in the case of the previously mentioned time series data cleaning for noise removal, different techniques are also available to determine the timing of specific seasonal events from VI time series analyses. According to Curnel et al., (2007) they can be grouped in the following categories:

i. Methods based on thresholds:

The philosophy of these techniques is based on the definition of a VI threshold. Here, the onset and end of greenness is defined as the moment when the VI values become higher/lower than a defined threshold. Some authors follow a simple threshold method, applying a threshold to the VI value (Delbart et al 2006), applying a threshold to a pre-defined day of the year (DOY), i.e. DOY 120 and 270 (Shabanov et al., 2002), fixing a threshold on the long term mean of the VI (Piao et al. 2006, Philippon et al., 2007) or identifying the timing of SoS and EoS at the point of minimum and maximum incremental ratio on the VI serie, (Jeong et al., 2011).

ii. Methods based on moving averages:

This category of techniques involves the use of a moving average filter to the time series which creates a new time series characterized by a certain time lag. The original and the moving average time series are then compared and whenever an intersection between the two occurs, a trend change is considered. The number n of observation to select in order to compute the moving average is user defined. For example, Brown et al., (2002) suggested 5 observations.

iii. Methods based on first derivative, inflection point and maximum slope:

Given that VIs present a bell shape (Gaussian like) for annual crop cultivated areas, with the first derivative of time series signal it can be possible to identify occurrences such us crop onset and the end of crop greening by considering that these points correspond to inflection points (Sakamoto et al., 2005; Dash et

al., 2010). Yu et al., (2003) for example, defined the SoS and EoS points when vegetation begin its rapidly increase or decrease through the identification in the time series of points of maximum and minimum slope respectively. This category of techniques aims therefore to identify precisely the moment when the VI time series start increasing or stop decreasing.

iv. Methods based on the Curvature Change Rate (CCR):

In these methods, important transitions dates (such as green-up, maturity, senescence and dormancy) are defined as local minima and maxima in the curvature-change rate (You et al., 2013). Applications of these methods are in the work of Zhang et al., (2003), Sakamoto et al., (2010), Manfron et al., (2012).

v. Methods based on harmonic analyses:

In harmonic analyses a Discrete Fourier Transform (DFT) is used (Moody & Johnson, 2001). The analysis of the DFT harmonics provides a basis for linking the DFT results to basic vegetation types according to their characteristic phenologies. For example, Moody & Johnson, (2001) applied an approach based on DFT to derive SoS and EoS points by analysing the phase of the harmonics.

Among the various techniques, threshold based techniques are the most used. However different crops have their own phenological stages during the growing seasons and the use of a single threshold tends to ignore the differences among crop types (You et al., 2013). Crop type, planting patterns and climatic conditions can affect crop phenological events within a region. Therefore, it is critical to choose the “right” method for the “right” place (Cong et al., 2012) and for threshold methods to choose the “right” threshold for the “right” place.

In this research work a number of algorithms for the analysis of time series were developed considering many of the techniques above introduced. The timings of specific seasonal events were indeed determined according to threshold based approaches (1), derived from bibliographic resources or defined after the analyses of reference (high reliability) time series and (3), based on the analyses of first derivative and on the research of inflection points within the time series.

2.2 Application examples

2.2.1 Contribution of remote sensing in agro-practices estimation

An important applications of remote sensing time series analyses approach in agriculture, concern the identification of the temporal and spatial variability of agro-practices. The monitoring activities on such variabilities is helpful to derive informations on farm management but can also give information about the farm adaptation strategies to factors such as climate seasonality and agricultural policies. Examples in this case involve agricultural practices such as paddy rice flood events and flood duration, forage seasonal cuttings and cutting occurrences, crop tillering, crop yield prediction models or crop sowing periods (as in

the case of chapter 2 of this work). These informations are useful to monitor and better describe crop systems and crop management practices. Furthermore they concretely contribute to better manage natural resources, such as water saving, soil quality maintenance, nitrate leaching prevention. Time series of vegetation indices have been analysed to monitor agricultural flooding occurrences and flood duration. These informations are particularly important for rice cultivated areas, where water plays a key role to protect the culture from sudden changes in temperature. For example, in the work of Xiao et al., (2006) seasonal rice flooding and transplanting periods were identified when the time series values of the water sensitive Land Water Surface Index (LWSI, Xiao et al., 2002) are greater than NDVI (or EVI) vegetation indices time series values. Tornos et al., (2014) assessed the dynamics of NDVI and other spectral indices in relation to rice management practices and flood periods in the Ebro Delta and Orellana Spanish case studies. These authors proposed specific combination of indices to assess rice flooding events, and rice sowing periods in relation to different crop growing techniques. Another example on the application of time series for monitoring water management is in a recent contribution of Le Page et al. (2014). In this work, a real-time experiment of irrigation scheduling driven by time series of satellite images was carried out for durum wheat cultivated test site in Morocco. A reference irrigation scheduling plot was compared with a test plot, with irrigations managed following the FAO-56 method and driven by remote sensing data. The “crop coefficient” was inferred from NDVI time series data by modulating a reference evapotranspiration locally measured. Results showed comparable crop yields between reference and test field plots but with a 14% less irrigation water consume for the test field (hence saving 14% of irrigation water). Time series have been also exploited in order to individuate cutting practices in forage cultivations. The contribution Halabuk et al., (2015) reported the possible usage of VI time series (NDVI, EVI) for detection of cut periods in hay meadows. Authors found that the optimal period for detection lay between June, 1st and August, 20th. They moreover noticed that the 16-day compositing period seemed to be enough for the cutting detection. As pointed by Zheng et al., (2012), remote sensing is an efficient and cost-effective tool to obtain information concerning crop residue cover and tillage practices. Starting by multi-temporal analyses of Normalized Difference Tillage Index (NDTI, Van Deventer et al., 1997) authors found that minimum values extracted from multi-temporal NDTI profiles reliably indicate the surface status when tillage or planting occurred. The crop sowing practice represents another important example of information that could be estimated from satellite VI time series. Representative examples in the estimation of sowing dates can be found in the work of Sakamoto et al. (2005) and Chen et al. (2010). Sakamoto et al. (2005) estimated paddy rice sowing dates at national (Japan) scale from the analyses of EVI time series data. Authors filtered time series using the wavelet and Fourier approaches and then depicted the occurrence of rice planting dates in correspondence of points of local minima in the time series signal with 12.1 days of root mean square error (RMSE). Time series of NDVI data derived from SPOT Vegetation satellite, were used by Chen et al. (2010) in order to estimate rice planting calendar in the Taiwan case study. Time series

were filtered by empirical mode decomposition (EMD) and wavelet transform approaches and rice planting dates were detected from crop heading date by searching the earlier local minimum point along the NDVI profile. The results were validated with the government rice planting statistics and indicated that EMD-based filtered data for gave remarkably good results in comparison with other cases using wavelet transform.

2.2.2 Contribution of remote sensing on farm typology definition through crop shift monitoring

Despite their fundamental ability to provide primary productivity, agricultural practices have had a wide range of harmful effects on the environment, such as the degradation of soils, the loss of biodiversity, and the decrease of water quality (Tilman et al. 2002). Both the composition and the configuration of agricultural landscapes are the result of farmer's cropping plan choices made at the farm level. These decisions are critical because they modify farm productivity and profitability in the short and long period (Dury et al., 2012). A farm "cropping plan" is composed of the crop acreages that refer to the farm area, usually devoted to one or a group of crops each year (Wijnands 1999) and the crop allocation, which is the assignment of a particular crop to each plot on a given piece of land (Aubry et al. 1998). Crop rotation is defined as the practice of growing a sequence of plant species on the same land and is a concept that has long been used to represent the temporal dimension of cropping plan decisions (Bullock 1992). Crop rotations undergo to different criteria, for example the return period of crops, prohibited crop sequences, or soil fertility improvement sequences. Farmers cropping plan and crop rotations are often spatially explicit at farm scale (Rounsevell et al., 2003) and depends by many factors including biophysical factors (e.g. rainfall, soil types), or socioeconomic factors (e.g. farm size, subsidies).

Considering this, decisions that are at the core of the farm management have strong impacts on resource use efficiency and on environmental processes at both farm and landscape scale (Dury et al., 2011) the "farm typology" individuation is of a great importance for understanding the determinants of crop acreage changes at the regional scale and to help decision makers to formulate farm-scale policies intended to modify farming systems. A "farm typology" approach aims in categorizes farms into homogeneous groups with similar crop "crop allocations". Comparisons of these groups are important to understand farmers' decision processes for crop choices (Iraizoz et al. 2007) and conduct or influence at regional level farmers cropping plans through agricultural policies.

According the contribution of Iraizoz et al, (2007) two are the main techniques followed to design farm typologies: the (i) "a priori" approach and the (ii) "quantitative typification" approach.

- i. The "a priori" approach, or what Rosenberg and Turvey (1991) refer to as the "pre-specified method", refers to the subjective knowledge of the researcher to define the characteristics (rules) for the segmentation process. Therefore the quality of this approach depends on the choices made by researchers. The method has been heavily criticised for failing to make full use of available data

(Gloy and Akridge, 1999). Moreover, given a lack of statistical foundation, there is no evidence that this approach lead to (fairly) define homogenous farm groups (Gebauer, 1987). For example, many application based on this approach has been group farms on the base of geographic area, which ignores the heterogeneity of farming systems within particular locations (Kobrich et al., 2003).

- ii. "Quantitative typification" approach (Kobrich et al., 2003) can be based on a small number of variables, such as followed by USDA (2000, 2001) or employ multivariate statistical techniques. USDA (2001) segmented farms into seven categories based on just two variables: the occupation of operators and the volume of sales. When a classification is based on so few variables there is a danger that the typology will fail to accurately capture and segment the state of farms. For example, while the USDA (2001) look for understand the economic aspect of farms considering a limited number of indicators they ignore a number of factors that might influence future performance such as the degree of financial stress and the farm ownership level. Given this, some other authors preferred to adopt multivariate statistical techniques so that a greater range of variables can be involved in the typology design (Bernhardt et al., 1996; Kobrich et al., 2003). In the quantitative typification based on a multivariate approach, the most commonly used technique has been cluster analysis. For example, Gebauer (1987) employs cluster analysis to segment farms into four groups based on 13 socio-economic variables.

Quantitative typification multivariate analysis appears as the most robust approach to design farm typologies. However, its application usually relied on data for a single year, limiting the ability to trace the evolution trajectories of farms (Landais, 1998). An approach of farm typology definition based on multi temporal data could provide reliable information concerning the future dynamics of structural changes at farm and regional level (Righi et al., 2010). Farm typologies are static they are made for a particular year and do not show changes over time and cannot, therefore, reveal the changes in farm cropping plans across time and space or the determinants of changes in farm cropping plans (Chopin et al., 2015).

Considering a multi temporal perspective, satellite data time series represent a good candidate approach to depict the multi annual variabilities of farm management and therefore it can represent a reliable and consistent tool to design farm management typologies. Remote sensing approach has proven to be useful for depict farm management changes, in particular through the mapping of crop cycles (crop intensity) and crop rotation patterns (Casasnovas et al., 2005). Some examples are hereafter presented:

Casasnovas et al., (2005) introduces a methodology for mapping the main multi-year cropping patterns in agricultural areas from crop maps derived from supervised classification of satellite images. The method used seven year time series of Landsat 5 TM and Landsat 7 ETM+ data. In the contribution of Conrad et al., (2011) is presented a mapping procedure for crop rotations that exploit classification and regression trees (CARTs) applied to 250m MODIS NDVI time series. The method was validated with reference sample derived by high resolution (15m) ASTER data and achieved overall accuracy value s of 84%. Osman et al.,

(2015) proposed instead a machine learning approach to model crop rotation managements. This approach was able to predict crop types before the beginning of crop season with accuracies of 60%. Le li et al., (2014) presented an algorithm for the automated mapping of cropping intensity in China and estimated agricultural intensity on the base of EVI time series analyses reaching overall accuracies of 91%.

In this research framework, we took in consideration the “farm typology” approach as a methodology to describe crop management variability at farm scale level. The specific bibliographic review highlighted the need to derive farm typologies by considering the temporal evolution of farms management changes estimated from long term time period and define as “farm trajectories” (i.e. Landais, 1998). In reason of this we evaluate the possibility to identify farm management typologies through the analysis of time series of satellite data to provide helpful information for the farm characterization.

2.2.3 Combining remote sensing with crop simulation modelling

Remote sensing derived parameters, retrieved from single image or extracted from satellite time series are used with crop simulation models and improve their capability to predict regional crop yields. Two main families of approaches can be distinguished in agricultural crop models according to the level of detail at which crop development processes are described:

- i. Simplified approaches are mostly based on Monteith’s efficiency equation and are also known as NPP (Net Primary Production) models.
- ii. Sophisticated approaches are represented by the so called SVAT (Soil Vegetation Atmosphere) group of techniques, also known as “crop growth models” or “agro-meteorological models”.

Generally speaking, crop growth models reproduce general knowledge about plant physiology in a mathematical way. These models describe the primary physiological mechanisms of crop growth (e.g., phenological development, photosynthesis, dry matter partitioning), as well as the interactions of these mechanisms with the main environmental driving variables (temperature, nutrient availability, rain events). In the SVAT models, state variables such as phenological development, biomass and leaf area index are updated during successive computational loops usually performed at a daily time step and retrieve continuously a set of feedbacks. These loops (and feedbacks) are not used in the simplified approaches based on Monteith equation (Monteith, 1971): those models assume that the local biomass production is equal to the sum of the (daily) Net Primary Production (NPP) calculated in a simplified manner. Both families of approaches that have been successfully coupled with remotely sensed inputs are synthetized in the following.

In the simplified approaches, remotely sensed data are used in Monteith’s efficiency equation through the estimation of the seasonal cycle of the fraction of Absorbed Photosynthetically Active Radiation fAPAR (if enough images are available so that the full temporal profile can be reconstructed).

$$\text{NPP} = \text{PAR} \times f\text{APAR} \times \epsilon_b \quad (\text{Eq. 1})$$

Where NPP: net primary production ($\text{g}\cdot\text{m}^{-2}\cdot\text{d}^{-1}$), PAR: incident Photosynthetically Active Radiation ($\text{MJ}\cdot\text{m}^{-2}\cdot\text{d}^{-1}$), fAPAR: fraction of incident PAR which is intercepted and absorbed by the canopy (dimensionless), ϵ_b : light-use efficiency of absorbed photosynthetically active radiation ($\text{g}\cdot\text{MJ}^{-1}$). The light-use efficiency (ϵ_b) is relatively constant for crops like winter wheat (with a value of about $2.0 \text{ g}\cdot\text{MJ}^{-1}$).

At the same time, the light-use efficiency (ϵ_b) must either be relatively known or should be assessed using other remote sensing inputs (e.g., from thermal data). Provided that enough images are available, the seasonal integration of time series radiometric measurements theoretically improves the capability of estimating biomass compared to one-time measurements, since the approach is based on sound physical and biological theory, whereas the relationship between instantaneous measurements of canopy reflectance and biomass is mainly empirical, and, to some degree, chance (Baret et al., 1989). Figure 2-5 shows the close correspondence between seasonally integrated absorbed PAR ($f\text{APAR} \times \text{PAR}$) and the dry matter at harvest for nine commercial winter wheat plots in the Camargue region of France (Atzberger, 1997). The slope (1.7434) corresponds here to ϵ_b in equation 1.

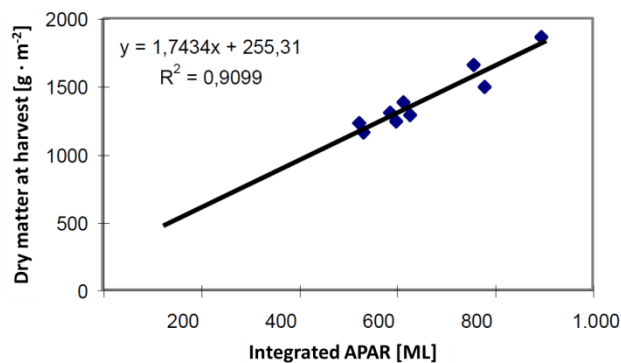


Figure 2-5 - Linear regression between the seasonally (from sowing to harvest) integrated absorbed PAR and dry matter at harvest ($\text{g}\cdot\text{m}^{-2}$) of nine commercial winter wheat plots. From Atzberger (1997).

SVAT crop growth models differ from the previous for three main characteristics (Delecolle et al., 1992): (i) they are dynamic, because they update state variables at a defined time-step; (ii) they contain parameters that can be changed according to different crop species; (iii) they include a strategy to describe phenological development of a crop. The strength of these models, as research tools, resides in their ability to capture the soil-environment-plant interactions; however their initialization and parameterization generally require a number of physiological and pedological parameters that are not easily available.

Crop growth models and remote sensing complement one another since crop growth models provide a continuous estimate of crop growth over time, whilst remote sensing provides spatial pictures of crop status (e.g., LAI) within a given area. In spatially distributed modeling all model inputs and parameters have to be provided in spatialized form. As remote sensing provides spatial status maps, the use of remotely sensed information makes the crop growth models more robust (Moulin et al., 1998; Guerif et al., 2000).

According to Moulin et al. (1998) and Rembold et al. (2013), the most straightforward way to couple remote sensing data with crop growth models is the “model parametrization” or the “model initialization”. The parameterization of crop growth models consist in provide parameters to the model, for example, remotely sensed data is used to provide information about crop type and With known crop types, plant specific parameter settings can be assigned. The initializations of crop growth models consist in providing the model of state variables at the start of the simulation (note that all the state variables need to be initialized). It is reasonable to assume the initial value of LAI at sowing to be zero. However, the soil water content at sowing may be highly variable. Satellite imagery may be used to provide an estimate of soil water content at the beginning of the simulation run.

Besides the direct parameterization and initialization of crop growth models, remote sensing can be coupled to spatially distributed crop models at least in four other valuable ways:

- i. Re-calibration or (re-parameterization)
- ii. Re-initialization
- iii. Forcing
- iv. Updating

(i) The “re-calibration” or (re-parameterization) approach is used when it is assumed that some parameters of the crop growth model are inaccurately calibrated. This is usually achieved by (iteratively) adjusting the model parameters until measured and simulated profiles of the state variables match each other. In spatially distributed modeling this re-calibration has of course to be done pixel by pixel. Here, the remote sensing derived state variables are considered as important reference for the model simulation.

(ii) In the “re-initialization” approach a tuning of the initial values of state variables is done until a good match between observed and simulated state variables is obtained. Here again, remote sensing derived state variables are considered as reference for the model simulation.

(iii) In the forcing strategy approach, the complete time profile of a crop state variable (i.e. LAI) is reconstructed from remote sensing time series data and the corresponding value introduced into the dynamic crop growth model at each time step of the simulation.

(iv) The updating of crop growth models consists in the replacement of simulated values of crop state variables by remotely sensed values each time these are available (not necessarily at each time step).

The more satellite observations are available and the better they are distributed across the growing season, the more/better model parameters can be calibrated and/or initialized.

2.3 Operational crop monitoring systems exploiting satellite time series data

Agricultural primary productions follow patterns depending on the physical landscape (e.g., soil type), climatic driving variables (e.g. temperature, rain) agricultural management practices (i.e. sowing, irrigation

and fertilization scheduling) and also on un-predictable climate events. These main drivers (and many other more) are furthermore variable in space and time and contribute to define the “seasonality” characterizing agricultural production fluctuations.

In reason of seasonality, an agricultural monitoring system has to be able to provide timely and spatially distributed informations on crops during the agricultural season. As pointed out by the Food and Agriculture Organization (FAO) (2011), the need for timeliness is a major factor underlying agricultural statistics and associated monitoring systems. Information is of little interest if it is available too late.

Today, a regional to global agricultural monitoring system information service can provide added value information useful for stakeholders such as national and international agricultural policy makers as well as global agricultural trade and organizations dealing with food security issues heavily depend on reliable and timely crop production information (Becker-Reshef et al., 2010).

An ideal Agricultural monitoring system service should be characterized by the following features:

- a. provide timely information on crop status and crop production;
- b. provide these informations regularly, from a (sub) regional to national scale level;
- c. provide information as early as possible during the growing season and update many times in the season, until the harvest;
- d. provide homogeneous data sets, statistically based, precise and with high accuracy;

Satellite remote sensing (in combination with modeling tools) can provide such information in a timely manner, over large areas, in sufficient spatial detail and with reasonable costs (Roughgarden et al., 1991). Currently, several regional to national (and global) operational agricultural monitoring systems provide reliable informations on agricultural crop production during agronomical season. Hereafter some of them will be introduced, with particular consideration on the contribution that remote sensing provide within them.

i. The USAID Famine Early Warning System (FEWS-NET).

The FEWS-NET is a leading provider of early warning and analysis on acute food insecurity. It was created in 1985 by the US Agency for International Development (USAID) to help decision-makers plan for humanitarian crises. FEWS NET provides evidence-based analysis on some 35 countries. The main information carried out concern in reports and maps detailing current and projected food insecurity, timely alerts on emerging or likely crises and specialized reports on weather and climate, markets and trade, agricultural production, livelihoods, nutrition, and food assistance. Remote sensing plays a central role in all the FEWS-NET outcomes. (<http://www.fews.net>).

ii. *The Global Information Early Warning System (GIEWS).*

Established during the world food crisis of the early 1970's, the Food and Agriculture Organization (FAO) GIEWS remains the leading source of information on food production and food security for every country in the world. GIEWS aims is to provide policy-makers and policy-analysts with the most up-to-date and accurate information available on all aspects of food supply and demand. In doing so, it provides regular bulletins on food crop production and markets at the global level and situation reports on a regional and country scale level.

Data from four satellite systems are used for monitoring the various crop seasons throughout the world: the European Meteorological Satellites (METEOSAT), the Japanese Geostationary Meteorological Satellite (GMS), the US National Oceanic and Atmospheric Administration (NOAA) and the French Satellite Pour l'Observation de la Terre (SPOT-Vegetation). GIEWS operatively provide global information on rainfall and drought by comparing satellite images from the current season to those from previous years or the historical average. In addition to rainfall monitoring, the System makes extensive use of NDVI images that provide an indication of the vigor and extent of vegetation cover. These informations allow analysts to assess vegetation conditions during the current growing season as compared to the historical average or previous years. (<http://www.fao.org/giews/english/about.htm>).

iii. *The Monitoring Agricultural ResourceS (MARS) action of the European Commission (Ispra, Italy).*

Two are the main topics of MARS action: agricultural production estimates of EU countries (Agri4Cast) and food security assessments in food insecure countries (FoodSec). MARS project started in 1988, with the aim to apply emerging space technologies for providing independent and timely information on crop areas and yields. Since 1993, MARS contributed towards a more effective and efficient management of the Common Agricultural Policy (CAP) through the provision of a broader range of technical support services to DG Agriculture and Member-State Administrations. Since 2000, the expertise in crop yields has been applied outside the EU. Services have been developed to support European capability for global agricultural monitoring and food security assessment. The expertise developed within MARS integrates research and techniques in: Statistics, Image processing and interpretation (satellite or air-borne), GIS management & web-based information technology, Geomatics and GPS (orthophotos, large scale mapping, and parcel measurement), Agrometeorological models (crop growth / yield). (<http://mars.jrc.ec.europa.eu/mars/About-us/The-MARS-Unit>).

iv. *The Global Monitoring of Food Security (GMFS) program.*

GMFS is an activity started by the European Space Agency (ESA) under the joint ESA and European Commission (EC) Global Monitoring for Environment and Security (GMES) initiative. Through GMES, ESA and the EC have combined forces to unite the research, development and operational user communities across Europe in a coordinated effort to establish a European capacity for Global Monitoring for

Environment and Security. GMFS aims to provide earth observation based services of early warning agricultural monitoring and services in support of food security monitoring activities in Africa. (<http://www.gmfs.info>).

- v. *The China Crop Watch System (CCWS) program at the Institute of Remote Sensing Applications (IRSA) of the Chinese Academy of Sciences (CAS).*

Since 1998, “Crop Watch” is operative in China as leading crop monitoring system. This service aims to assess national and global crop production and related information. “Crop Watch” analyze global production and environmental and agricultural trends on the base of remote sensing and ground data and a combination of well-established and innovative methodologies. Once every three months, a bulletin is carried out. “Crop Watch” uses a hierarchical approach for crop production monitoring. It involves the use of specific environmental and agricultural indicators on different scales, using the combined information to assess global, regional, and national (as well as sub-national) crop condition, production, and agricultural trends. The analysis covers the following four levels: sub-national, national, regional and global. During the analysis, each level is covered with specific indicators adapted to its scale, while the next broader level provides the overall background. Using the outputs on the four levels, a synthesis of crop production and crop condition estimates is provided. (<http://www.cropwatch.com.cn/htm/en/index.shtml>).

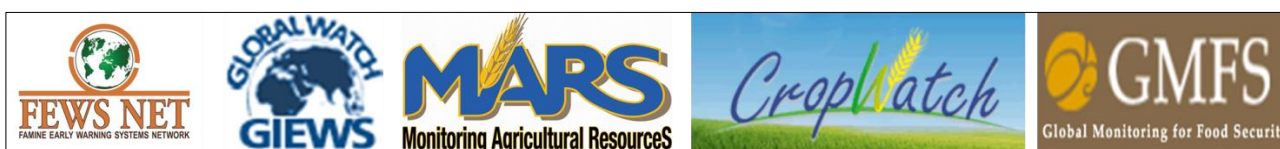


Figure 2-6 - Representative logos of Operational crop monitoring systems services. Left to right: Famine Early Warning System (FEWS-NET), Global Information Early Warning System (GIEWS), Monitoring Agricultural Resources (MARS) unit, Global Monitoring of Food Security (GMFS) program and China Crop Watch System (CCWS) program

2.4 Conclusions

Remote sensing and in particular the analyses of time series of satellite data represents a very interesting tool extensively used for studies on crop phenology and crop management. Application of time series analyses approach requires knowledge of benefits and limitation of vegetation indices, data smoothing techniques and crop key-stage extraction techniques. Different methodologies in this sense can be applied for each step of the time series production. In this review the most used for agricultural monitoring were documented. The selection of proper data processing techniques has to be chosen according to the peculiarities of the singular case studies in order to minimize unwanted disturbing factors and maximize the meaning of time series derived information. Long term databases containing satellite data are freely available (i.e MODIS or Landsat archives). Such a long period described by continuous series of data registered by the same instruments allow for studies on phenological and agro-practices changes and in temporal and spatial scales.

Two important considerations were derived from the analysed bibliography and taking into account the scope of the thesis:

- I. Only few contributions at present are target in the remote sensing discipline to estimate specific crop practices, such as the sowing periods, through the analyses of time series. In particular concerning the analyses of winter crops inter- and intra- annual sowing period variability;
- II. As pointed by Landais et al. (1998), Righi et al. (2010) and Chopin et al. (2015); an approach of “farm typology” definition based on multi temporal data could provide reliable information concerning the future dynamics of farm changes. A time series analyses contribution approach could therefore be an innovative and meaningful approach to describe farm diversities at regional level.

3 Inter-annual variability of winter wheat sowing dates through satellite time series analysis: 2003-2013 estimation in Camargue, France

3.1 Introduction

Cropping systems are highly diverse due to many different factors, such as environmental condition, cultivated varieties, agro-practices, growing conditions and climate. European cropping systems in particular are diversified in both space and time in reason of a high field fragmentation and of the multiple cultivated crop varieties. Observing cropping systems, we are also facing a great source of variability due to the diversified strategies implemented by the farmers, the presence of specific constrains (i.e. soil types, water availability) and due to unavoidable factors affecting their practices, such as climate hazards and seasonality. This leads to high intra-annual (different space arrangement of crop) and inter-annual (diversification of crop establishment dates) differences. Furthermore, the cropping systems are changing rapidly due to different sources of pressure: climate change, population growth, decreasing of arable lands and innovations in crop practices and (in Europe) according to policies and communitarian subsidies.

In order to be able to provide suggestions for the adoption of more sustainable systems, we need to analyse the current situation (base-line scenario) characterising their evolution in the past as an indicator of farmers attitude to react to external (biotic and abiotic) factors.

To do this, we need to characterize the variability and diversity of practices, and therefore to quantify the actual spatial diversity and temporal variability of the system under analysis (Zhang et al., 2003). We also need to identify the main sources and reasons of the observed diversity and variability, to be able to project it into the future (Doraiswamy et al., 2005).

Often, it is difficult to get information about the variability of crop management at regional level, which is the target of territorial approaches aiming to explore future scenarios. Generally, the main sources of information are provided by governmental agencies or regional institutions through census. This data are aggregated and it is not possible to reconstruct single farmer practices. Moreover, these data are auto declared and consequently it represents another possible source of error. Other sources of data are the ones coming from specific studies conducted through farmers' interview. These data are more complete but, due to the required effort to acquire the information, sometimes lack of representativeness to

characterise the diversity in space (few samples) and time (sporadic year of analysis does not provide a complete picture of the dynamics) of a region (Chen et al., 2002).

Indirect data such as the ones provided by Earth observation satellite data archives can be a valuable alternative when direct field information are not available for territorial studies. Remote sensing data can greatly contribute to the characterization of the cropping systems by providing timely, synoptic, cost efficient and repetitive information about the status of the Earth's surface (Justice et al., 2002). Today, a large range of satellite sensors provide data covering a wide spectral range (from visible to microwave) and at different spatial (from sub meter to kilometre) and temporal resolutions (from 15 minutes to on demand acquisition). For deriving vegetation information from satellite images, a large number of spectral analysis tools have been developed. Besides the spectral signature, useful information can also be retrieved by analysing the temporal signature properties of vegetation (Atzberger, 2013). Considering satellite images data there is a trade-off between temporal resolution, spatial resolution and information content (spectral dimension). MODIS data can be considered a good compromise of these three features. This data tends to be used when agricultural-related long term information (> 10 year) needs to be analysed at regional scale (< 1km resolution) with a good revisiting time (availability of weakly data).

For example, remote sensing time series analyses has been used to discriminate temporal signature of cultivated crops types and investigate their management practices at regional scale in Kansas (U.S.A.) for the 2001 season (Wardlow et al., 2002). Sakamoto et al., (2005) instead, characterized the variability of paddy rice (i.e. planting, heading and harvesting periods) for the 2002 season in Japan. Satellite time series were also been used to investigate inter-annual variability of cropping systems. For example Xin et al., (2002) worked in the Huang-Huai-Huai plan (China) observing inter-annual fluctuation of winter wheat heading period and summer maize tasselling period through the analyses of 1990-2000 NOAA time series. MODIS derived NDVI time series were considered to produce inter-seasonal estimation analyses of paddy rice emergence, heading and maturity periods in Northern Italy for the 2001-2005 period by Boschetti et al., (2009). Son et al., (2013) assessed MODIS time series in the 2002-2012 period to investigate inter-annual variability of paddy rice crop management systems.

In this framework, this paper presents the results of the research conducted to analyse vegetation indices of MODIS time series for the estimation of inter-annual variability of winter wheat crop establishment in Camargue, France. These informations are a fundamental pre-condition to adopt crop modelling approaches to assess the impact of climate change scenarios on crop yield. A key issue for modelling future scenarios, notably related to climate change, is the capacity to properly parameterize crop models, including information related the variability of critical crop practices, such as the period of crop establishment which is for most of the crops, a critical variable to explain the crop performance (such as the yield). Different drivers can explain the variability of crop establishments, such as the climate (cold period,

rainy events), the farm organization and availability of labour and machineries and the presence of preceding crops.

In Camargue, the establishment of rice (the main crop) is quite stable through years (low inter and intra annual variability) because the farmers tend to prioritize this crop and the window for establishing the crop in optimal conditions is small (about three weeks). However, the conditions of establishment for durum wheat are greatly variable; with respect to rice, wheat is not a prioritized crop, and the sowing operation can be realized in good conditions in a window of approximately 2.5 months. Therefore analysing the inter and intra-annual variability of sowing conditions, and understanding the factors that affect the timing of this operation is fundamental to use crop models for the characterisation of actual condition (baseline scenario) and the simulation of future scenarios (e.g. climate change and/or agro-polices). In the Camargue case study, no data are already available to reconstruct reliable information at a regional level about the variability of crop practices, and the option to retrieve it through farmers' interview was not sustainable due to the risk of error and to the high cost for data acquisition. This is therefore an important topic for which remote sensing could significantly contribute to improve agronomic knowledge.

Various approaches have already been exploited to derive the period of establishment of winter wheat crop from satellite time series analyses. Huang and Lin, (2009) estimated winter wheat onset of greenness adopting a threshold approach. The approach focused on evaluating half maximum of wheat-related time series (dynamic threshold value) and deriving then the date at which the half max value is exceeded (during spring period). Onset greenness estimations showed a general agreement with in situ phenology observation. More recently Lu et al., (2013) presented a curve-fitting method to derive winter wheat phenology from SPOT-VEGETATION S10 NDVI data products. Here winter wheat start of the season (SOS) was derived considering the date when the derivative of the NDVI composite series reaches its maximum. This occurrence well fitted ($r=0.724$ and $RMSE= 18.7$ days) with wheat jointing (when the first node of the stem is two cm higher than the soil surface) phenology-stage of wheat. Vyas et al., (2013) instead, proposed a mathematical model able to capture persistent positive slope of NDVI profile after an inflection point and estimated the crop establishment occurrence seven days after this point. The onset dates were validated obtaining RMSE value of 3.2 (n=45).

The objective of this work is to develop a remote sensing based approach to characterize and analyse the wheat crop establishment. MODIS derived time series were analysed with a rule based method to estimate the variability of wheat crop establishment for the period 2003-2013 and to make hypothesis about the factors explaining such variability.

The paper presents in the second section the satellite data and the ancillary data exploited in the work and the work flow adopted to design and validate the methodology. Results, concerning the developed methodology and the long term estimation of winter wheat crop establishment in Camargue, are presented

in section three and discussed in section four. Finally, section five provides a general conclusion of the work highlighting the usefulness of the obtained results.

In this manuscript we used the definition “crop establishment” with reference to an approximate period between crop sowing and crop emergence and we referred to “crop sowing” to identify the moment for which we estimate when this crop practice is conducted.

3.2 Material and Methods

3.2.1 Study region

The Camargue is a geographic region situated in south-eastern France at the mouth of the Rhône River. This is a flat (0-5 meters of elevation) delta shaped territory of about 180.000 ha. Most of the Camargue region is protected by environmental authorities that manage the territory at different administrative scale. For what concern agriculture, the most important authority is the Regional Natural Park of Camargue (PNRC), which protects nearly 108.000 ha and includes almost all the land enclosed in the two branches of the Rhône River (Grand Camargue) and other smaller areas on the East and West sides of this central part (Figure 3-1).

From Figure 3-1-A and 1-B it is possible to appreciate the study area as it appears from high spatial resolution satellite images (Landsat, 30 m) and moderate satellite spatial resolution (MODIS, 250 m). According to the PNRC land use datasets of the year 2006 and 2011 (Figure 3-1-C and 1-D), agricultural land uses represent respectively the 31% and 25% of the park area (32.713 ha in 2006 and 28.733 ha in 2011). The two most representative cultivated crops are Rice (*Oryza Sativa* L.) which accounted 36% (11.684 ha in 2006) and 56% (16.037 ha in 2011) of the cultivated area and Winter Wheat (*Triticum Durum* L.) with 22% (7.350 ha in 2006) and 10% (2.927 ha in 2011) of the cultivated area. These crops represent together two thirds of the cultivated area of the park.

Rice and winter wheat are in Camargue two complementary crops in terms of agronomy and crop rotation: while rice is a summer irrigated (flooded) crop, winter wheat is a winter-spring rainfed crop. Flooded rice cultivation (irrigated with freshwater from the Rhône River) allows dealing with soil salinity problem. However, after a few years of cultivation, weeds pressure tend to decrease rice yields and durum wheat and other not irrigated crops are sown in rotation with rice.

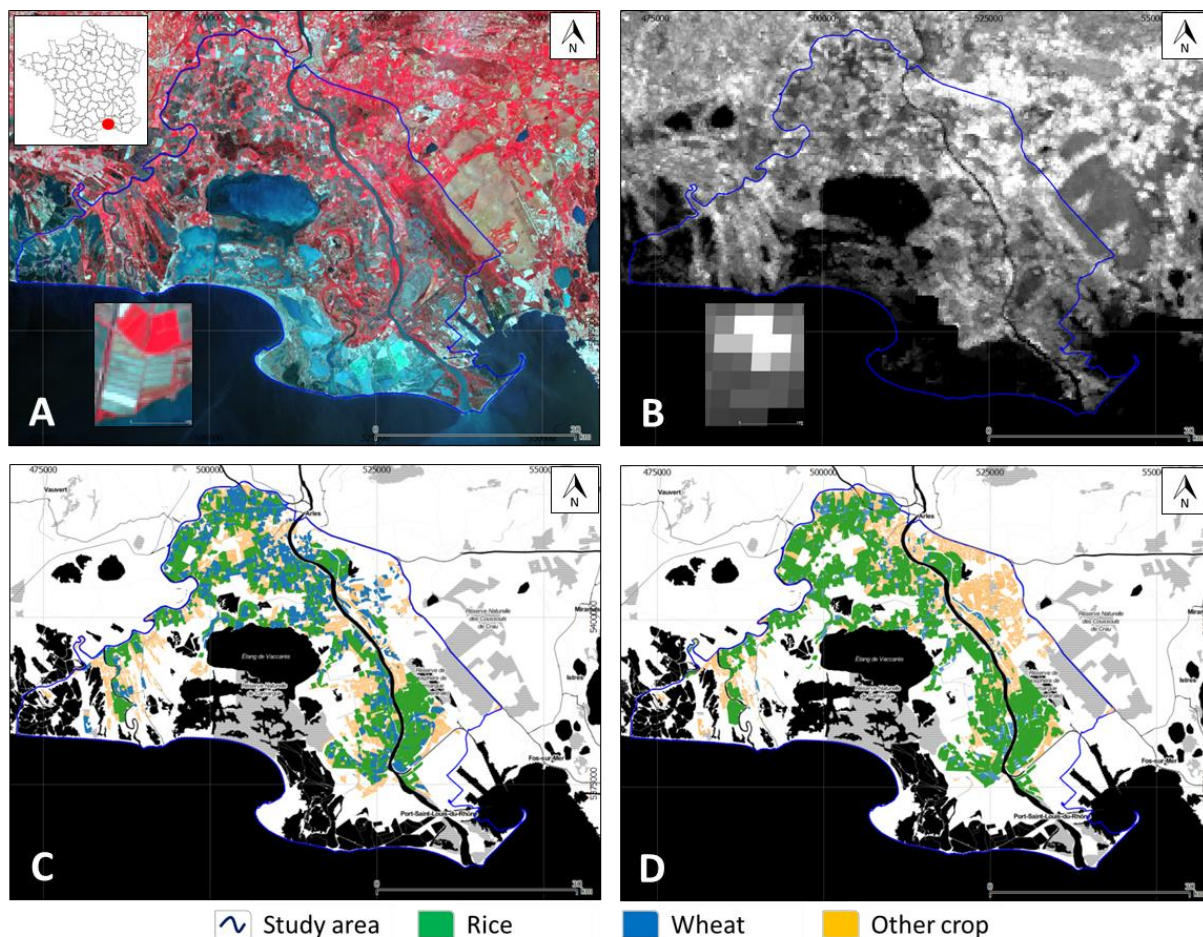


Figure 3-1 – Main cultivated areas in the study site of the *Parc naturel régional de Camargue* (PNRC). Figure 1-A: Study area at Landsat high spatial resolution (Landsat-8, DOY.163, RGB-543). Figure 1-B: Study area at MODIS moderate spatial resolution (MODIS MYD13Q1, DOY.161, EVI grey scale). Figure 1-C: Land use map of Camargue 2006 (*Occupation du sol 2006 du PNR de Camargue*). Figure 1-D: Land use map of Camargue 2011 (*Occupation du sol 2011 du PNR de Camargue*). The borders of the study area are represented in dark blue lines. Rice, winter wheat and other crops are reported in green, light blue and orange respectively in figure 1-C and 1-D. In figure 1-C and 1-D, water bodies, non-agricultural areas and areas of not interest are coloured respectively in black, white and grey.

Table 3-1 – Average crop calendar for the main cultivated crop in Camargue

| Crop: | Jan | Feb | Mar | Apr | May | Jun | Jul | Aug | Sep | Oct | Nov | Dec |
|------------------|-----|-----|-----|-----|-----|-----|-----|-----|-----|-----|-----|-----|
| Rice | | | | | ■ | ■ | ■ | ■ | ■ | ■ | ■ | |
| Winter wheat | ■ | ■ | ■ | ■ | ■ | ■ | ■ | ■ | ■ | ■ | ■ | ■ |
| Corn | | | | ■ | ■ | ■ | ■ | ■ | ■ | ■ | ■ | |
| Sorgho | | | | ■ | ■ | ■ | ■ | ■ | ■ | ■ | ■ | |
| Alfalfa (fall) | ■ | ■ | ■ | ■ | ■ | ■ | ■ | ■ | ■ | ■ | ■ | ■ |
| Alfalfa (spring) | ■ | ■ | ■ | ■ | ■ | ■ | ■ | ■ | ■ | ■ | ■ | ■ |
| Alfalfa | ■ | ■ | ■ | ■ | ■ | ■ | ■ | ■ | ■ | ■ | ■ | ■ |
| Sunflowers | | | | ■ | ■ | ■ | ■ | ■ | ■ | ■ | ■ | |

■ Sowing ■ Growing ■ Harvesting

Table 3-1 shows the crop calendars for the main cultivated crop in Camargue. It is possible to notice that a narrow window concern rice sowing period due to favorable weather condition and due to the importance of this crop during the tillage scheduling (priority). A wide sowing window instead characterizes the crop calendar of winter wheat due to possible unfavorable weather in autumn and due to a variability in crop

practices. However, despite this general static representation of crop practices no detailed information are available concerning the actual sowing period in the study area.

3.2.2 Methodological work flow

In Figure 3-2 the activities conducted in the research are summarized in three main phases. The first phase, called the development phase consisted in the pre-processing procedures to analyse MODIS VI time series satellite data (section 2.3) and in the definition of a set of rules to identify (i) winter wheat cultivated area and (ii) the crop establishment period (section 2.4). The second phase consisted in validating the performance of the developed method by comparing i) mapping results with reference data derived from high resolution satellite data for the years 2003, 2006, 2009 and 2012 and ii) sowing date estimation with ground reference datasets acquired for 2011, 2012 and 2013 in three farms (section 2.5). Finally, the last phase consisted in the application of the algorithm to a long term time series of MODIS images (11 years) and to their analyses (section 2.6).

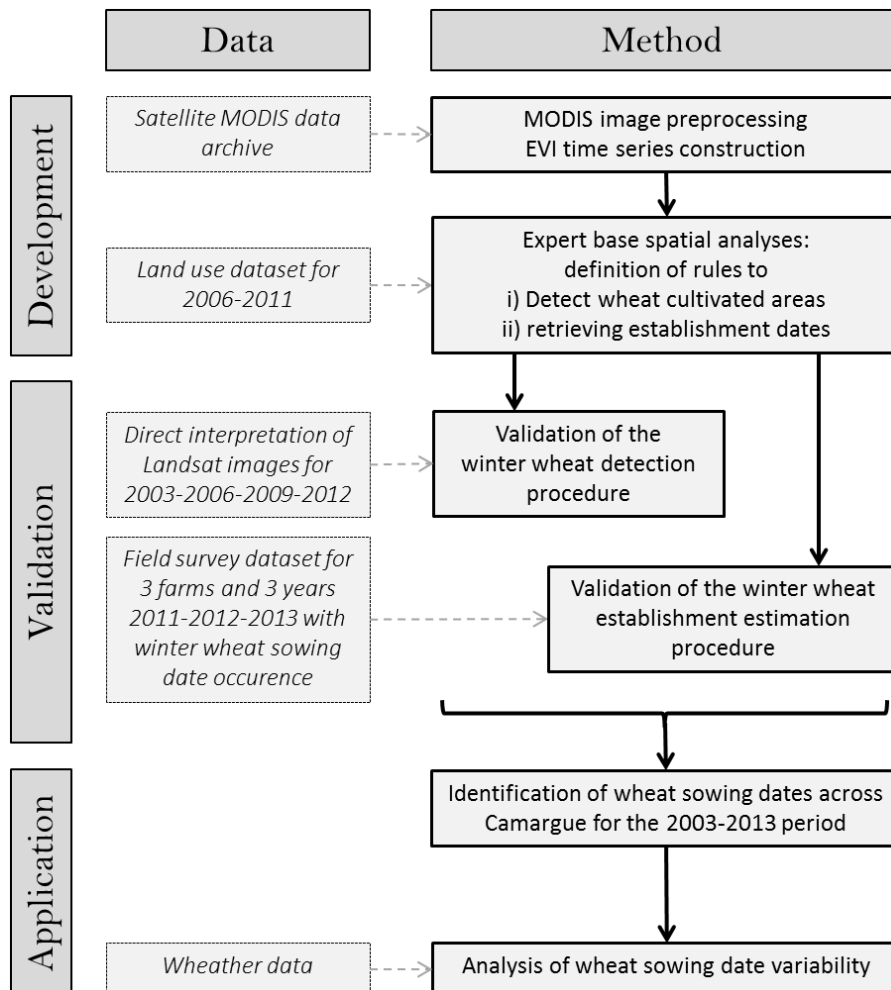


Figure 3-2 - Flow chart representing the key methodological steps and the data used during this work.

3.2.3 MODIS satellite data

The approach we followed is based on the analyses of time series of Moderate Resolution Images Spectroradiometer (MODIS) satellite data. We analyzed time series of Enhanced Vegetation Index (EVI - Huete et al., 2002) data, acquired from MODIS Terra and Aqua satellites and released in the MOD13Q1 and MYD13Q1 16-days composite product respectively. The MOD/MYD 13Q1 Level-3 products are calculated using the Constrained View angle-Maximum Value Composite (CV-MVC) compositing method to reduce the noise (mainly due to clouds) affecting MODIS images. The composites method takes into account a time span of 16 days to retrieve the best observation in the period (Solano et al., 2010). These products are provided with 8 days nominal time shift and once combined they allowed reconstructing EVI values with an improved temporal frequency of eight days. The MOD/MYD 13Q1 have nominal 250-m spatial resolution (blue and medium infrared reflectance band are resampled from 500 to 250m) and they're delivered in a Sinusoidal projection. These data are provided according the Hierarchical Data Format (HDF) standard and they are free to be download from the Land Processes Distributed Active Archive Center (LP DAAC) through the GloVis data provider. In this work, MODIS data were collected from the Day of the Year (DOY) 177 of 2002 (end of June), to the DOY 361 of 2013 (end of December). A total of 484 MODIS MOD/MYD 13Q1 image products were downloaded for the reference grid tile h18v04.

VI time series construction and analyses

The Enhanced Vegetation Index (VI) EVI was chosen for time series analysis due to its performance recognised in vegetation monitoring studies. Pan et al. (2012) in their study on wheat area estimation reported how inter-annual variation of EVI can reflect the crop phenology during the growing seasons and intra-annual variability of EVI intensity can reflect areal coverage of a given crop. It is well known that agricultural crops can hardly been classified using moderate spatial resolution single-date reflectance bands (Sun et al., 2012), however VI's time signatures of moderate resolution remotely sensed data, have been used to detect agricultural land covers (Sakamoto et al., 2005; Wardlow et al. 2007; Wardlow and Egbert 2008). Time series of the EVI (Eq. 1) for the period 2002 – 2013 were generated for a specific subsample of MODIS images that covers the study area.

$$EVI = 2.0 * \frac{\rho_{NIR} - \rho_{Red}}{\rho_{NIR} + 6.0 * \rho_{Red} - 7.5 * \rho_{Blue} + 1} \quad (Eq. 1)$$

Two main processes were involved in time series production: (i) the extraction of the necessary information from the MODIS MOD/MYD 13Q1 products and (ii) the smoothing of the EVI temporal series.

During the first phase, information on EVI was extracted from the MOD/MYD 13 product on the HDF layer 2 and then stacked according to a chronological order to create a multi-band array (three dimensional array: space-space-time) of EVI information data. Together with EVI data, additional information about the VI

quality flags, the blue reflectance band, the DOY of acquisition and the pixel reliability quality flags were respectively extracted from the HDF (Hierarchical Data Format) layers 3, 6, 11 and 12.

A smoothing operation on EVI data was then applied to remove the residual rate of noise that still affect the data after the compositing procedure (as pointed in Pettorelli et al., 2005). EVI time series were smoothed following a two-step approach as described in Boschetti et al. (2015). In the first step, anomalous “spikes” due to residual cloud cover, cloud shadow, water or snow were detected and cleaned from the raw EVI temporal profiles following the approach already proposed in the TIMESAT algorithm (Jönsson and Eklundh, 2004). In the second step, EVI time series were smoothed according to a weighted Savitzky-Golay (SAV-GOL) filter procedure (Savitzky and Golay, 1964), using a symmetrical smoothing window of ± 3 periods and a second order polynomial fitting function (Manfron et al., 2012; Boschetti et al., 2014). The SAV-GOL filter is widely adopted in remote sensing of cultivated areas and different researches show the successful application of this method in the MODIS vegetation indices, by minimizing overall noise and preserving higher vegetation-index values (Chen et al., 2004; White et al., 2006; Abílio D.C. et al., 2015). Recently, Geng et al. (2014) compared eight techniques for smoothing multi-temporal NDVI data, considering different vegetation types and sensors, and concluded that the SAV-GOL filter achieved best results in most situations. In this study the SAV-GOL filter was used taking into account the quality of the data according to the information derived from quality reliability flags and blue reflectance data (Xiao et al., 2005). On the basis of this information, a noise-related judge in the form of: *Clean*, *Contaminated* or *Cloudy*, were assigned on each pixel of the EVI time series array and used as weight in the polynomial fitting. Annex 1 provides an example of the adopted method smoothing performances.

Extraction of representative crop temporal signature

Land use maps for the year 2006 and 2011 were available from the PNRC institution (Parc Naturel Régional de Camargue, 2013). In this dataset, the different land use that can be found in Camargue, including cultivated crops, are mapped at the individual field level (polygon format). The data were provided in France Lambert-93 geographic projection with a representation scale of 1:5000.

The land used data were used to characterize the presence of winter wheat cultivation within all the MODIS 250m pixels covering the study area. Geographic Information System (GIS) analyses were done to extract cultivated land use polygons and performing zonal statistic to calculate the percentage of specific crop presence in each MODIS pixel for the years 2006 and 2011.

Our aim was to select high confidence MODIS pixels related to winter wheat and other crop classes in order to identify a representative temporal signature of the crop (i.e. average EVI time series from homogeneous pixel). On the basis of these data, we derived rules for the automatic detection of winter wheat cultivated areas and crop sowing period. For this purpose, we selected the MODIS EVI time series belonging to those MODIS pixels having at least 80% surface covered by the winter wheat in 2006 or 2011.

3.2.4 Algorithm implementation

The detection criteria were derived on the basis of agronomic expert knowledge and by interpretation of high confidence EVI crop temporal signature. The details of this approach, previously used to analyse rice crop dynamics, are described in Manfron et al. (2012), Nelson et al. (2014) and Boschetti et al. (2015).

According to (Figure 3-3), the peculiarities of winter wheat crop cycle are:

- (i) the crop seeding is performed in late autumn (September-November) and followed by the crop emerging phase after 6 - 10 days;
- (ii) a vegetative period of 2-3 weeks occurs until three leaf stage when dormancy period stops plant grow in winter (December-February, ends when cold amount is satisfied);
- (iii) a tillering period and green up vegetative phase starts at the end of the winter (February–March), in this phase the plant increases rapidly its biomass and leaf area;
- (iv) a crop heading, that precede the reproductive phase (April-May); plants reach the higher vegetative growth (height, green biomass and leaf area index);
- (v) a grain filling and a successively ripening process determines the drying of the plant in June (senescence).

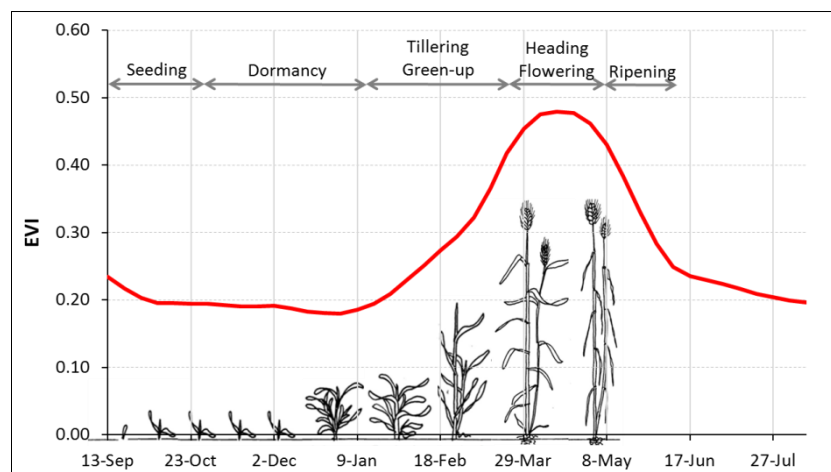


Figure 3-3 - Comparison between winter wheat agronomic cycle and the EVI time series (red line) extracted for a winter wheat cultivated area

According to these observations, the distinction of winter wheat from others crop in a clear and unambiguous way can be based on the detection of specific features in the EVI temporal profiles. The most typical features are (i) the occurrence of the heading period in late spring (e.g. April to June) and (ii) the length of the crop cycle that starts in late autumn. The heading period is in fact anticipated of nearly two months with respect to summer crops and the crop cycle, that last from autumn to the end of spring (up to 8 months), is usually longer than other seasonal (and shorter than perennial) crop types.

Wheat detection

In the literature, it is accepted that peculiar minima and maxima points in a time series are respectively indicators of (i) the start of the active growth cycle (i.e. sowing date and/or period of crop establishment)

(Sakamoto et al., 2005; Lu et al., 2014) and of (ii) the crop “heading” period (i.e. described as the transition between the end of the vegetative stage and the beginning of the reproductive cycle and correspond to the maximum vegetative seasonal crop stage) (Curnel et al., 2008; Boschetti et al., 2009; Atzberger et al., 2013).

In order to identify these points in the EVI series, a temporal signal analysis was conducted. For every smoothed VI time series the first derivative was calculated. The derivatives allowed to automatically identify all the local minima and maxima points when the first derivative changed from negative to positive (MIN_{rel} , eq. 2) and from positive to negative (MAX_{rel} , eq.3) respectively.

$$MIN_{rel}(t) = EVI'_{(t-1)} < 0 \ \& \ EVI'_{(t+1)} > 0 \quad (Eq.2)$$

$$MAX_{rel}(t) = EVI'_{(t-1)} > 0 \ \& \ EVI'_{(t+1)} < 0 \quad (Eq.3)$$

Time series of local MAX and MIN points were subsequently checked in order to detect the ones that are related to crop characteristics. Defining a series of rules, winter wheat crop cultivation was identified for those time series characterized by the presence of (i) a crop related maxima point (crop heading) occurring in the second quarter of the year, together with the presence of (ii) a crop related minima point at the defined distance to the heading during the preceding year.

Wheat heading

The heading moment is assumed to correspond to the maxima point related to crop development that is identified implementing the following rules, which have to be simultaneously satisfied:

1. An high vegetation presence: Individuation of an EVI value at the maxima point, greater than 0.42;
2. Rapid growth: Individuation of the rapid growth in the vegetative phase (February – March) preceding the crop heading by detecting a sequence of at least three positive derivative points in a temporal window of 40 days (5 composites) before the maxima point;
3. Senescence: individuation of a sequence of at least three negative derivative points in a temporal window of five after the maxima point together with the individuation of a decrease of 1/3 of the EVI maxima value, in a temporal window of the 48 days (6 composites) following the maxima point.
4. Crop calendar: The absolute maximum must occur in the second quarter of the year, from the end of March (DOY 89) to the beginning of June (DOY 153);

Crop establishment period

The beginning of winter wheat crop cycle is searched in correspondence of the minima point, identified by derivative analysis that occurs in the autumn period of the year preceding the harvesting (128 to 224 days before wheat heading). The crop establishment is characterised by the succession of the following events: (i) the field preparation indicated by low EVI values corresponding to bare soil conditions after plowing and

(ii) sowing and successive crop emergence corresponding to a moderate EVI increase. These criteria are formalised in the following rules:

1. Bare soil condition: candidate minima points must have an EVI value lower than 0.32.
2. Crop emergence: Individuation of a sequence of at least three positive derivative points in a temporal window of 40 days (5 composites) after the minima;
3. Crop calendar: the minima has to fall between 128 to 224 days before the previously individuated heading point.

Sowing date estimation

Once a MODIS pixel is identified as winter wheat, an additional set of rules were designed to detect a more robust sowing date in proximity of the identified crop establishment moment. The procedure involves two steps: (1) identification of the searching time windows and (2) selection of a crop minima point related to sowing within the window.

Search window

The first step is to define the limits (WIN_{start} and WIN_{end}) of the searching temporal window (WIN_{sowing}). WIN_{start} is fixed at DOY 273 (September, 30th) which is identified by agronomist knowledge as the earliest date for the crop sowing in the study area. WIN_{end} is then identified considering additional agronomic aspects such as (i) the shortest possible crop growth ($WIN_{end(1)}$) and (ii) the delay of the winter wheat crop cycle due to the presence of a preceding summer crop ($WIN_{end(2)}$). WIN_{end} is calculated considering the lower WIN_{end} DOY value (earlier date) between the two retrieved with different methods

$$WIN_{end} = \min (WIN_{end(1)}, WIN_{end(2)}) \quad (Eq.4)$$

$WIN_{end(1)}$ is set as the shortest possible duration of vegetative phase, 140 days from sowing to heading. Where $WIN_{end(1)} = (DOY_{heading} - 140)$.

To define $WIN_{end(2)}$ we assume that the delay in agro practices connected to sowing, is related to the dates of the preceding crop harvesting period. The more harvest is delayed the more winter sowing is delayed. The summer crop harvest (preceding winter wheat) is assumed to correspond to the lower EVI value in the period from late summer (DOY 209) to the end of the year (DOY 353). Once this moment, identified as DOY (MIN_{EVI}) is detected, the criteria to define $WIN_{end(2)}$ is formalised as follow:

$$if \ DOY (MIN_{EVI}) < DOY_{250} \ (September, 6^{th}) \ then \ WIN_{end(2)} = DOY_{310} \ (November, 5^{th}) \quad (Eq.5)$$

$$if \ DOY (MIN_{EVI}) > DOY_{305} \ (November, 10^{th}) \ then \ WIN_{end(2)} = DOY_{350} \ (December, 15^{th}) \quad (Eq.6)$$

$$\text{if } DOY_{250} < DOY(MIN_{EVI}) < DOY_{305} \text{ then } WIN_{end(2)} = 310 + \frac{DOY_{350} - DOY_{310}}{DOY_{305} - DOY_{250}} \times [DOY(MIN_{EVI}) - DOY_{250}]$$

(Eq.7)

A graphic representation of these criteria is reported in Figure 3-4.

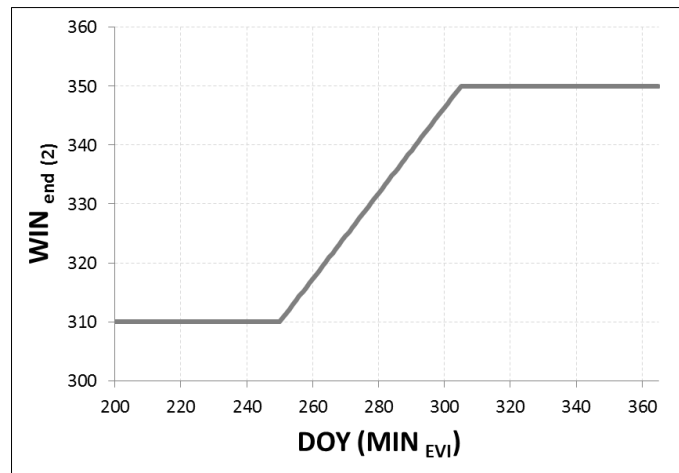


Figure 3-4 – Identification of WIN_{end(2)} as function of DOY (MIN_{EVI}) values.

Selection of minima

Once the limits for the crop establishment research window are defined, all the minima points that fall within this window are checked according to a “flatness” criteria. Previous experiment, not reported here, highlighted that “false” sowing date detections can take place in correspondence to random minima points generated due to noise in periods of several consecutive low EVI values. Once these points are detected and discarded the final estimation of the sowing date is considered as the MIN point with the earlier occurrence (lower DOY value). The flatness criteria is formalised by checking the EVI values neighbouring the detected minima points (+/- 2 composites). The minima points surrounded by values of similar magnitude ($\pm 5\%$) are filter out as following:

$$\begin{aligned} EVI(t-2) &= \pm 0.95 EVI(tMIN) \text{ and } EVI(t-1) = \pm 0.95 EVI(tMIN) \text{ and } EVI(t+1) \\ &= \pm 0.95 EVI(tMIN) \text{ and } EVI(t+2) = \pm 0.95 EVI(tMIN) \end{aligned}$$

(Eq.8)

3.2.5 Validation

Winter wheat mapping accuracy assessment

A dataset of Landsat satellite images was collected with the aim to retrieve reference information to be compared with maps of winter wheat derived from MODIS. Landsat images have a spatial resolution of 30m and are freely distributed from the United States Geological Survey (USGS) institution thanks to the Earth Explorer service catalog (<http://earthexplorer.usgs.gov>).

Landsat images were used for an expert based visual interpretation process aimed at characterize the land use presence for a sample of the MODIS 250m pixels. The visual interpretation of high resolution satellite images is a widely accepted practice in remote sensing, especially in the case of lacking of suitable in situ data to build reference datasets. This approach is particularly useful when applied to remote areas or on large scale areas (regional to continental), where collection of ground data becomes too expensive (Chen et al., 2002; Wulder and Franklin, 2003; Sun et al., 2012; Zhao et al., 2014; Azar et al., 2015).

According to land cover information, winter wheat is the only winter crop cultivated in the study area, then Landsat images were selected in the most suitable periods to distinguish winter crop from the other cultivated crops. Two Landsat images were chosen per year: (1) around the mid-April period, where winter wheat is close to the seasonal heading and summer crops are in bare soil condition or just at the beginning of the season, and (2) after the second half of July, where winter wheat is harvested and summer crops are in the heading phase.

For each year analyzed (see Table 3-2), a total of 300 pixels were randomly chosen from the MODIS 250m pixel grids covering the study area, afterwards pixels were labelled through a multi temporal visual interpretation process of Landsat images. During this process, randomly selected MODIS cells were overlapped to Landsat high resolution images displayed in form of RGB 4-3-2 combination (“R” – visible near infrared VNIR: 0.76 - 0.90 μm , “G” - red: 0.61 - 0.69 μm , “B” - green: 0.51 - 0.60 μm) these bands are combined to make a 'traditional' false color composite able to enhance vegetation covers. In the comparison with Landsat images each MODIS pixel was labelled as belonging to “winter wheat” or “other crop”. The random selection of MODIS pixel was repeated recursively until at least 50 MODIS pixels were labelled as winter wheat for each year. A final database of 1200 labelled MODIS pixels was used as reference dataset to evaluate detection performance. Validation accuracy metrics were then calculated in form of error matrix (Congalton, 1991; Brivio et al., 2006).

Table 3-2 – Summary of the Landsat images dataset

| DATA SET: | YEAR: | IMAGE: | DOY: | DATE: | CLOUD COVER %: |
|----------------|-------|-----------------------|------|--------|----------------|
| Landsat 7 ETM+ | 2003 | LE71960302003112EDC00 | 112 | 22-Apr | 2 |
| Landsat 7 ETM+ | 2003 | LE71960302003224EDC01 | 224 | 12-Aug | 1 |
| Landsat 7 ETM+ | 2006 | LE71960302006104ASN00 | 104 | 14-Apr | 0 |
| Landsat 7 ETM+ | 2006 | LE71960302006200ASN00 | 200 | 19-Jul | 15 |
| Landsat 7 ETM+ | 2009 | LE71960302009112ASN00 | 112 | 22-Apr | 2 |
| Landsat 7 ETM+ | 2009 | LE71960302009240ASN00 | 240 | 28-Aug | 2 |
| Landsat 7 ETM+ | 2012 | LE71960302012105ASN00 | 105 | 14-Apr | 18 |
| Landsat 7 ETM+ | 2012 | LE71960302012201ASN00 | 201 | 20-Jul | 23 |

An example on how winter wheat cultivated areas was identified from Landsat images is presented in Figure 3-5. In the RGB images, it is possible to appreciate that pixels labelled as “winter wheat” (highlighted in blue color) are red at DOY 105/2012 (mid-April) due to the presence of vegetation and they’re white in the image acquired at DOY 201/2012 (mid-July) due to a bare soil condition. Summer crops instead (highlighted in yellow color) presented the opposite behavior, with a bare soil or a flooded condition in mid-April and vegetation presence in mid-April.

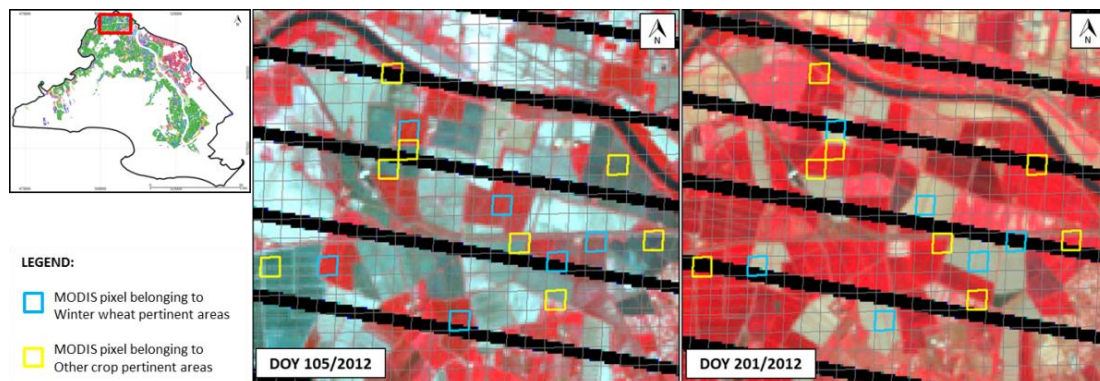


Figure 3-5 - Visual interpretation process of randomly selected MODIS pixel. Pixels were overlapped to RGB Landsat high resolution images and labelled as “winter wheat” (blue pixels) or “other crops” (yellow pixels). Landsat-7 images are in RGB false colour composite (bands: 4-3-2) representation.

Wheat sowing estimations assessment

A dataset of agro practices and phenological observations at field level was used to evaluate the accuracy of the algorithm in estimating winter wheat sowing occurrences. The field survey provides data on three different farms located in the middle of the *Parc Naturel Régional de Camargue* (see Figure 3-6), accounting a total of 1334 ha of the study area (4.6% of the 2011 park cultivated extent). The database provides crop typology and crop phenological information (including crop sowing dates) for 324 single fields in three consecutive years (2011, 2012 and 2013). Winter wheat fields in the three years are 83 (261 ha), 94 (343 ha) and 111 (363 ha) fields; a total of 288 fields (967 ha). Sowing dates information associated to winter wheat polygon fields were summarized to the MODIS 250 m spatial resolution through a majority GIS spatial analysis operation. The sowing dates were then associated to the nearest MODIS temporal composite. A comparison between field surveys information and the crop sowing occurrence estimations for the years 2011, 2012 and 2013 was finally done.

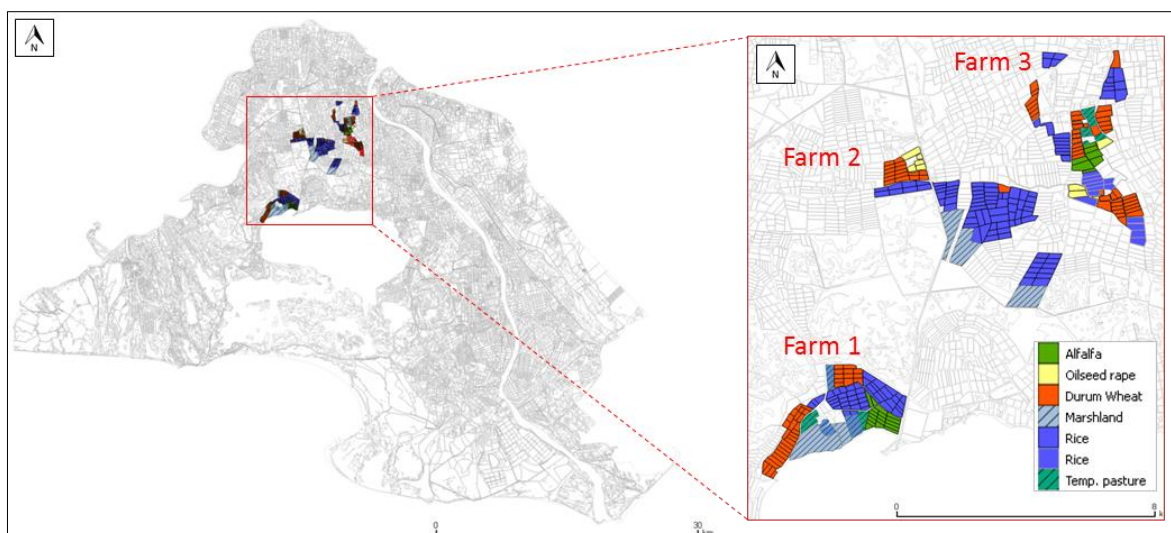


Figure 3-6 – Three farms in Camargue for which it was available a field survey database for the year 2011, 2012 and 2013. Farm 1: Mejanes, farm2: Megias, farm 3: Arnaudo. The 2013 land use informations are displayed.

3.2.6 Analysis of wheat sowing inter-annual variability

The final part of this study aimed to retrieve information to analyse the variability of winter wheat crop establishment during the period 2003 ÷ 2013. In this phase, the methodology for the time series analyses was applied for each year of the study period, retrieving 11 years sowing estimations. The results obtained were analysed with the specific aim to understand to which extent the inter-annual variability of sowing estimation is influenced by meteorological seasonality in comparison to other criteria that guide farmers' management decisions. According to agronomist (INRA personal communication) rain events are the main meteorological factors that influence the sowing practices. To perform this analysis, rainfall data were acquired from the meteorological station of Arles for the period 2003-2013 and analysed together with frequency distribution of sowing estimates.

3.3 Results

3.3.1 Effect of detection criteria on Camargue crops time series

Figure 3-7 reports EVI time series characterizing for the main crop cultivations in Camargue during 2006 and 2011. Only MODIS pixel time series for which corresponded at least 80% of land cover presence in the 2006 and 2011 land cover datasets were considered. Time is represented in the x-axis and ranges from DOY 177 of the year before the harvest to DOY 365 of the harvesting year. The y-axis (that crosses x-axis on Jan, 1st) reports EVI index values multiplied for the scale factor of 10000.

From Figure 3-7A, it is possible to note two main "humps" characterizing winter wheat time series. The first one appears at the beginning of August (first year) with EVI values near to 0.4, this is related to the summer crops that preceded winter wheat cultivations. The second peak instead, clearly indicate the highest vegetative phase period (crop heading) of winter wheat crops, that occurs around mid-April with EVI values greater than 0.4. From the figure it is possible to note an initial phase, from October to January, where the

EVI values are low and, this signal response occurs from the initial phase of the crop cycle (sowing) to the end of the vernalisation period. After that a rapid increase of EVI signal occurs, indicating the rapid growth of the crop (green-up) until reaching the heading point of the culture around April (crop heading and flowering). An EVI decrease occurs in May and June. It can be interpreted as the crop senescence stage. The collected winter wheat EVI profile characteristics were consistent with the crop's distinctive crop calendar. A marked standard deviation appears in all of the points that made the AVG time series (not highlighted in the figure). This variability is primarily due to differences in crop managements and environmental conditions but also to some noise due to mixture generated from the coarse spatial resolution of MODIS data (Boschetti et al., 2004) and also due to the geometries of acquisition (Duveiller et al., 2015). A qualitative analysis and observation on reliable winter wheat related time series, together with agronomical expertise and local crop calendar information led us to formulate and implement a set of rules for the identification of winter wheat crop cultivated areas and the crop establishment occurrence estimation.

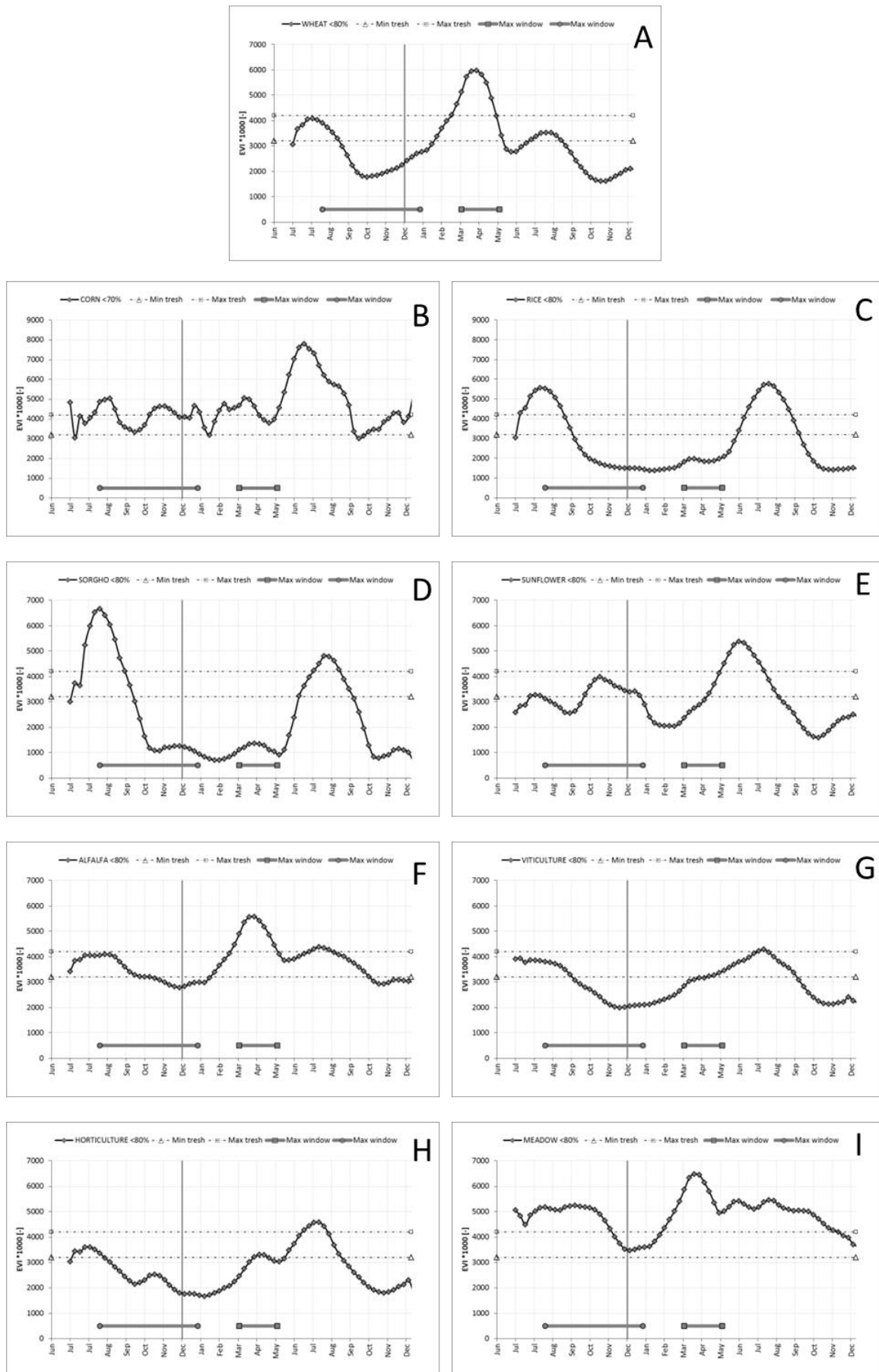


Figure 3-7 - Example of typical EVI temporal trend for principal crop categories in Camargue: winter wheat (A), CORN (B), RICE (C), SORGHO (D), SUNFLOWER (E), ALFALFA (F), VITICULTURE (G), HORTICULTURE (H) and MEADOW (I).

In Figure 3-7, panels from B to I show the EVI temporal trends for the main crop categories of Camargue. Each temporal trend can be compared with the rules we designed for the individuation of winter wheat crop: on the bottom of the panels two bars represent the crop establishment research window (left) and the heading research window (right) and the two horizontal dotted lines, represent the crop MIN threshold value (EVI=0.32) and the MAX threshold value (EVI=0.42).

The EVI time series of summer crop cultivations are presented in panel B (maize), C (rice), D (sorghum), E (sunflower), G (vineyard) and H (orchards). As they are summer crops or perennial trees, their crop headings occurs during the third quarter of the year and they can hardly be confused by the algorithm, in reason of a crop heading research window set during the second quarter of the year. Alfalfa cultivations (F) usually generate two or three periods of maximum development as a consequence of the seasonal cuts of the cultivations. One of these max periods occurs in correspondence of the defined winter wheat heading research window. Nevertheless minimum values are very close to the threshold and some alfalfa pixels could therefore refused. Moreover, the defined decreasing criteria allow avoiding commissions. Winter wheat cultivations have an EVI signal decreasing after the heading greater than alfalfa. Also meadow cultivations have an EVI time signature that can be confused with the one of winter wheat. Here, thanks to the imposed thresholds to the minima point, it is possible to separate the individuation of this culture from winter wheat.

3.3.2 Mapping results

Figure 3-8 reports an example of the outputs generated by the algorithm we designed. Figure 3-8A represents the map of the estimated winter wheat cultivated areas in Camargue during 2006. In the zoom box of Figure 3-8C it is possible to identify the algorithm's omissions, as well as the low level of commission errors. Figure 3-8B shows the map of winter wheat sowing date estimations, with reference to the 2006 harvest season (occurring in 2005). In the zoom image of Figure 3-8D, the sowing estimations are more visible. The winter wheat fields placed on the West size of Rhone river appears as sowed before the fields placed on the East side of the river. These mapping results put in evidence the contribution of remote sensing data in information retrieval in a spatial distributed manner.

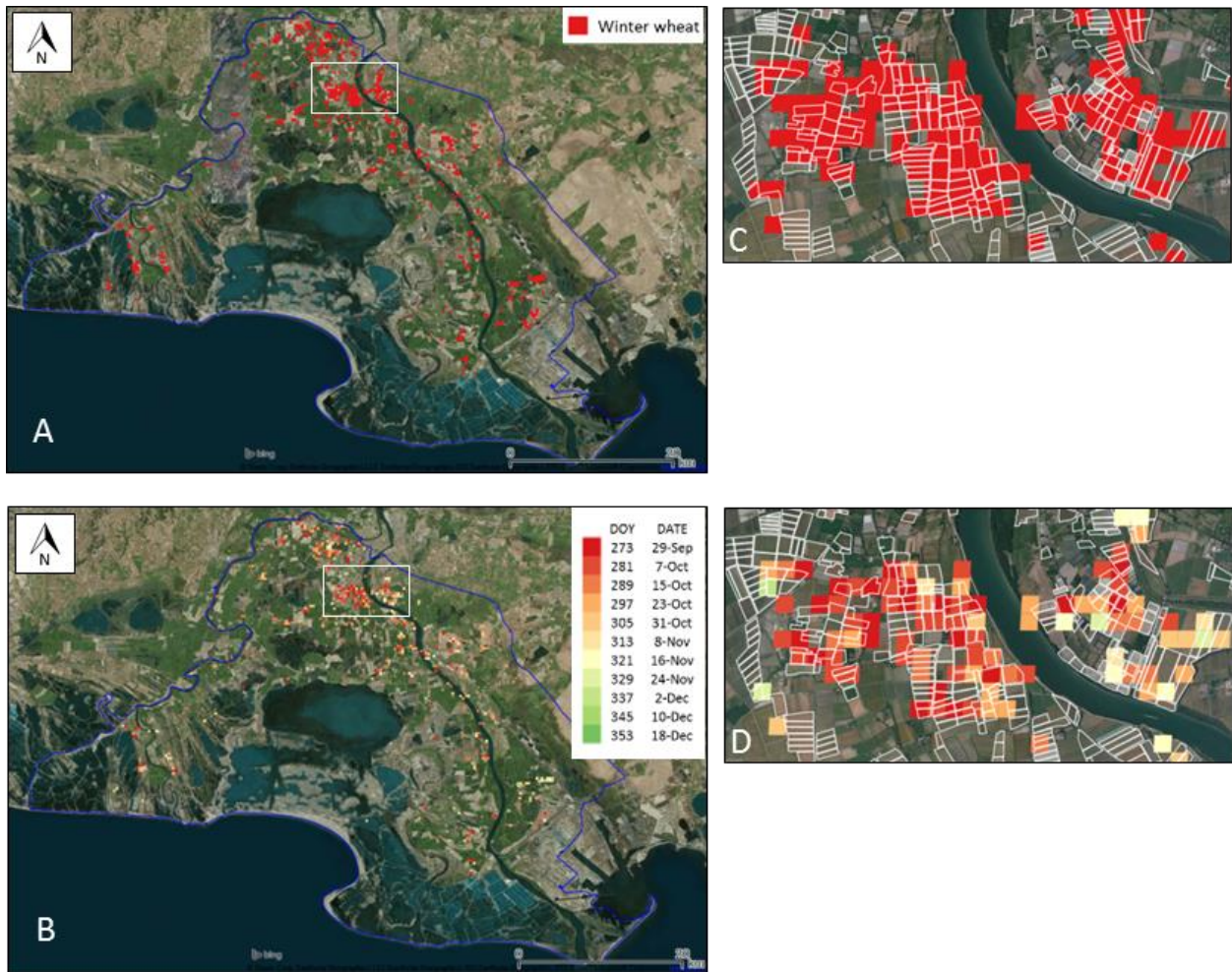


Figure 3-8 – Example of winter wheat mapping results obtained for the year 2006. (A) 2006 winter wheat detection map, the estimated wheat cultivated areas are shown in red. (B) 2006 winter wheat sowing date estimations map, the color ramp (red to green) indicates sowing estimations occurrences. (C) Zoom of the detection map. (D) Zoom on the sowing date estimations map. Figure C and D report in white color winter wheat polygons of the 2006 land use map of the Camargue region.

3.3.3 Validation of winter wheat detection

In Table 3-3 are reported the validation results concerning winter wheat cultivated areas detection, compared with the previously presented reference dataset. Validation's results are presented in the form of error matrices for the year 2003, 2006, 2009 and 2012 and all together. The error matrices showed good overall accuracy (OA) results, with annual values ranging from 84% (2006) to 93% (2009) and an average value of 89%. Satisfactory results were obtained from K coefficients (K), which are based on the difference between the actual agreement in the error matrix and the chance agreement. K estimators ranged from 54% (2006) and 76% (2009) with an average value of 62%. Predictions of winter wheat cultivated areas, reached very good results in terms of commission errors (3% to 19%) and acceptable results for omission errors (28% to 56%). Commissions were very low, with annual values between 3% (2012) and 19% (2003) and an overall value of 11%.

Table 3-3 – Comparison between Landsat visual interpretation based reference dataset and estimations based on MODIS EVI time series analyses. UA = user accuracy, PA = producer accuracy, CE = commission error, OE = omission error, OA = overall accuracy, K = Cohen’s k coefficient.

| | | | | | | | | | |
|------------------|----------|----------------|-------|------|--|------------------|------|------|------|
| Validation 2003: | | REFERENCE DATA | | | | Accuracies 2003: | | | |
| | | wheat | Other | tot. | | UA | PA | CE | OE |
| MODIS ESTIMATION | Wheat | 44 | 10 | 54 | | 0.81 | 0.66 | 0.19 | 0.34 |
| | No Wheat | 23 | 223 | 246 | | 0.91 | 0.96 | 0.09 | 0.04 |
| | tot. | 67 | 233 | 300 | | | | OA: | 0.89 |
| | | | | | | | | K: | 0.66 |
| Validation 2006: | | REFERENCE DATA | | | | Accuracies 2006: | | | |
| | | wheat | Other | tot. | | UA | PA | CE | OE |
| MODIS ESTIMATION | Wheat | 40 | 2 | 42 | | 0.95 | 0.47 | 0.05 | 0.53 |
| | No Wheat | 45 | 213 | 258 | | 0.83 | 0.99 | 0.17 | 0.01 |
| | tot. | 85 | 215 | 300 | | | | OA: | 0.84 |
| | | | | | | | | K: | 0.54 |
| Validation 2009: | | REFERENCE DATA | | | | Accuracies 2009: | | | |
| | | wheat | Other | tot. | | UA | PA | CE | OE |
| MODIS ESTIMATION | Wheat | 39 | 5 | 44 | | 0.89 | 0.72 | 0.11 | 0.28 |
| | No Wheat | 15 | 241 | 256 | | 0.94 | 0.98 | 0.06 | 0.02 |
| | tot. | 54 | 246 | 300 | | | | OA: | 0.93 |
| | | | | | | | | K: | 0.76 |
| Validation 2012: | | REFERENCE DATA | | | | Accuracies 2012: | | | |
| | | wheat | Other | tot. | | UA | PA | CE | OE |
| MODIS ESTIMATION | Wheat | 28 | 1 | 29 | | 0.97 | 0.44 | 0.03 | 0.56 |
| | No Wheat | 35 | 236 | 271 | | 0.87 | 1.00 | 0.13 | 0.00 |
| | tot. | 63 | 237 | 300 | | | | OA: | 0.88 |
| | | | | | | | | K: | 0.55 |
| Validation all: | | REFERENCE DATA | | | | Accuracies all: | | | |
| | | wheat | Other | tot. | | UA | PA | CE | OE |
| MODIS ESTIMATION | Wheat | 151 | 18 | 169 | | 0.89 | 0.56 | 0.11 | 0.44 |
| | No Wheat | 118 | 913 | 1031 | | 0.89 | 0.98 | 0.11 | 0.02 |
| | tot. | 269 | 931 | 1200 | | | | OA: | 0.89 |
| | | | | | | | | K: | 0.62 |

3.3.4 Validation of sowing date estimations

Figure 3-9 shows the results obtained during the validation of winter wheat sowing estimations. Estimations were compared with information provided by farmers in Camargue during the year 2011, 2012 and 2013. The scatter plot of Figure 3-9A shows the relation between observed and estimated data; most of the estimations fall within the error confidence interval of ± 16 days (see also Figure 3-9C). Underestimations tend to be produced for late sowing periods (from November 9th, DOY 313, onward), overestimations instead during the early sowing period (From September, 30th to November 9th, DOY 273 to 313). Analysis of residuals is presented in Figure 3-9B and C. In the histograms, zero class (no estimation error) were the most represented with 19% of the estimation falling in (27 on 142 comparisons). Figure 3-9C shows the distribution of residual errors according to the observed sowing date. The methodology produced the following indices of performance: RMSE = 21.5, MAE = 16.5, CRM = -0.002.

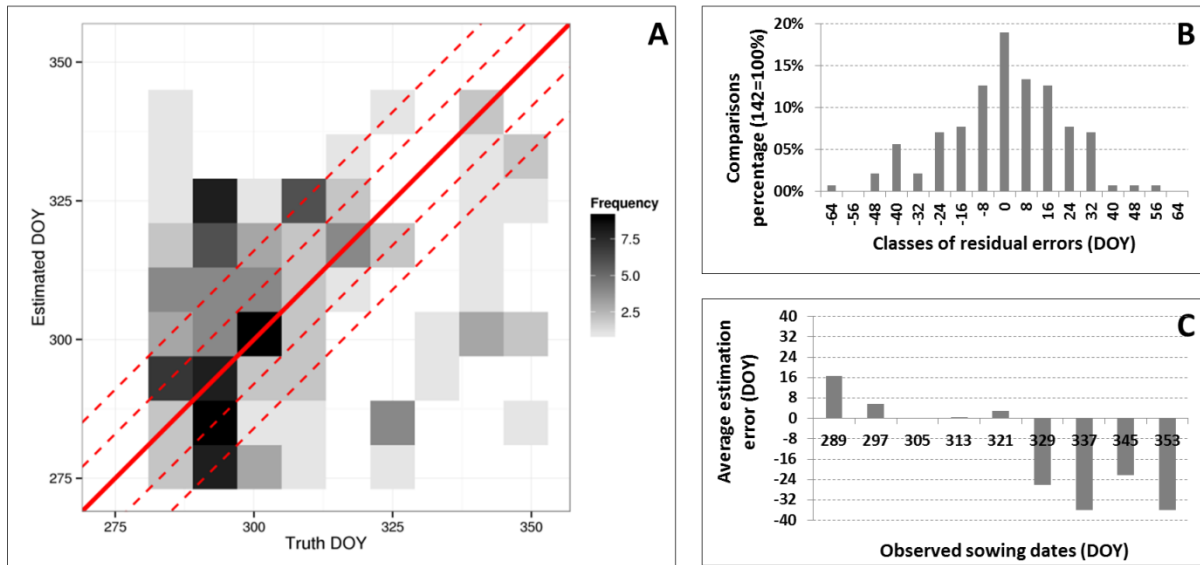
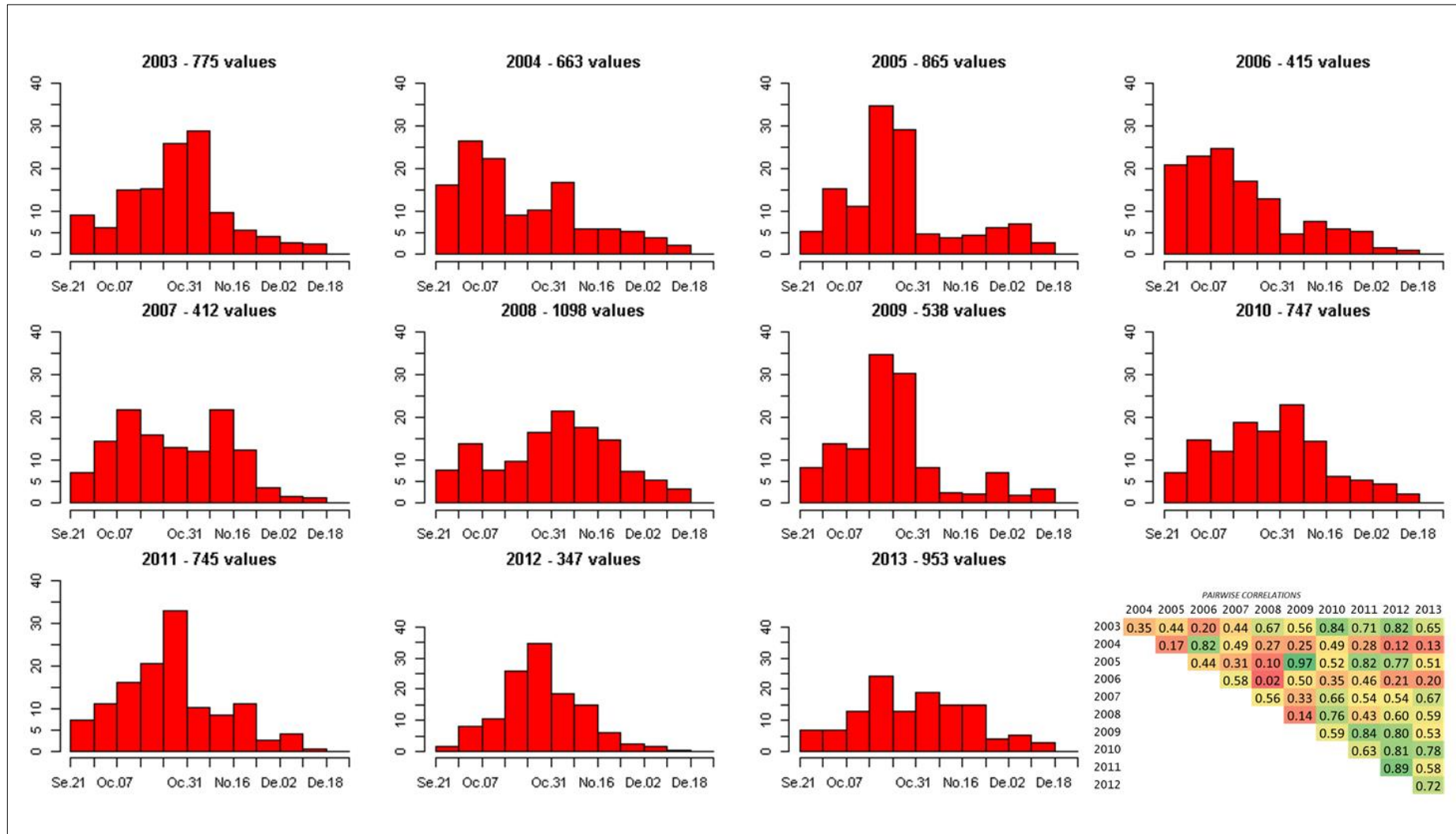


Figure 3-9 - Comparison between winter wheat sowing dates and crop sowing estimations for three farms during the year 2011, 2012 and 2013, n=142 comparisons. (A) Scatter plot among observed and estimated data, with 8-days and 16-days interval of confidence. In grey colours are reported the comparison's frequency. (B) Distribution of validation residual errors according to the MODIS time composite. (C) Distribution of residual errors according to the observed sowing date.

3.3.5 Intra-annual variability of winter wheat sowing

The methodology was applied for the years from 2003 to 2013 in order to analyse the inter-annual variability of crop sowing. Results are reported in the histograms of Figure 3-10. Similarities of the different years were quantitatively analysed through a pairwise correlations between seasonal estimation distribution frequencies. Results are reported in the lower right panel of Figure 3-10. From the figure it is possible to appreciate how similar seasons ($r = 0.82$) such as 2004 and 2006, characterized by an anticipated sowing, show estimations that mainly falls in the September-beginning of October period. For the seasons 2005, 2009, 2011 and 2012 instead (pairwise correlation greater or equal to 0.77), sowing estimations were mainly concentrated in October. In 2008, 2010 and 2013 sowing estimations (pairwise correlation greater or equal to 0.59) were almost equally distributed during the season. 2007 resulted to be a peculiar year with low similarity with respect to the others ($0.31 < r < 0.67$) because the sowing estimations showed two modes centred in the middle of October and the middle of November respectively.



1
2
3

Figure 3-10 - Inter-annual variability of crop sowing estimation for winter wheat in Camargue. Frequency histograms of the estimation values from the year 2003 to 2013. In the lower-right corner: pairwise correlations between estimations years.

3.3.6 Comparison with meteorological indicators

Figure 3-11 reports the results of the comparisons between winter wheat sowing estimations and the rainy events in Camargue for the period 2003-2013. Graphics reports with bins the frequency of sowing dates estimations between DOY 260 and DOY 360 (lower graphics) and with lines seasonal rainy events. Sowing seasons as for example the 2004's, 2006's or the 2012's shows an anticipation of the rainy events with respect to the periods of high concentration of sowing. On the contrary, in seasons such as the 2007's, the 2008's and the 2011's high concentrations of rainy events occur after periods of high concentration of sowing dates estimation. In season as the 2003's rainy events occurs both before and after the period where sowing estimations mainly fall. Comparison results put in evidence the absence of correlation between sowing estimations and seasonal rainy events. This lead to hypotise that the inter-annual variability in winter wheat sowing dates in Camargue cannot be described by the seasonal occurrence of rains. A possible hypothesis to explain such variability is that sowing dates could be much more influenced by the harvest date of the preceding crop and the soil moisture, that are related to rains but also to the date of last irrigations and to the wind.

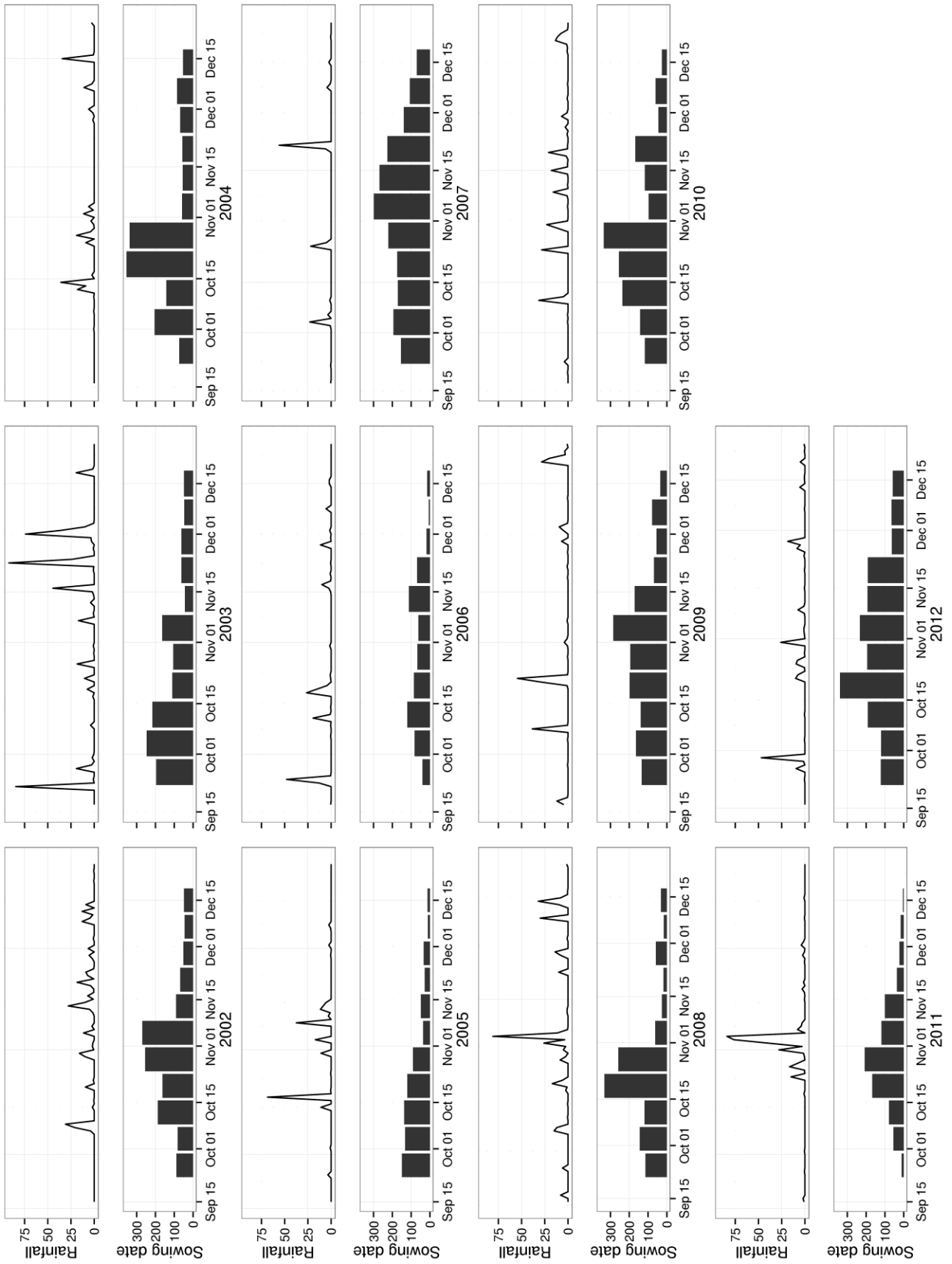


Figure 3-11 – Comparison between winter wheat sowing date estimations and rain meteorological data for the period 2003-2013 in Camargue.

3.4 Discussion and conclusions

On the basis of winter wheat time series analyses and thanks to agronomical expert knowledge, we designed and implemented a rule-based methodology able to automatically analyse MODIS satellite time series and to retrieve crop sowing occurrence information.

The first step of the procedure was dedicated to the detection of winter wheat cultivated areas. Results showed that winter wheat is accurately identified; with an omission error of 44% and a commission error of 11%, meaning that even if not all the fields of winter wheat were detected, but that the detected one have a very high probability to have been effectively cultivated in winter wheat. Taking into account that the proposed method aims to automatically identify a reliable sample of time series referred to winter wheat crop to further retrieve statistics of sowing date. On average 56% of our target crop in the study area was automatically detected. We consider these results satisfying due to the very low commission error. During the validation of sowing date estimations, the method we implemented was able to capture the seasonal variability of sowings with errors within an 8 days period in 45% cases and 16 days in 65% cases. Since we aimed to analyse seasonal variability of sowing date in a period that can usually last in 75 days, we considered our methodology as able to capture the sowing variability and we then extended it for a long term period to depict crop sowing inter-annual variability. We estimated winter sowing in Camargue from 2003 to 2013, observing seasons such the 2004 and 2006, where crop establishments were anticipated at the beginning of October and seasons such us the 2005, 2009 or 2011 where the establishment were shifted in the late October period. The sowing date occurrence estimations were not correlated to the seasonal rainy events; this led us to formulate the hypothesis that sowing dates could be much more influenced by the harvest date of the preceding crop and the soil moisture, that are related to rains but also to the date of last irrigations and to the wind.

Finally, we produced information that were not available for the considered study area and that represent a step forward with respect to the current available crop calendar information, that is static. This information is furthermore important for crop simulation modelling. They are particularly helpful in producing base-line scenario and to improve the simulation performances of cropping systems future scenarios.

Although the good result achievement in intra and inter-annual establishment variability estimation, some features of the methodology as well as critical issues have to be discussed. The method is mainly rule and threshold dependent and these features tend to increase robustness but reduce the exportability to study areas different from the one for which it has been calibrated. Despite this, it is important to highlight that only few contributions at the present are addressed in deriving winter wheat crop management or crop phenological information from the analyses of satellite time series and the present work represent a contribution in this direction.

The MODIS spatial and temporal resolutions demonstrated to be suitable to describe the crop establishment variability. With the perspective to investigate more detailed crop management information, time series with improved spatial and temporal resolution are needed. Improved spatial resolution will be important to decrease the rate of noise in time series due to mixed pixel contaminations. Improvements in time frequency resolution can contribute to identify new patterns in winter wheat time signatures to be associated with crop phenological occurrences. Time resolution improvements could be furthermore important to decrease the rate of noise affecting winter wheat time series at low magnitude levels during the autumn period. This kind of noise produce not meaningful features (i.e. false local minima point). Alternative strategies to analyse improved resolution time series, could be adopted using available high spatial-temporal resolution dataset (i.e. Sentinel-II data) with reference to actual or future analyses, while, with the purpose to enhance spatial and temporal resolution of already acquired archives (i.e. MODIS) the adoption of particular data processing techniques, such as the “data fusion” techniques appears indispensable to improve the spatio-temporal resolution of time series.

3.5 Annex 1: smoothing process

Figure 3-12 reports the steps to pre-process the EVI signal, from raw to smooth, and to retrieve the min and maxima points. The graphs show the condition of a rice pixel in Philippines (Lat. 15.69; Lon. 121.08) for the period 2007-2009 (77 composites). Vertical lines indicate the start/end of the analyzed year.

- Panel A, reports the raw EVI data in red;
- Panel B, shows the effect of spike detection and removal producing the blue line;
- Panel C, shows the effect of small drop detection and filling (orange lines with points);
- Panel D, shows the results of weighted smooth (green line) grey points on the X axis report data that have a low weight (0.0) corresponding to complete noisy data;
- Panel E, red and green filled points represent relative minima and maxima respectively detected by derivative analysis.

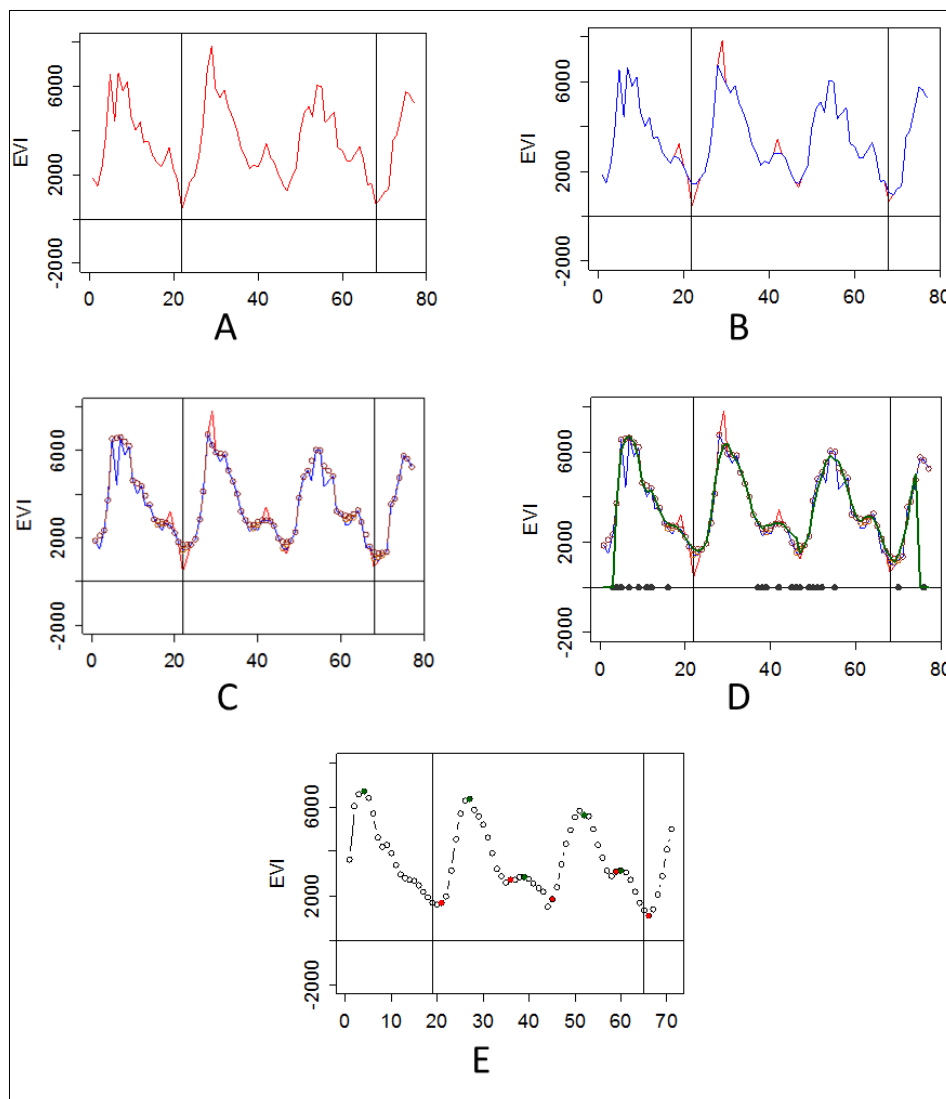


Figure 3-12 – Main steps during the preprocessing of the EVI time series. (A) EVI raw, (B) spike detection and removal, (C) small drops detection and gap filling, (D) weighted SAV-GOL smoothing, (E) local minima and maxima individuation

4 Analysis of crop changes through satellite time series for the definition of farm typologies in Camargue, France

4.1 Introduction

Farming systems are rapidly changing due to farmers' decisions in term of management, according to the evolution of different driving forces such as changes in the economic conditions (e.g. market and input cost changes), agro-policies (e.g. subsidies or environmental laws) or in the natural resources characteristics (e.g. water availability, soil quality and meteorological trends). Farmers yearly decide how to allocate fields to different crops with the purpose to optimize farm productivity and farm profitability. These decisions mainly concern crop management in reason of spatial distribution within the farmland and crop rotation strategies. These changes have direct impact on the performance of the farms, on the resources use efficiency and on environmental impacts. However, the farming systems of a given region are diverse and evolve in different direction according to the farmers choices. Therefore, to anticipate future changes and to drive adaptation, information is needed about the diversity of farming systems and their management. Usually this analysis is performed building a typology of farming systems able to summarize their diversity (Righi et al., 2011; Andersen et al., 2007). By farm typology we refer to a classification of farms according to their homogeneity regarding criteria related to performances (e.g. economic or environmental performances) and/or farm management practices (Andersen et al., 2007). The relevance of a farm typology depends on its ability to capture the differentiation of farming systems, showing a maximum amount of heterogeneity between the types, while obtaining maximum homogeneity within particular types (Kobrich et al., 2003). Typologies are used to assess and design farming policies taking into account the differences in farm management between different farm types (Andersen et al., 2004). They can also be used to target different innovations to different farm types (Lopez-Ridaura, 2011). Finally, they play a major role for up-scaling from farming systems analyses to regional level assessment.

Different methods have been used to design farm typologies. The first, most classical method, lies on statistical analyses of database in which different variables are describing the farming systems (Gebauer, 1987; Köbrich et al., 2003; Olaizola et al., 2008; Blazy et al., 2009). A second (often preferred) approach relies on expert knowledge (Rosenberg and Turvey., 1991; Iraizoz et al., 2007). The reason is that the former are characterized by objective reproducibility built in their statistical foundations and to the possibility of making an efficient use of information (Iraizoz et al., 2007; Righi et al., 2011). The majority of previous studies employed factorial analysis, multi-correspondence analyses or principal component

analyses to reduce the initial number of variables which are subsequently processed with hierarchical clustering techniques to group the farms (Poussin et al., 2008).

In the above mentioned approaches, all the farm typologies were defined on the basis of data describing the farms for single/specific year. They were therefore based on a “static picture” of the farming systems, taken at a given time, and in most cases without any information about the inter-annual variability of management and performances. However, the farmers are adapting their farm management to the variability of external factors (such as climate, prices of production and prices of inputs). They can also be engaged in a middle term trajectory of change (e.g. the conversion from traditional to organic farming) that implies an important redesign of their farming system and a long process of adaptation before reaching an (hypothetical) equilibrium (Bowler et al., 1996; Maton et al., 2005).

The specificity of the data needed to take into account inter-annual variability and farm trajectories to build a farm typology is that the data must be representative of farms of a region both in time and space. However, obtaining this type of data is a major issue because in most regions of the world no database, containing information related to a large sample of farms for a continuous series of years, exists. Traditional sources of information such as individual farmers’ interviews and census have two major drawbacks especially when applied for large areas analysis (i.e. regional level): they are expensive and time consuming to conduct, but can also be of low reliability or biased, especially when looking for data related to the past, as not all the farmers keep track of their practices in details.

In this perspective, a potential new source of information for these studies can rely on time series analysis of satellite images archives. Satellite data can provide spatially distributed information on large scale areas concerning vegetation (crop) presence, seasonal dynamics and conditions. Given this, multi-temporal analyses of satellite data could allow to describe some aspects of the variabilities in farming systems management. For example several applications have demonstrated that it is possible to provide spatial explicit information on crop intensity (Le li et al. 2014), or crop rotation (Manjunath et al., 2006; Conrad et al., 2011; Waldhoff et al., 2012; Osman et al., 2015).

In this framework, the research activities reported in this chapter have the objective to retrieve land use trajectories of the Camargue’s farms from satellite time series analyses. These informations are fundamental to build farm typologies on the base of time variability of land use. Despite, the monitoring of the land use change at the regional level with remote sensing is performed since several years (Weng et al., 2002; Shalabay et al., 2007; Nutini et al., 2013), the adoption of this approach to analyze farm management trajectories and to formulate hypotheses for different possible future scenarios is definitively innovative.

To perform this analysis, we designed a rule based methodology able to automatically detect winter and summer crops cultivation at farm level from the analyses of MODIS time series data. Crops identification were performed for the 2003-2013 time period, the retrieved database allowed to build land use

trajectories within each farm of the Camargue to be used as an indicator of farm management. Farm typologies were finally derived applying clustering method on this indicator.

The manuscript is structure as follow: in the first and second sections, the general context of this study together with its main objective and the study area are introduced. In the third section, the data handling and method developed are described. Results are presented in section four while section five is dedicated to the discussion of the results obtained.

4.2 Study area

This study focuses on the Camargue region, a delta area placed in South-Eastern France. This region has been labelled as a Biosphere Reserve (Man and Biosphere Program of UNESCO) since 1977. Being recognized for the exceptional environment, agricultural activities also play an important role, particularly in economy and on the environmental equilibria of the region. The Regional Natural Park of Camargue (PNRC) covers notably the land enclosing the two branches of the Rhone river over an extension of almost 112.000 ha (Figure 4-1). According the land use dataset provided by the PNRC for 2011, 25% of this area is occupied by arable land, nearly 29.000 ha. Rice and winter wheat are here the most cultivated crops, having a complementary role in terms of agronomy and crop rotation. Rice and winter wheat account almost two thirds of the total arable land (19.000 ha). Other (minor) cultivated crops in Camargue are alfalfa, sunflower, maize, soybean, oil seed rape and sorghum. About 340 farms are present on over 62.000 ha of this territory. Many of these include activities linked to farming (such as hunting or tourism). About 200 farms are identified as rice producer accounting for almost 44.000 ha of this area. The average total farm surface is 240 ha with an average arable land of 130 ha. Rice farmers usually grow rice and winter wheat in rotation, what allows maintaining a low soil salinity levels (through the inundation of rice) and contribute to weed control through the alternation of dry and irrigated crops. The balance between rice and winter wheat fields is mainly driven by the prices of the two commodities as well as by the European subsidies: when rice price and subsidies are favourable, farmers go toward rice monoculture. Otherwise when rice is not profitable, farmers increase wheat surface and other kind of summer crops are considered instead of rice. Other (low represented) cultivation schemes in Camargue are due to the presence of livestock and consist in an increase of forage cultivations (mainly alfalfa, grown for three consecutively years).

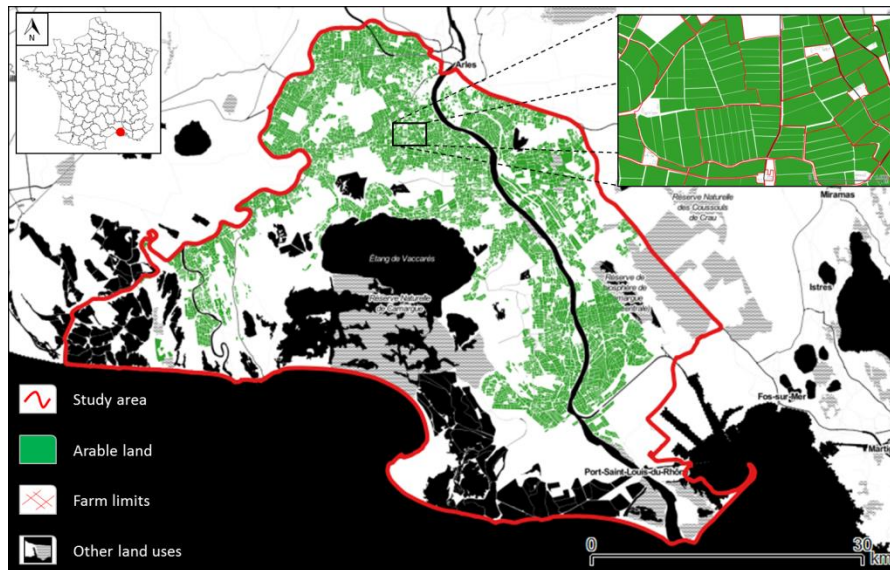


Figure 4-1 - The Camargue study area. In red colour: PNRC boundaries. In green colour: arable land surface, according 2011 PNRC land use dataset. In the zoom on the upper-right corner it is possible to appreciate farm limits and single fields boundaries.

4.3 Material and Methods

The methodological framework followed during this work is presented in Figure 4-2. In an initial “developing” phase, multi-years EVI time series were produced from MODIS satellite images archives and analysed in order to design a rule based detection method to automatically identify the presence of winter and summer crop cultivations. The “validation” phase allowed to assess method performance. Crop detection at full resolution (250m pixel scale) was summarised to “homogeneously cropped areas units” (group of fields in the same farm managed in the same way) and then compared to reference information extracted by high resolution satellite data (Landsat Image, 30 m resolution) interpretation.

Once the detection method was validated and considered having satisfying performance, the amount of estimated summer and winter crop for each farm was assessed for the period 2003-2013. This information allowed to derive land use trajectories at farm scale. Farm trajectories were clustered with the aim to define farm management typologies and identify the farms belonging to these.

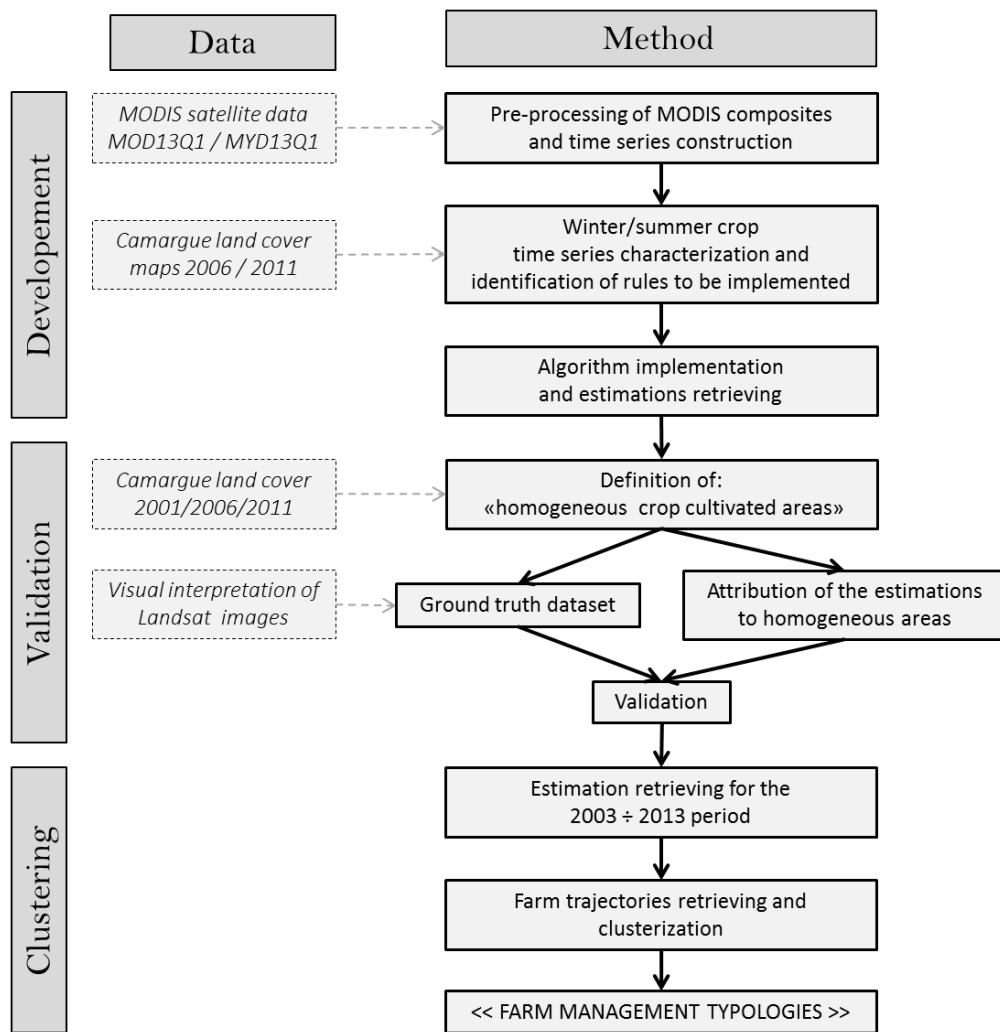


Figure 4-2 – Flow chart representing the data involved in the work and the main methodological steps identified to retrieve main farm management typologies in Camargue.

4.3.1 Development phase

MODIS satellite data

Moderate Resolution Imaging Spectroradiometer (MODIS) sensor data, on-board on Terra and Aqua satellites were used to produce satellite time series of the Enhanced Vegetation Index (EVI - Huete et al., 2002). Among vegetation-related spectral indices, EVI is frequently taken into consideration to observe vegetation dynamics by means of moderate resolution time series (Wardlow et al., 2007; Arvor et al., 2011; Li et al., 2014). It is well accepted that the intensity of EVI within a season can reflect the areal coverage of a given crop (Pan et al., 2012), for this reason the exploitation of vegetation indices (VI) time series is a common approach in the remote sensing discipline for agricultural monitoring purposes (Sakamoto et al., 2005; Atzberger et al., 2011; Eerens et al., 2014).

We exploited MOD13Q1 (Terra satellite) and MYD13Q1 (Aqua satellite) 250 m resolution vegetation indices products; in the production atmospheric correction for gases, thin cirrus, clouds and aerosols are implemented (Vermote and Vermulen, 1999). These data are 16-days composite products, it means that given the daily revisit time of satellites, a 16-days images composite is generated through a multi-step process called Maximum Compositing Value – MCV (Holben and Brent, 1986) that eliminates low quality observations and then select for each image the pixel the less contaminated by clouds and with the higher value in the 16-days period. For both sensors, these data are provided with an 8 days nominal shift (Terra 16-day composites start at the day of the year (DOY) 001, while the Aqua compositing period starts at DOY 009), once combined they can provide EVI data values with an improved temporal frequency of eight days. MODIS products are organized in a “tile” system with the sinusoidal projection grid; each tile covers an area of 1200 km by 1200 km. For this study we downloaded all the available MOD13Q1 and MYD13Q1 data from the Day of the Year (DOY) 177 of 2002 (end of June), to the DOY 361 of 2013 (end of December). A total of 484 MODIS MOD/MYD 13Q1 image products were collected for the reference grid tile h18v04 and resized to overlap the study area extension.

Time series production and smoothing

A pre-processing procedure of MOD13Q1 and MYD13Q1 composite products was done in order to produce time series of EVI vegetation index and remove residual noise (mainly due to cloud contamination). We produced time series by extracting the EVI information contained in each composite product during an 18-month time window starting from DOY 177, before the reference year (harvesting season), and ending in DOY 361 of the reference year. Once extracted, EVI information was stacked into a multi-temporal raster array of totally 70 bands, according to the chronological criteria. The reference years in time series production correspond to the harvesting season (June-July for winter crop and September-October for summer crop) for the period 2003 to 2013 (11 years). All the multi-temporal EVI data were finally resized for a region of approximately 60 km per 45 km (250 by 190 MODIS pixels grid) covering the study area of

the PNRC. We then smoothed the EVI time series to reduce the residual rate of noise that still affect the data after the compositing procedure (Pettorelli et al., 2005). A weighted Savitzky-Golay (SAV-GOL - Savitzky and Golay, 1964) approach was applied, as described in section 2.3.1. of chapter 2.

Characterization of summer and winter crops time signatures

The land use polygon datasets “*Occupation du sol du Parc Natural Regional du Camargue*”, were available for the reference year 2001, 2006 and 2011. These products result from aerial photo-interpretation activities and field work for validation, and describe the land uses, including the different crop observed (e.g. rice, durum wheat, alfalfa). These datasets were provided in France Lambert-93 geographic projection, with a representation scale of 1:5,000. Camargue land use datasets for the year 2006 and 2011 were used as reference information to analyse the temporal behaviour of EVI (extracted by MODIS) in correspondence of winter and summer crops of the study area. A zonal statistic procedure between vectorial data (land use polygon) and 250 m raster grid was performed to estimate the percentage of winter and summer cultivations for each MODIS pixel in the reference years. Those MODIS grid pixels that were at least 80% covered by winter or summer crops in the 2006 and 2011 land covers were selected. Their corresponding EVI time series, considered as high confidence for winter and summer crop cultivations, were analysed to derive a set of rules for the automatic detection of winter or summer crop cultivated area. Figure 4-3 presents the average EVI time series of high confidence pixel’s time series selected for winter and summer crops during 2006 and 2011 years.

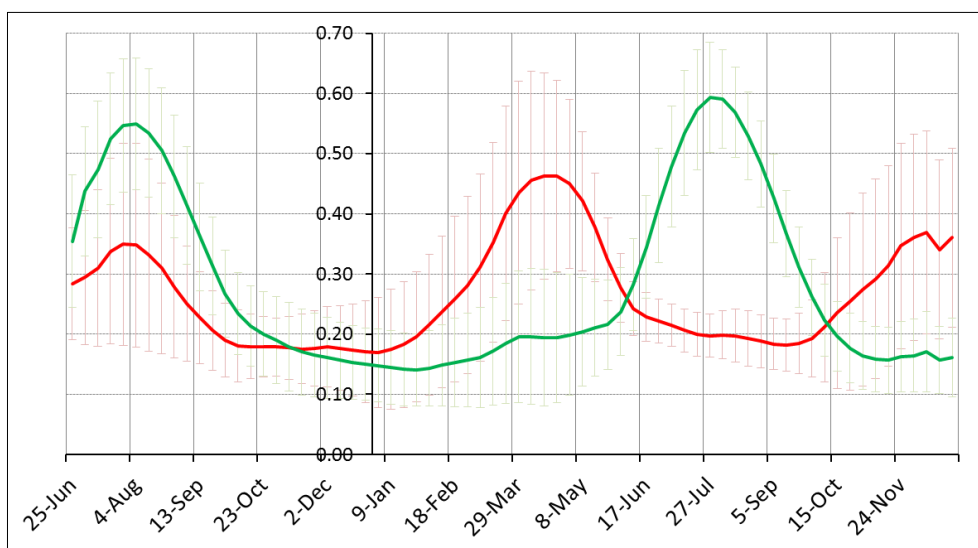


Figure 4-3 – Time series of MODIS 250m EVI index for winter and summer crops for the period DOY 177, before the harvest seasons, to DOY 365 of the harvesting (reference) season. The red (181 pixels) and green (3446 pixels) series represent the winter and summer crop respectively.

The average time series of winter and summer crops are mainly characterised by winter wheat and rice cultivations respectively. These two crops cover 85% of the total arable lands in Camargue. The average time series of winter crops (Figure 4-3, red temporal series) is characterized by an increase of EVI values during the January - March period (vegetative phase). The heading periods occurs in mid-April, and EVI

decrease in May up to late July (crop senescence). Summer crops instead (Figure 4-3, green temporal series), begin the vegetative growth in April. EVI values rapidly increase until the beginning of August (crop heading). The index decreasing then takes place until mid-October, the usual crop harvest period of rice in Camargue.

Time series standard deviations of winter crops are greater than the one of summer crops. This is mainly due by the reduced and more scattered surface of winter crops on the study area. This feature considering the coarse spatial resolution of MODIS data, tend to introduce noise in the time series due to mixed pixel situations. The 250 m pixel size is greater than winter crop field size. However, another important aspect is related to the diversity in management of winter wheat in particular in relation to the sowing dates (See Chapter 2). The qualitative analyses of reliable time series, together with agronomical expertise and local crop calendar information led to formulate a set of rules to be implemented in an algorithm for the automatic identification of winter and summer crop cultivated areas.

Definition of rules for the crop automatic detection

The algorithms were developed on the basis of an already existing approach called “PhenoRice” (Manfron et al., 2012; Nelson et al., 2014; Boschetti et al., 2015) aimed to estimate paddy rice field presence and rice phenological stages from the analysis of satellite time series. For summer crops, the rules of PhenoRice were modified to take into account specific crop calendar of Camargue. For winter crops, the rules implemented in this algorithm were designed based on (i) the derived pixels with high confidence about winter crop cultivation presence in 2006 and 2011, (ii) agronomical expert knowledge and (iii) considering the crop calendar for the study area. The algorithm involves three different steps detailed in the following paragraphs.

Step 1: Individuation of time series local maxima and minima points

We calculated the first derivative from every smoothed EVI time series. The derivatives allowed to identify automatically all the local minima (MIN, where the first derivative changes from negative to positive) and local maxima (MAX, where the first derivative changes from positive to negative) points (Eq. 1 and 2).

$$MINrel_{(t)} = EVI'_{(t-1)} < 0 \ \& \ EVI'_{(t+1)} > 0 \quad (Eq.1)$$

$$MAXrel_{(t)} = EVI'_{(t-1)} > 0 \ \& \ EVI'_{(t+1)} < 0 \quad (Eq.2)$$

Step 2: Selection of reliable crop related maxima and minima points

Every identified local MIN and MAX point was subjected to a series of checks in order to identify the ones related to crop cultivation (here after defined as “crop related MIN point” and “crop related MAX point”). In literature, these crop related MIN and Max points are respectively reported as indicators of the start of the active growth cycle (Sakamoto et al., 2005; Lu et al., 2014) and of the crop “heading” period (Curnel et al., 2008; Boschetti et al., 2009; Atzberger et al., 2013).

Crop related MIN points were identified as the inflection points followed by a sequence of at least three positive derivatives in a (time series) temporal window of five values. This is an inflection-based criteria defined to depict the growing phase succeeding the establishment. A second threshold-based rule (Zhou et al., 2003; Delbart et al., 2006; De Beurs and Henebry, 2010) concerned the exclusion of the minima points with high and unrealistic EVI values above 0.25 for summer crops and 0.32 for winter crops.

Crop related MAX-points (considered as representative of the crop heading phase) were identified as the inflection points that occurred after a rapid growth period and followed by the beginning of a senescence process. The rapid growth was defined in the time series as a sequence of at least three positive derivative (time series) points in a temporal window of five, before the relative maxima point. The senescence period were defined using two criteria: (i) a sequence of at least three negative derivative (time series) points in a temporal window of five, and (ii) a decrease of one third of the MAX-EVI value within a temporal window of 6 MODIS composites (48 days) occurring after the relative maxima point. The relative maxima points with EVI value lower than 0.5 (for summer crops) and 0.42 (for winter crops) or the one that do not respect the above described criteria were excluded.

Step 3: Estimation of winter and summer crop cultivation presence

We then applied a second set of rules that associate mutual relation between occurrence of crop related MIN and MAX points, identified during step 2, to individuate winter and summer crop.

We identified a winter crop cultivation for those time series characterized by the presence of a crop related maxima point (crop heading) occurring in the second quarter of the year (from the end of March -DOY 89- to the beginning of June -DOY 153-), together with the presence of a crop related MIN-point at a distance from the heading, set from DOYMAX minus 224 DOY's (28 time series composites) to DOYMAX minus 128 DOY's (16 time series composites). This criteria was established on the basis of the average length of the winter wheat cycle in the study area.

Similarly, summer crops were identified selecting the crop related maxima point occurring in the third quarter of the year (from DOY 185, beginning of July to DOY 273 end of September) for which it was possible to associate a crop related MIN-point over a time window starting from DOYMAX minus 120 DOY's (15 time series composites) and ending 48 DOY's before DOYMAX minus (6 time series composites 48 DOY's).

The output of the algorithm is a thematic map, consisting in a geo-referenced raster file of 250 by 190 pixels, of 250 m pixel size. Each pixel is labelled with one of the following thematic information: "detection of summer crop cultivation", "detection of winter crop cultivation" and "no cultivations detected".

4.3.2 Validation phase

Ground truth validation data

Ground truth information to validate the estimations produced at MODIS pixel scale (250m pixel size) was collected through an expert-base visual interpretation of Landsat (30m spatial resolution) satellite images. The visual interpretation of high resolution satellite images is a widely accepted practice in remote sensing, especially in the case of lacking of suitable in situ data to build reference datasets (Chen et al., 2002; Wulder and Frankin, 2003; Sun et al., 2012; Zhao et al., 2014; Azar et al., 2015).

A total of eight Landsat-7 satellite images were selected from the Earth Explorer service catalogue of the United States Geological Survey (USGS) (<http://earthexplorer.usgs.gov>) (Table 1).

Table 4-1 – List of the selected Landsat images for the validation process.

| DATA SET: | YEAR: | IMAGE: | DOY: |
|----------------|-------|-----------------------|------|
| Landsat 7 ETM+ | 2003 | LE71960302003112EDC00 | 112 |
| Landsat 7 ETM+ | 2003 | LE71960302003224EDC01 | 224 |
| Landsat 7 ETM+ | 2006 | LE71960302006104ASN00 | 104 |
| Landsat 7 ETM+ | 2006 | LE71960302006200ASN00 | 200 |
| Landsat 7 ETM+ | 2009 | LE71960302009112ASN00 | 112 |
| Landsat 7 ETM+ | 2009 | LE71960302009240ASN00 | 240 |
| Landsat 7 ETM+ | 2012 | LE71960302012105ASN00 | 105 |
| Landsat 7 ETM+ | 2012 | LE71960302012201ASN00 | 201 |

Four different years, 2003, 2006, 2009 and 2012, were identified to perform the validation. For each of those years we selected two Landsat images: the first chosen around the 15th April and the second around the 15th of July. These periods were chosen because considered the most suitable from a remote sensing point of view for visually distinguish summer crops from winter crops. While in mid-April summer crops are at the beginning of the crop cycle and winter crops are close to the heading period, in mid-July summer crops are close to the heading phase and winter crops fields are harvested. During the visual interpretation process, the expert used an RGB false colour combination (“R” - VNIR: 0.76 ÷ 0.90 µm - B4; “G” - red: 0.61 ÷ 0.69 µm - B3; “B” - green: 0.51 ÷ 0.60 µm – B2) that is proved to be useful to enhance soils vegetation cover (http://gdsc.nlr.nl/gdsc/en/information/earth_observation/band_combination). Ground truth pixels were labelled by experts as belonging to “winter crop cultivation” or “summer crop cultivation”. This validation step represented only a preliminary validation stage. The definitive validation was conducted after the representation of estimation on a most reliable representation scale (see next section).

Spatial unit for thematic map production and validation

Scale problem between moderate resolution satellite images (MODIS 250m) and agricultural targets (average crop field sizes and fields fragmentation) can produce noise in remote sensing data and reduce the accuracy of thematic products also known as “low resolution bias” (Boschetti et al., 2004; Moulin et al.,

2009). Figure 4-4 provides an example of this problem. Preliminary analysis (not reported) demonstrated that the algorithm identified well the presence of summer or winter crops in situations where time series belonged to MODIS pixels with high and homogeneous presence of crop fields (i.e. Fig. 4A and 4C) and tended to produce omissions for pixel with mixed land use. In the latter condition signals are unclear and affected by noise (i.e. Fig. 4B and 4D) and, because of this, the algorithm (conservatively) omits to classify that time series.

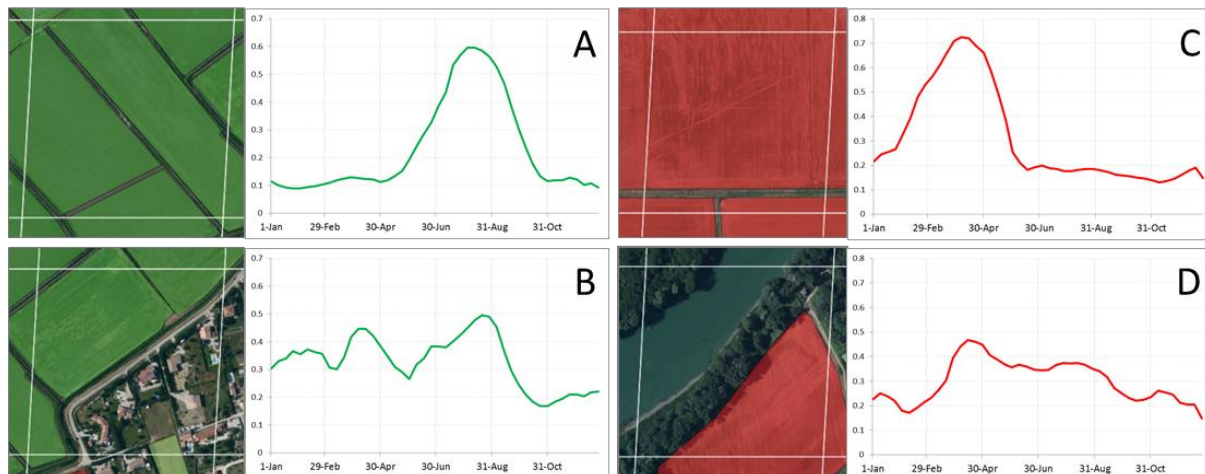


Figure 4-4 - Time series of summer crops (green color, fig. 4A and 4B) and winter crops (red color, fig. 4C and 4D) in different pixel purity conditions (high homogeneity, fig. 4A and 4C and mixture condition on fig. 4B and 4D). Green colored fields represent single fields for which land use datasets attributed summer crop cultivations presence and red colored fields related where it was for winter crop presence. The white grid represents the MODIS 250m pixel resolution for which time series was retrieved.

Due to the fact that we targeted to analyse the land use trajectories at the farm level, this require to obtain as much as possible the information for all the fields of a given farm. To produce more representative estimations, we decided to use an intermediate level of analysis, called “homogeneously cropped area”. Indeed, a peculiarity of Camargue’s cropping systems is the homogeneous management of group of fields within each farm. While the average farm area is large (about 240 ha farm surface and 130 ha of arable land), the fields in Camargue are strongly fragmented, with an average area around 2.5ha. This is mainly due to the presence of strong wind and the need for rice field to have a homogenous level of water (in large field, the wind would push the water on one side of the field, with therefore different levels of water depending on the wind direction). However, to simplify their work and notably the water management, the farmers tend to homogeneously manage groups of nearby fields within their farm.

Given this, we decided to perform a GIS analyses on 2001, 2006, 2011 Camargue land use with the aim to identify within each farm groups of neighbouring fields with the same land use, called “homogeneously cropped areas” (hereafter indicated as HCA). The criteria to identify them were the following:

- i. Fields in the HCA must have the same land use in the 2001, 2006 and 2011 years;
- ii. Fields in the HCA must belong to the same farm;
- iii. Only neighbouring fields belonged to the defined HCA.

A total of 891 HCA were identified. These spatial units were cover 19.300 ha (the 67% of the PNRC arable land). The average size of the HCA was 21.3 ha area, corresponding to the area of 6.8 MODIS pixels. 85% of the 180 farms had at least two HCA and in general about five homogeneous areas were found for each farm.

Spatial analysis at HCA level

We synthesized the crop detection from MODIS images at the level of HCA spatial unit by considering a majority criteria. For example, if within one homogeneous unit there were 7 pixels labelled as summer crop and 2 as winter crops, the HCA was assigned to summer crop class. When for a HCA the algorithm doesn't performed estimations or performed an equal number of winter crop and summer crop estimations, we defined the unit as "un-classified". This operation allowed to overcome commission/omissions error typical of moderate resolution data. Figure 4-5 presents the example of two farms (Farm ID 1605 and farm ID 221 in figure) for which each field limit was known (Figure 4-5A, in yellow). The field grouping operation allowed to identify the farm HCA (blue polygon in Figure 4-5B). Time series of MODIS satellite data were then analysed to retrieve estimations of winter or summer crop cultivated areas at a 250m MODIS pixel scale (Figure 4-5C, red and green pixels). Estimations were then aggregated at the HCA scale (Figure 4-5 D, red and green pixels homogeneous areas).



Figure 4-5 - Homogeneously cultivated areas (HCA) winter and summer crop estimations. A) - Farms limit (white color; ID 1605 and ID 221) and fields border (yellow color); B) identification of all the HCA inside the farm (blue colored areas) and MODIS 250m pixel grid (white lines); C) Time series based estimations of winter (red) and summer (green) crop; D) The final estimation representation at HCA level for each farm.

For the final validation, 100 HCA were chosen for each validation year through a stratified random sampling procedure (70% summer crops and 30% winter crops) and then visually labelled following the procedure described in section 3.2.1. A final database of 400 HCA labelled as belonging to “winter crop cultivation” or “summer crop cultivation” was produced.

Figure 4-6 presents an example of Landsat image on which the HCA areas have been overlapped. In the RGB images areas labelled as “winter crop cultivated areas” have a blue border. This corresponds to reddish areas at DOY 112/2009 (end-April) due to the presence of vegetation (while summer crop are not sown yet) and grayish colored at DOY 208/2009 (mid-July) as the crop has been harvested. Summer crop cultivated areas instead, (identified with a yellow border) showed the opposite behavior: a bare soil or a flooded condition in mid-April period (grayish or dark colors) and vegetation presence in mid-July period (reddish color).

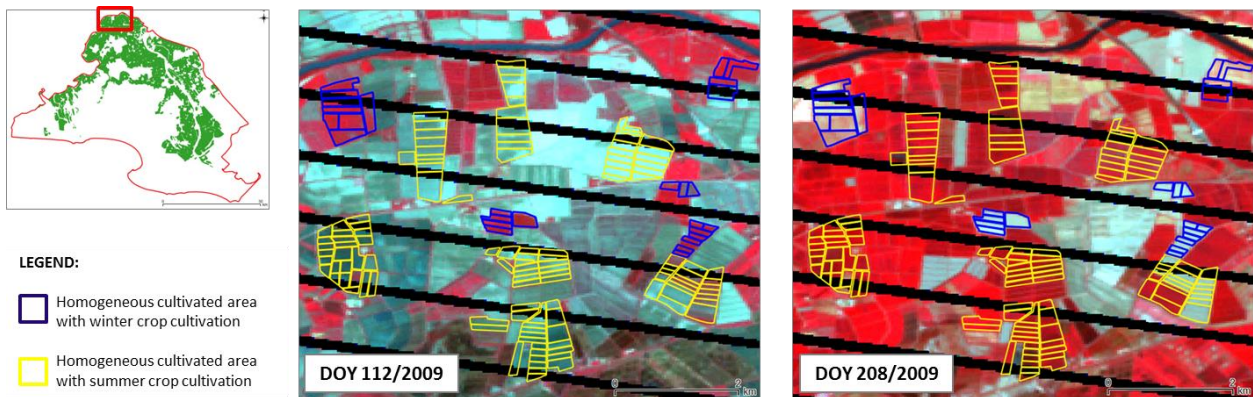


Figure 4-6 - Production of the reference dataset by visual interpretation of homogeneous cultivated areas (HCA). Landsat-7 images are in RGB false color composite (4-3-2) representation: spring and summer acquisition is reported in left and right panel respectively.

Algorithm validation

The validation was finally conducted comparing the visual interpretation of HCA against the estimation synthesis retrieved on this spatial unit. The validation was conducted in form of error matrix (Congalton, 1991; Brivio et al., 2006). Table 4-2 shows the accuracy metrics that have been evaluated.

Table 4-2 – Description of the accuracy metrics evaluated from the confusion matrix.

| METRIC | ACRONIM | DESCRIPTION |
|---------------------|---------|--|
| Overall accuracy | OA | ratio between the total agreements and the total sample on the testing set |
| User Accuracy | UA | ratio of the total right predictions of the class on the total pixel assigned at the class |
| Producer Accuracy | PA | ratio of the total right predictions of the class on the total estimation produced at the class |
| Commission Error | CE | ratio of failed prediction of the classification on the total prediction |
| Omission Error | OE | amount of the target class not detected on the total of this class |
| Cohen's coefficient | K | relationship between “observed agreement”(OA), and “expected random agreement” that is the percentage of classification that can be expected between the random coincidences from the two maps |

In particular, the Cohen’s coefficient (k) can be considered as a measure of agreement between model predictions and reality (Congalton, 1991), the estimator determines if the values contained in the error matrix represent a result significantly better than a casually random one (Jensen, 1996).

4.3.3 Farm clustering phase

Farm selection

Detailed farm limits information of the study area was available in a GIS polygons format from the French national agency for the payment of the subsidies from the European Common Agricultural Policy. We retrieved for each farm, the total amount of arable land occupied by summer and winter crop for the 11 years of the analysis. We selected the farms with at least an arable land surface above 25 ha and for which the sum of the HCA identified within the farm boundary represented at least the 70% of the total arable land. This allowed to discard farms with a high level of fragmentation that determines i) uncertainty in the classification predictions (targets too small compared to size of the Modis pixel) or ii) a high level of missing estimations (the land use was not retrieved for the majority of the farm's fields). The adoption of these criteria led to select a sample of 140 farms. These samples represents 50% and 75% of the total and rice producer farmers respectively. On the basis of the 2011 land use dataset, the selected farms cover a total of 32.000 ha of which 21.500 ha of arable land that correspond to the 29% of the PNRC entire surface and 75% of the cultivated areas.

Clustering of farm trajectories and management typology definition

We applied a clustering procedure on the dataset of 140 farms to identify groups of farms that share the same land use trajectories. For each farm the input dataset correspond to 11 years of winter and summer crop cultivated areas percentage in the farm. In addition an evaluation of the uncertainty in the farm labelling (percentage of crop estimation) was calculated considering the percentage of undetected area for each farm. These three informations are then used to define the "farm trajectories".

A hierarchical clustering procedure, with binary split at each hierarchic level was applied using the data mining software WEKA (Hall et al., 2009). The sample clustering membership was attributed according the major consensus of three different clustering algorithms: Expectation Maximization, K-means, Density based (k-means with local density based seed initialization). Splits were stopped at a threshold value of maximum 35 samples. The clusterization process was weighted according to the uncertainty of the estimations. Once farm management typologies (clusters) were retrieved, we described and analysed them according the main farm management drivers of the study area, identified by agronomy experts.

4.4 Results

4.4.1 Crop detection accuracy

Table 4-3 reports the results of the validation process regarding the accuracy of the detection of the winter and summer crops. Results are reported as error matrix comparison between reference and estimated dataset.

Table 4-3 - Error matrices between reference and estimated data for 400 homogeneous cultivated spatial units. Validation results are reported individually for each year (2003, 2006, 2009, and 2012) and also all together. Results are reported as sums of areas (in hectares). UA: user accuracy, PA: producer accuracy, CE: commission error, OE: omission error, OA: overall accuracy and K: Cohen's coefficient.

| Validation 2003: | | REFERENCE DATA | | Total. |
|------------------|--------------|----------------|-------------|---------|
| | | Summer crop | Winter crop | |
| MODIS ESTIMATION | Summer crop | 4012.89 | 126.59 | 4139.48 |
| | Winter crop | 141.56 | 731.96 | 873.52 |
| | Unclassified | 104.59 | 145.47 | 250.06 |
| Total. | | 4259.04 | 1004.02 | 5263.06 |

| Accuracies 2003: | | | |
|------------------|------|------|------|
| UA | PA | CE | OE |
| 0.97 | 0.94 | 0.03 | 0.06 |
| 0.84 | 0.73 | 0.16 | 0.27 |

| | |
|-----|------|
| OA: | 0.90 |
| K: | 0.67 |

| Validation 2006: | | REFERENCE DATA | | Total. |
|------------------|--------------|----------------|-------------|---------|
| | | Summer crop | Winter crop | |
| MODIS ESTIMATION | Summer crop | 5542.48 | 210.05 | 5752.53 |
| | Winter crop | 0 | 953.54 | 953.54 |
| | Unclassified | 161.8 | 93.1 | 254.9 |
| Total. | | 5704.28 | 1256.69 | 6960.97 |

| Accuracies 2006: | | | |
|------------------|------|------|------|
| UA | PA | CE | OE |
| 0.96 | 0.97 | 0.04 | 0.03 |
| 1.00 | 0.76 | 0.00 | 0.24 |

| | |
|-----|------|
| OA: | 0.93 |
| K: | 0.75 |

| Validation 2009: | | REFERENCE DATA | | Total. |
|------------------|--------------|----------------|-------------|---------|
| | | Summer crop | Winter crop | |
| MODIS ESTIMATION | Summer crop | 4954.48 | 174.48 | 5128.96 |
| | Winter crop | 58.75 | 518.94 | 577.69 |
| | Unclassified | 225.23 | 72.34 | 297.57 |
| Total. | | 5238.46 | 765.76 | 6004.22 |

| Accuracies 2009: | | | |
|------------------|------|------|------|
| UA | PA | CE | OE |
| 0.97 | 0.95 | 0.03 | 0.05 |
| 0.90 | 0.68 | 0.10 | 0.32 |

| | |
|-----|------|
| OA: | 0.91 |
| K: | 0.56 |

| Validation 2012: | | REFERENCE DATA | | Total. |
|------------------|--------------|----------------|-------------|---------|
| | | Summer crop | Winter crop | |
| MODIS ESTIMATION | Summer crop | 5471.63 | 179.36 | 5650.99 |
| | Winter crop | 0 | 369.81 | 369.81 |
| | Unclassified | 30.46 | 146.6 | 177.06 |
| Total. | | 5502.09 | 695.77 | 6197.86 |

| Accuracies 2012: | | | |
|------------------|------|------|------|
| UA | PA | CE | OE |
| 0.97 | 0.99 | 0.03 | 0.01 |
| 1.00 | 0.53 | 0.00 | 0.47 |

| | |
|-----|------|
| OA: | 0.94 |
| K: | 0.64 |

| Validation ALL: | | REFERENCE DATA | | Total. |
|------------------|--------------|----------------|-------------|----------|
| | | Summer crop | Winter crop | |
| MODIS ESTIMATION | Summer crop | 19981.48 | 690.48 | 20671.96 |
| | Winter crop | 200.31 | 2574.25 | 2774.56 |
| | Unclassified | 522.08 | 457.51 | 979.59 |
| Total. | | 20703.87 | 3722.24 | 24426.11 |

| Accuracies ALL: | | | |
|-----------------|------|------|------|
| UA | PA | CE | OE |
| 0.97 | 0.97 | 0.03 | 0.03 |
| 0.93 | 0.69 | 0.07 | 0.31 |

| | |
|-----|------|
| OA: | 0.92 |
| K: | 0.67 |

The error matrices showed good overall accuracy (OA) results, with values always greater or equal to 90% and K values from 0.56 and 0.75 with an average value of 0.67. According to Brivio et al., (2006), positive values of the K-estimator, lead to an agreement between reference and estimated datasets that are greater than the casual matching. Algorithm results summarized to HCA units demonstrated to be very accurate in terms of user and producer accuracies (UA, PA), therefore producing low commission and omission errors. As expected winter crop estimation presented the highest omission error (30%) as a consequence of the fragmentation of this target. However, we consider the results satisfactory for the purpose to reconstruct shift in land use at farm scale. In particular, the validation results highlighted to be consistent for the three analyzed years showing very low inter-annual effect. This indicates that the algorithm performances are consistent in time confirming the possibility to produce accurate estimations for the entire 2003 – 2013 time series.

4.4.2 Farm trajectories retrieving

EVI time series were analyzed for the period of 2003-2013, retrieving estimations on summer and winter crop cultivation presence for each HCA. These data represent for a single farm the amount of area allocated to summer and winter crop cultivations. Figure 4-7 shows an example of “farm trajectories”. The figure reports for two farms the percentage of winter and summer crop (as percentage on the total arable land) for the 2003-2013 periods. The trajectories of farm ID.221 (Figure 4-7, upper panel) indicates a farm where summer crops (most probably rice) are constantly cultivated for about the 80% of the farm arable surface. The analysis of farm ID.1605 trajectory (Figure 4-7 lower panel) reveals a different situation with a general smaller gap between summer and winter crops proportions; summer crop was the main crop before 2010, while winter crop started to occupy most of the lands after this year. This farm shows certainly a management orientation devoted to more crop diversification. On the basis of each farm trajectory, we classified the farms using clustering algorithms in order to retrieve a set of farm management typologies.

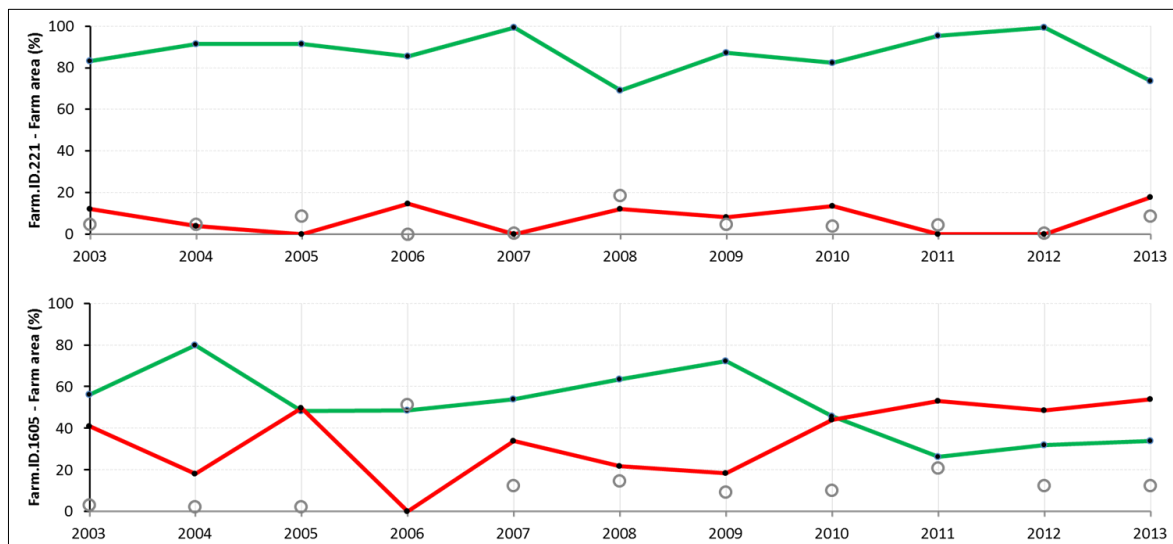


Figure 4-7 – Farm trajectories for two farms in Camargue, farm ID.221 (upper panel) and farm ID.1605 (lower panel). Green lines represent temporal trajectories of those farm portion dedicated to summer crop while red lines represent winter crop ones. Grey circles indicate the portion of farm for which no estimations were produced.

4.4.3 Identification of farm management typologies

The temporal dynamic of winter and summer crop proportions for 140 farms in Camargue (farm trajectories) was the input dataset for the clustering process aimed to group the farms on the basis of their land use trajectories. Figure 4-8 reports the general scheme resulting from the clustering; a total of 6 different groups according to farm trajectories were identified (in the figure from letter A to F). Cluster A and cluster B were identified during the second hierarchic level. These clusters respectively grouped a total of 17 and 29 farms having average arable land surfaces of 67 and 193 ha. Clusters C, D, E, F, were identified at the third clustering level, they respectively grouped a total of 35, 17, 33, and 9 farms having average arable land surfaces of 131, 117, 180 and 247 ha.

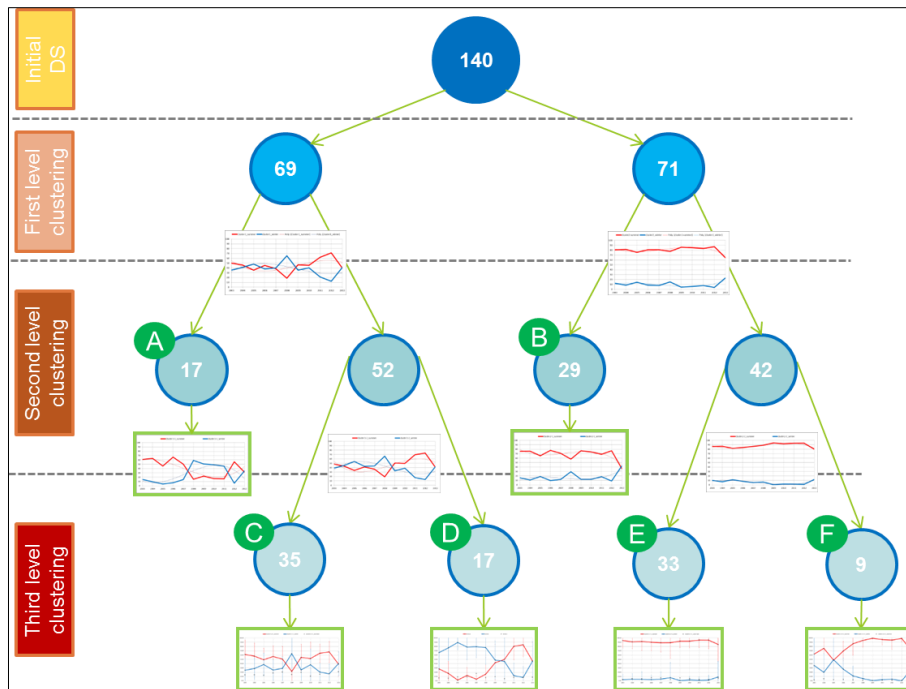


Figure 4-8 – Schematic representation of a three levels hierarchical clusterization process. The clustering produced six groups identified by the letter from A to F; the number of farms in each cluster is also reported.

For each of the six clusters, the average farm trajectories were evaluated (see Figure 4-8). These trajectories were interpreted as representatives of different kind of farm management typologies of Camargue.

The 69 farms of clusters A, C and D are separated at the first level of the hierarchical clusterization and have in common a shift between winter and summer crop cultivations during the years (Figure 4-9). In particular, cluster A includes farms that dedicated more arable land to summer crop from 2003 to 2007, in the period 2008 to 2011 an inversion of crop repartition is evident with dominance of winter crops compared to summer. Farms belonging to cluster C, show a more equal allocation of summer and winter crops, with always a predominance of winter crops on summer crops. An exception appears in 2008, where a shift of the two main crops occurs. The trajectories of cluster D underline two main phases, the first one from 2003 to 2009, where summer crops are more represented than winter crops, and a second one from 2010 to 2012 where winter crops became dominant.

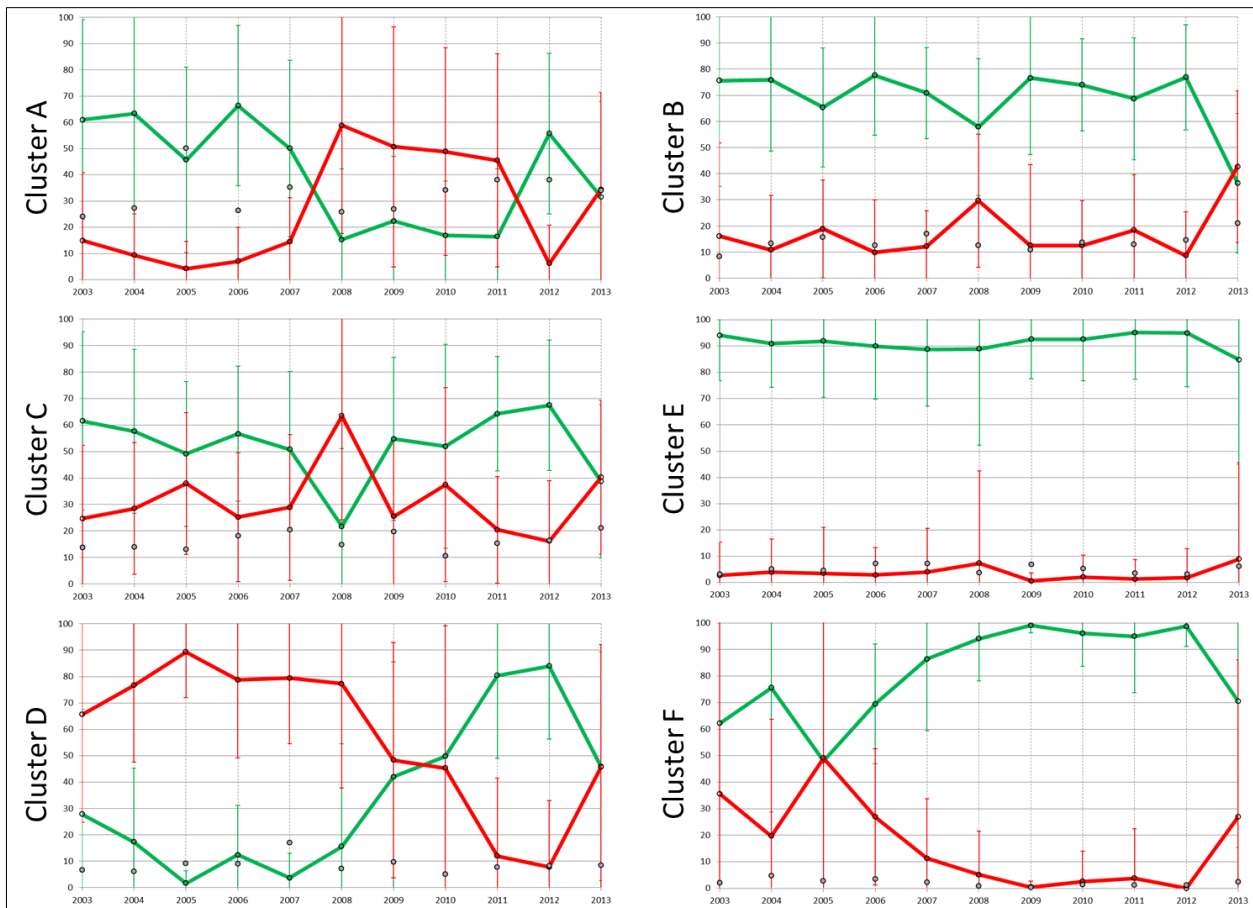


Figure 4-9 - Trajectories of winter and summer cultivation presence for six farms clusters in Camargue. Each graph reports in the x-axis the time line from year 2003 to 2013 and in the y-axis the percentage of farm area occupied by summer (Green lines) and winter crop (Red lines). Grey circles highlight the portion of farm for which no estimations were produced.

The trajectories of the 71 farms belonging to cluster B, E and F show a greater proportion of summer crop cultivation level compared to winter crop cultivation. No shift happens during the time period (Figure 4-9). In clusters B, summer crops are dominant compared to winter crops, but fluctuations of about 20% in crop changes occurred through time. Cluster E instead describes farms having high and stable levels of summer crop cultivations (i.e. rice) that are always around 90% and show low fluctuations. Finally, cluster F, highlights the average trajectory of farms that since 2005 progressively increase the portion of summer crop cultivation in the farm, until reaching a level similar to those of cluster E. In all of the clusters a decrease in summer crop cultivations happen in 2013.

4.4.4 Spatial explicit assessment of farm typology

Figure 4-10 provides a map representation of the identified clusters. It is interesting to notice that the cluster constantly characterized by summer crop presence (B, E and F) are mainly distributed in the southern-eastern part of the study area closer to the sea. This confirms that those farms are typically specialized in rice cropping. On the contrary the winter crop cluster (D) are more in the northern part. Cluster C, that includes farms with a diversification between summer and winter crop are generally distributed in all the study area.



1

2

Figure 4-10 – Spatial distribution of six clusters representing different farm land use managements for the study area of Camargue.

4.5 Discussion

4.5.1 Discussion on the main result

A farm trajectories clusterization led us to identify six different farm types, which referred to different farm land use management during the analysed period. A semantic interpretation of those (see Figure 4-9), allowed formulating some hypothesis to describe the farming systems.

A preliminary observation can be done focusing at the first clustering level, where a distinction can be done between i) farms having a common inclination to shift winter and summer crops, from ii) farms with high and stable summer crop. The first group (clusters: A, C, D) is characterized by farms having average arable land of 112 ha and can be interpreted as including farms with attitude to a general crop diversification and to shift crops in the mentioned period. On the other hand, the second group (clusters: B, E, F) is characterized by farms with average arable land of 193 ha (60% greater than the previous). These farms can be interpreted as extensive farms prone to homo-succession of crops. Rice farmers tend to be among these management typologies. The size of the farms seemed to be an explanatory variable of the intensive or extensive farming system.

Following, are reported the hypothesis we formulate to semantically interpret the resulting farm types:

- **Farm type A:** these farms tend to shift their crops, likely from alfalfa to winter wheat, due to the possible presence of livestock or due to high crop diversification for organic farm management.
- **Farm type C:** according to the equal allocation of lands for summer and winter crops, this farm type could include diversified crop producers. The crop allocation inversion, occurring in 2008 could be explained by the rapid increase in wheat prices occurring since July 2007, as demonstrated in the statistics provided by the *Association Générale des Producteurs de Blé et autres céréales* (AGBP. <http://www.agpb.com/documentation-et-publications/prix/200-evolution-des-prix-des-principales-cereales-francaises>).
- **Farm type D:** these farms seem to have progressively converted (since 2007) their land use to rice production (the most representative summer crop in the study area), facilitated by the PAC subsidies arrived since 2012, that was paid by considering the previous five years rice cultivated area.
- **Farm type B:** farms belonging to type B can be considered “reactive” because show an average 20% of fluctuations between winter and summer crop in land use; these farms are potentially the ones characterized by a high tendency to adapt their crop allocation strategy according to external factors (i.e. subsidies, grain prices etc.).
- **Farm type E:** according their trajectories these farms seem to be specialized rice producer. These farms are then the most inclined to monoculture and therefore the one having worst environmental impact (due to the higher use of herbicides to control weeds).

- **Farm type F:** since 2005, farms belonging to this cluster progressively increased the portion of summer crop cultivation until reaching the general trait of the E typology. This could be explained in a management strategy of farm that changed from diversified producer to specialized producer. This is the less represented farm type group (9 farms) but also the one characterized by the higher average arable land farm size (247 ha).

A decrease in summer crop cultivation in the 2012 to 2013 period occurs in all the farm types. A general decreasing of summer crop was therefore estimated for the entire study area. This decreasing trend was confirmed by statistics data relative to the total rice cultivated area in Camargue region: 31% decrease of rice cultivation during the 2011-2014 periods (Source: Agreste. The French statistical agency for agriculture. <http://agreste.agriculture.gouv.fr/>)

The obtained farm typologies were compared with other different farm types designed by Delmotte et al. (2015). These typologies, related to the same study area and produced for the reference year 2007, were realized considering key variables such as: rice and wheat proportion in the farm area, presence of livestock and style of production (organic or conventional). A general agreement was found between the two farms classification systems: “farm type B”, “farm type E” and “farm type F” match with “middle rice producer” and “large size rice producer” farm types (Delmotte et al. 2015) for the 72%, 88% and 100% respectively. These similarities are in agreement with the hypothesis we previously formulate.

Validation results were satisfactory and comparable with already published contribution aimed to depict crop rotations and land use changes exploiting time series of remote sensed data. For example, Conrad et al. (2011) achieved overall accuracy values of 84% ($\pm 1\%$) mapping crop rotations in Central Asia and Le Li et al. (2014) mapped agricultural intensity in China with overall accuracy of 91%. The algorithm validation was conducted summarising the pixel based estimations to homogeneously cultivated areas (HCA). This operation was done considering the peculiarities of the study area (groups of nearby fields homogeneously cultivated) and was necessary to attenuate the omission errors generated due the mismatch between MODIS 250 meters spatial resolution and Camargue crop field sizes and fields fragmentation. The final validation results, compared with results obtained with a pixel based approach (data not showed) reveals a decrease of the omission errors: for summer crop estimation, from 43% to 3% (-40%) and for winter crops, from 44% to 31% (-13%). A consequent increase of the overall accuracy from 59% to 92% (+33%).

4.5.2 Conclusion and further development

Farm typology approaches, oriented on capture over time the farm land use management variabilities are rare and provide important information to (i) summarize and classify farm diversity and (ii) formulate short term scenario assessment. In this work, remote sensed time series data were successfully exploited with the aim to identify farming system management typologies for the Camargue’s case study. Six farm types were defined by a clusterization of farm land use trajectories, assumed as an indicator of farm

management. Results were in agreement with previous contribution. Further research efforts are needed to improve the robustness of the methodology and to take into account during the farm clusterization new different variable able to depict the temporal variability of farming systems.

The results of this study demonstrate the potential of moderate resolution satellite data time series to individuate farm land use typologies. However, several refinements might improve the proposed methodology:

- I. The detection of summer and winter crops from EVI time series were mainly driven by a rule based methodology. A time series analyses approach less constrained by thresholds or rules based on local crop calendars could be took in consideration to make the algorithm more robust for applications outside the study area of Camargue.
- II. The clusterization phase, involved 140 farms, selected according the size (>25 ha) and the representativeness of HCA in the farms (>70%). This selection could negatively affect the individuation of those farm typologies characterize by small farm size.
- III. During the clustering procedure, the methodology considered the un-estimated areas as a proxy of the detection reliability. In this sense, further improvements could involve the definition of new metrics to better assess the mapping capacity (e.g. the number of pixels belonging to an HCA for which it was possible to produce estimations).
- IV. Remote sensed data allowed defining farm typologies by identifying temporal changes in farm land use management. This is an innovative feature in farm typology definition. Further analysis will be aimed to improve the understanding of farm systems by including other variables, such soil types or farm dimensions.

5 Improving satellite time series resolution with data fusion techniques. Advantages for crop monitoring

5.1 Introduction

Agricultural monitoring needs updated information on both type and dynamic of cultivated crops. Usually, the agricultural environment is fragmented into fields with heterogeneous vegetation dynamics due to differences in cultivated varieties, agro-practices and weather influence. Thus, a monitoring system based on the analysis of time series of satellite data, requires data featuring both high spatial resolution (single field detail) and high temporal resolution (revisiting time). Currently, only heterogeneous data in terms of spatial and temporal resolutions are available for operational monitoring purposes. For example MODIS data have high temporal resolution (quasi daily) but a low spatial resolution (250-100 m) and Landsat satellite data has moderate spatial resolution (30 m) and low temporal resolution (16 days). The launch of Sentinel-2A (23 June 2015) and the forthcoming launch of Sentinel-2B (mid-2016) satellites, in the context of the European Earth observation programme *Copernicus* (<http://www.copernicus.eu/>) will offer for the first time the chance for the coexistence of high spatial (20-30 m) and temporal resolution (up to 5 days when two satellites constellation will be available). These key features will bring considerable added value in crop monitoring especially for time series analyses approaches. However, cloud obstruction represents a major constraint reducing the potential revisiting time, and actually decreasing the number of scenes per season exploitable for monitoring purposes.

In this perspective and in order to understand in advance the potentiality of Sentinel-2 data, it is important to find a method suitable to exploit data from sensors with high spatial resolution and sensors with high revisiting time, fusing them into a new time series dataset featuring both high spatial and time resolutions. The SPOT4 Take5 experiment proposed by the *Centre National d'études Spatiales* (CNES), *Centre d'Etudes Spatiales de la BIOSphère* (CESBIO) and European Space Agency (ESA) gives the opportunity to simulate Sentinel-2 data, providing the best benchmark to evaluate the improvements offered by the coexistence of high spatial and temporal resolution.

During the following study we (i) implemented in an automatic routine an innovative approach (Bisquert et al., 2015) to perform the “data fusion” of heterogeneous resolution satellite images and generate new time series characterized by high spatio-temporal resolution and then we (ii) verified the quality and the usefulness of the generated time series for the monitoring of the main European cultivated crops.

5.2 Study area and Materials

As for the activities carried out in chapter two and three, this research took place in the Camargue region, Southern France. This region is characterized by an important agricultural land use vocation. Figure 5-1.

We worked on heterogeneous satellite images datasets, made of SPOT-4 and MODIS sensors images, collected for the acquisition period of February-June 2013. The SPOT-4 data were acquired and processed within the CNES “SPOT-4 TAKE-5” project (<https://spot-take5.org/client>) these data simulate the main features of the forthcoming Sentinel-II sensor: 20m of spatial resolution and 5 days of time resolution) and were used as reference low spatial resolution data in the data fusion process. Regarding MODIS sensor we used the MOD09A1 composite product, provided at 500m spatial resolution and 8 days of temporal resolution. A total of 20 SPOT-4 images and 21 MODIS images were available.

Land use informations collected at field level for three farms in Camargue were used as reference data. These informations referred to 2013 and accounted 324 polygons (fields) for a total surface of 1334 ha.

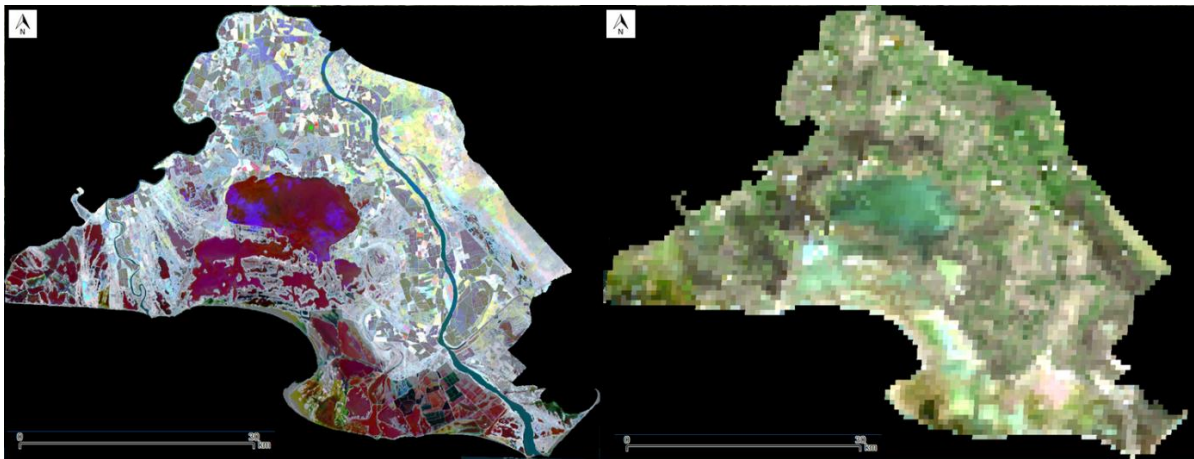


Figure 5-1 – The study area of the *Parc naturel régional de Camargue* (PNRC). On the left, *SPOT-4 TAKE-5 image at 20m resolution (NDVI RGB DOY 74:124:139)*. On the right, *MODIS MOD09A1 image product at 500m resolution (RGB true colour.)*

5.3 Methods

5.3.1 Pre-processing of satellite images

Two spectral indices (SIs), Normalized Difference Vegetation Index (NDVI, Rouse et al., 1974) and the Normalized Water Index 2 (NW12, Boschetti et al., 2014) have been calculated from all the available “SPOT-4 TAKE-5” (here after S4T5) and MODIS images (Eq. 1 and 2). These indices are respectively developed to detect biomass and standing water presence and therefore are useful to investigate crop seasonal dynamics and irrigation agropractises. Time series analyses of NDVI and NW12 have been already exploited in literature for crop monitoring purposes (Sakamoto et al., 2005; Wardlow et al., 2007; Manfron et al., 2012).

$$NDVI = \frac{\rho_{NIR} - \rho_{Red}}{\rho_{NIR} + \rho_{Red}} \quad (\text{Eq. 1})$$

$$NW12 = \frac{\rho_{RED} - \rho_{SWIR1620}}{\rho_{Red} + \rho_{SWIR1620}} \quad (\text{Eq.2})$$

Once calculated, the spectral indices were used as input of the considered data fusion approach. Previously, the indices retrieved from the MODIS images were down-scaled to the S4T5 spatial resolution of 20m.

5.3.2 Data fusion approach

The data fusion methodology proposed by Bisquert et al. (2015) were applied on the S4T5 and MODIS dataset in order to reconstruct time series with high spatial and temporal resolution (20m – 5 days). This method uses soft operators and is based on the temporal distance between the input images and the timestamp of the image to be simulated. Figure 5-2 present a schematic simplification of the method.

The approach aims to fuse a synthetic high spatial resolution “HR” time series by evaluating the information contained in the available satellite images with low (LR) and high spatial resolution (HR). In the example of Figure 5-2 two HR images time series were fused at the timestamps t_1 and t_2 . The procedure of Bisquert et al. (2015) could be summarize in 3 main phases:

1. Parameters definition.
 - desired time stamps for the simulated series (t_1, t_2, \dots, t_n);
 - number of High/Low resolution pairs of Images to be fused (one in the example);
 - the “ t_o ” and “ t_e ” parameters, that represents the time lengths over which an input image does not contribute to the fusion (μ_{t_1} or $\mu_{t_2} = 0$);
 - the power “ p ” parameter which modulates the weight intensity.
2. Input images weights definition.
 - For each timestamp t_n (t_1 and t_2 in the example of figure x). The weight (μ_t) of each input HR image (H_0, H_1) and LR image (L_1, L_2, L_3) acquired before t_o and after t_e is Null, otherwise it is $\mu_t(t_H)$ and $\mu_t(t_L)$ where μ_t is evaluated as in the following example (referred to t_1, H_0 and L_2) :

$$\mu_{t_1}(t_{H0}) = \frac{1}{(t_{H0} - t_1)^p} \quad (\text{Eq.3})$$

$$\mu_{t_1}(t_{L2}) = \frac{1}{(t_{L2} - t_1)^p} \quad (\text{Eq.4})$$

3. Fusion process.
 - The fusion is a weighted average of input images within t_o and t_e . The data fusion consists in a weighted average of the pixel values co-registered in the HR and LR input images. Their weight is calculated according to the inverse of the distance between the image acquisition date in input and the instant t of the image to be generated. In this way, the more the input image is close to the image to be generated the more the contribution of the image to determine the final pixel value of the fused image is.

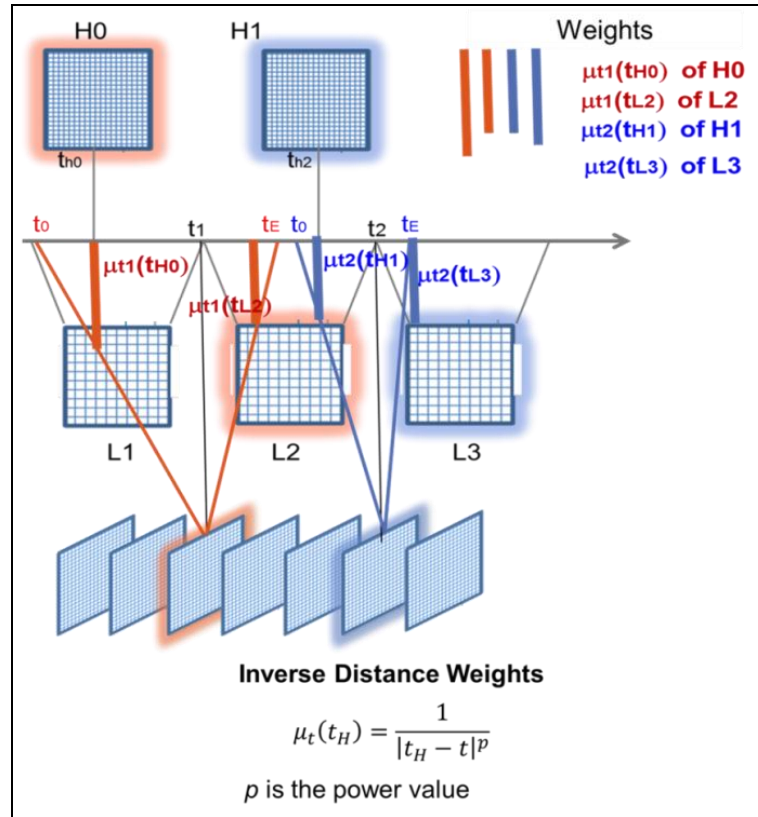


Figure 5-2 – Schematic representation of the data fusion approach proposed by Bisquert et al. (2015).

5.3.3 Calibration and application of the proposed methodology

A calibration test has been performed in order to evaluate the accuracy of the fused datasets under variations of the “ p ” parameter. To do this, the S4T5 together with the MODIS datasets have been divided into training and testing dataset. The training dataset has been used to assess the sensitivity of the method to the parameter. The fused time series resulting from different tests have been then validated through the testing dataset (not used in the fusion process). The Pearson’s coefficient (R), the Root Mean Square Error (RMSE) and the “Accuracy” estimator (see Eq. 3) were considered as validation’s estimators.

$$Accuracy\ estimator = 1 - AVG\left(\sum_{Test\ img=1}^{n\ Tesr\ img} (|Fused_{pixels} - Testing_{pixels}|)\right) \quad (Eq.3)$$

Finally, the most accurate parametrization of the algorithm have been used to assess the utility of the method for operational agronomical monitoring of specific agricultural areas of the Camargue

5.4 Results

5.4.1 Calibration of the proposed technique

The performances of the different configurations are resumed in Table 5-1. The comparisons between the new images after the fusion procedure with the validation dataset (SPOT4 images excluded by the fusion process) resulted with high level of accuracy, in particular setting the p value to 1, we achieved 0.92 accuracy level.

Table 5-1 – Statistical assessment of the fusion images database. IDW: Inverse Distance Weight approach statistics by setting the parameter “p” to values 1, 2 and 3. # HR/LR: pairs of Images to be fused. P: power parameter. R: correlation between data fusion images and testing dataset. RMSE: Root Mean Square Error. Accuracy: average of the residual values (see Eq.3).

| Statistics (Simulated vs Target) | | | | | |
|----------------------------------|---------|---|-------|-------|----------|
| Method | # HR/LR | p | R | RMSE | Accuracy |
| IDW1 | 3 | 1 | 0.806 | 0.181 | 0.926 |
| IDW2 | 3 | 2 | 0.727 | 0.226 | 0.912 |
| IDW3 | 3 | 3 | 0.686 | 0.249 | 0.904 |

A scatter plot comparison between the simulated image with “IDW1” method, obtained after the fusion process, and the reference dataset is reported in Figure 5-3A. Warm colors indicate high concentration of data while cold colors indicate low concentration of data it is possible to note the high correlation between the two, real HR data and simulated one, images. Figure 5-3B reports an example of pixel’s time series extracted by i) the input HR and LR data set and by ii) the output fused time series. The blue time series represents S4T5 NDVI pixel’s values, characterized by a low temporal resolution due to high presence of useless (cloud contaminated) data (set to zero). The red time series represents MODIS pixel’s values, characterized by higher temporal frequency but low spatial resolution. The green line represents data fusion pixel’s values, where the temporal resolution of S4T5 data was reconstructed through the “Inverse Distance Weight” (IDW) data fusion approach. Figure 5-3C and Figure 5-3D provide an example of “predicted” and “Target” images, to show how the fusion derived image is consistent to the respective target image of the testing dataset.

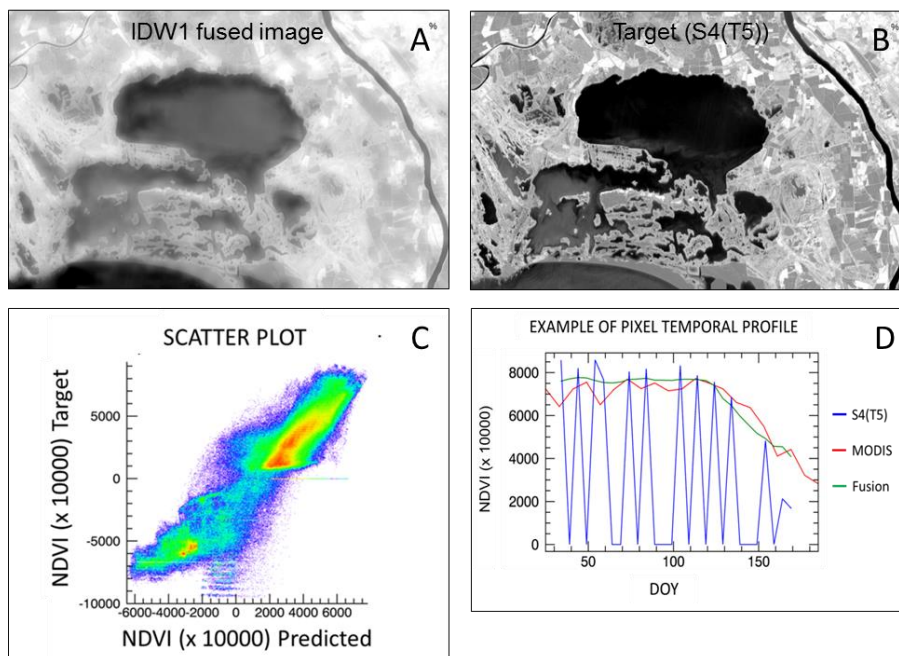


Figure 5-3 – Accuracy assessment of the fusion method. Resulting output image (A) compared to the corresponding reference one (B). (C) Scatter plot between the resulting fused datasets (Predictions) and the testing dataset images (Target). (D) Example of a pixel temporal profile for the input (blue HR image and read LR image) and resulting output “fused dataset” (green).

5.4.2 Improved time series for crop monitoring

Figure 5-4 reports a zoom image of the study area observed from different data sources: SPOT-4 image (left side), MODIS image resampled to the SPOT spatial resolution (in the center) and fusion resulting image (right side). Figure 5-4A, B and C are RGB composites obtained by multi temporal NDVI data (R = 15th of March; G = 4th of May; B = 8th of February). Two regions of interest (ROI) are highlighted in yellow: ROI#1 represents a region cultivated with winter wheat and ROI#2 a region with rice cultivations. In these images despite the coarse resolution of MODIS data (500m, Figure 5-4B), it is possible to appreciate how the synthetic output images (Figure 5-4C) maintains the initial high spatial resolution of the SPOT-4 data (Figure 5-4A) that allows to distinguish landscape structural pattern. The average NDVI time series extracted from the ROIs, in red (whiter wheat) and green (summer rice) colors, for the original SPOT data (HR), MODIS (LR) and fusion product (synthetic HR) are reported in Figure 5-4A1, B1 and C1 respectively. The period of interest of the data is from DOY 34 (February, 3rd) to DOY 169 (June, 18th). Time series referred to S4T5 dataset (A1), have an inconsistent time stamp due to cloud contaminations (see values set to zero), MODIS time series instead (B1) shows a regular temporal resolution despite characterized by some noise in relation to mixture of targets in the low resolution pixel. The contribution of the data fusion approach, highlighted in panel C1, is the possibility to reconstruct a S4T5 temporal frequency filling the gap with information from temporal neighboring HR and LR data. The application of this technique allows to improve the quality of Earth Observation input data used to perform agricultural monitoring activities.

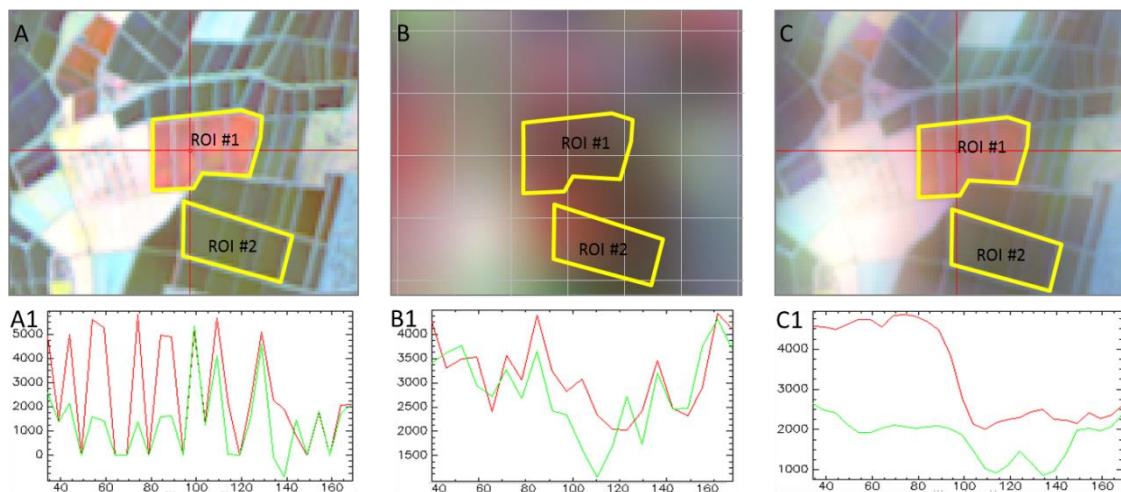


Figure 5-4 – Comparison between the spatial and temporal resolution in three dataset: S4T5 dataset (A, A1), MODIS dataset (B, B1), dataset resulting after “fata fusion” (C, C1).

Figure 5-1 provides comparisons of NDVI and NWI2 time series from original S4T5 sensor (A,C,E,G,I,K) and NDVI time series produced after the fusion process with MODIS data (B,D,F,H,J,L). The time series are represented with box plot of NDVI and NWI2 values extracted, from homogeneously cultivated area of rice, wheat and alfalfa. The analyzed areas are constituted by neighboring fields with same crop and date of sowing in 2013 according to available ground information. From the graphs it is possible to appreciate the

effect of the algorithm on the NDVI time signature reconstruction. The S4T5 time series were improved in the spatial and temporal domain in correspondence of situation where data were cloudy or missing.

From Figure 5-1 it is possible to appreciate the contribution of time series fusion for areas belonging to rice, winter wheat and alfalfa cultivations for the period February-June 2013. The fused time series of Figure 5-1B shows the beginning of rice crop vegetative period (DOY 124), occurring in the middle of May. The occurrence of a rice flooding event, is instead highlighted in Figure 5-1D, by an increase of the NWI2 indices around DOY 119.

Central panels of Figure 5-1 report the original and reconstructed winter wheat cultivated fields' trend. From this graph it is possible to appreciate the dynamics of the entire vegetative crop cycle. The crop (Figure 5-1F) starts to grow approximately in the middle February (from DOY 44), it reaches the heading point in middle April (DOY 109) and then decreases in June (until DOY 169).

In the NDVI fused time series of Figure 5-1J and L it is possible to appreciate the behavior of alfalfa cultivated fields. The graph highlights the complete crop cycle from the end of February (DOY 54) to the first cut at the end of May (DOY 144) and the beginning of a second alfalfa cycle in early June (DOY 154). All these observations, fully in agreement with local crop calendars and expert knowledge, could be made only after the application of the fusion process that allows to reconstruct an improved NDVI time series.

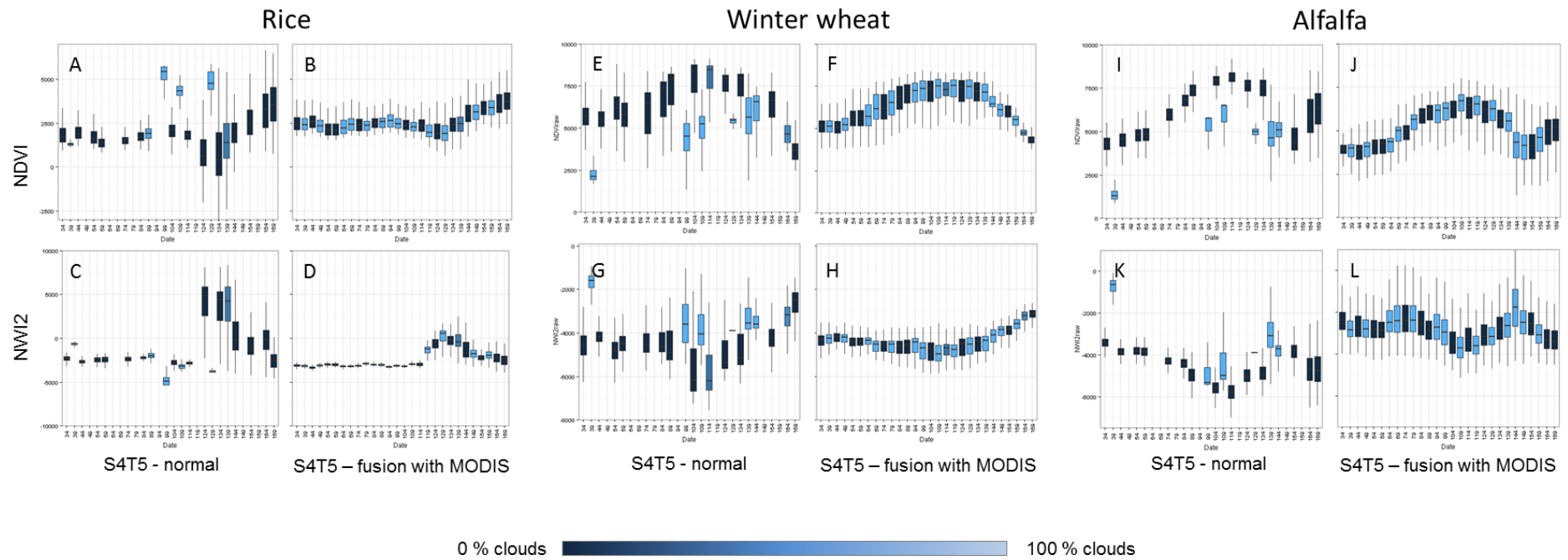


Figure 5-1 –Fusion of SPOT 4 Take 5 NDVI and NW12 time series for the three main cultivations in Camargue: rice, winter wheat and alfalfa in left, central and right panel respectively. Left panels (A and C; E and G; I and K) shows the original S4T5 data while right panels (B and D; F and H; J and L) the dataset obtained by the fusion process.

5.5 Discussions and conclusion

NDVI images, calculated from S4T5 and MODIS datasets were fused together to reconstruct NDVI time series at high spatial and temporal resolution. Validation tests have been performed changing the power parameter value “p” and evaluating the accuracy of the fused datasets. The utility of the method for operational agronomical monitoring purposes was finally assessed for some of the most represented cultivation of the study area.

The experiment positively demonstrated the contribution of data fusion techniques for the production of time series at high space-time resolution. A possible integration of data fusion techniques to the methodologies presented in this work seems to be of great interest. In particular with reference to a possible decrease of the algorithms omissions generated on winter wheat identification. Time series with improved temporal resolution (e.g. 20m) will better fit with winter wheat field size reducing the gap between the (exploited) MODIS 250m spatial resolution and Camargue average crop field sizes and fields fragmentation.

Further application will involve the use of time series obtained from data fusion approach as input in algorithms for the automatic classification of time series, in order to recognize different crop typologies and identify phenological key stages and agro practices occurrences. Another possible contribution of this technique could concern the possibility to produce historical archive of data with improved spatio-temporal resolution. This could be done for example involving MODIS and Landsat images in the fusion process. This could allow to perform long term time series analyses (e.g. farm typologies retrieving) at improved resolutions.

6 Summary and final Conclusions

The research activities presented in this manuscript were conducted in the framework of the international project SCENARICE (*Scenario integrated assessment for sustainable rice production systems: Exploring plausible, probable and possible futures for sustainable production systems*). The project wanted to demonstrate the contribution of different technical and scientific competences integration to assess current characteristics of cropping systems and define sustainable future agricultural scenarios taking into consideration environmental conditions and constrains (e.g. climate change), agro policy and technological innovations. The skills involved in the project are in the scientific domain of:

- Agronomy: to provide knowledge of the cultivated crops and characterize farming systems
- Crop model: to simulate current and future efficiency of cropping system
- Bio-economic and Agent Based model: to assess technological innovations and policies over a range of different geographic and climatic circumstances
- Geomatics and remote sensing: to provide spatio temporal information on environment condition and agro-practices that drives the cropping systems performance.

In this framework, dynamic simulation crop models were used first to evaluate efficiency of current cropping systems and their productivities in relation to environment, cultivated crop characteristics and farm management, secondly to predict the consequences of climate change scenarios on the cropping systems performances. Crop models require high quality input information (i.e. weather data, soil information, crop characteristics and agro management) to produce reliable prediction on farming system efficiency. For the study area of Camargue, a lack of information regarding the intra and inter-annual variability of crop practices was highlighted. In particular for crops like winter wheat, characterized by a great seasonal variability in crop establishment practices, quantitative sowing dates information is actually missing limiting the efficient exploitation of crop models. To address this issue satellite images can be analyzed and sowing dates retrieved for the available data archives.

A second important project topic, were represented by the description of possible future cropping systems adaptation strategies that will be happen at the farm level. To perform this analysis, it is fundamental to characterize the current diversity of farming systems through the proposition of different farm typologies representative for the study area. Different methods have been used to design farm typologies: (i) statistical analyses of database in which different variables are describing the farming systems and/or (ii) expert knowledge classification rule to identify categories of farms. In the above mentioned approaches, all the farm typologies are defined on the basis of data describing the farms for single/specific year. The methods are therefore based on a “static picture” of the farming systems, taken at a given time, and in most cases without any information about the inter-annual variability of management and performances.

The specificity of the data needed to take into account inter-annual variability and farm trajectories to build a farm typology is that the data must be representative of farms of a region both in time and space. To address this problem, time series of satellite data can be exploited to analyse the land use changes at farm level providing an important and innovative contribution in farm typology definition.

In this work satellite remote sensing represented the main tool exploited to deal with the previously mentioned issues related to data/information lacking. Remote sensed data greatly contribute in cropping systems characterization by providing timely, synoptic, cost efficient and repetitive information about the status of the Earth's surface. Moreover, remote sensing data can be free of charge and more than ten year data archives are nowadays freely available, for example in the case of the MODIS satellite.

Given this, the research work focused on the retrieval of information about crop cultivated areas at regional and farm scale, exploiting the analysis of long time series of satellite data. Taking into account the specific requirements of SCENARICE project, two objectives have been defined: (i) to provide winter wheat sowing dates estimation on a long term period (11 years) to contribute in Camargue base line scenario definition (Chapter 2) and (ii) reconstruct Camargue's farms land use changes through the analysis of time series of satellite data to provide helpful information for farm typologies definition (Chapter 3).

Chapter 2 described the rule-based methodology developed to automatically identify winter wheat cultivated areas and to retrieve crop sowing occurrence in the period 2003-2013. Detection criteria were derived on the basis of agronomic expert knowledge and by interpretation of high confidence EVI crop temporal signature. The distinction of winter wheat from other crops was based on the identification of the crop heading and crop establishment periods and considering the length of the crop cycle. Once winter wheat was detected, additional set of rules were designed to properly identify sowing occurrence. The detection of winter wheat cultivated areas showed that the 56% of the target in the study area was correctly detected with a low level of commissions (11%). This is an important result because it demonstrates that is possible to automatically select a reliable sample of winter wheat cultivated area to further analyse their seasonal behaviour. The validation of sowing date estimations demonstrated that the method was able to capture the seasonal variability of crop establishment practises with errors of ± 8 and ± 16 days in 45% and 65% of cases respectively. Since the sowing date period in Camargue usually last in 75 days, we considered our methodology able to capture in a reliable way the seasonal variability of sowings. We then extended the estimates for the 2003-2013 period to analyse inter-annual variability. We were able to observe that in Camargue the most frequent sowing period was October 31th (± 4 days of uncertainty). The 2004 and 2006 seasons showed early sowings (late September) the 2005, 2009, 2011 and 2012 seasons were in line with the average estimations and the 2003 and 2008 seasons were slightly delayed at the beginning of November. The sowing date occurrence estimations were not correlated to the seasonal rainy events; this led us to formulate the hypothesis that external factors that can influence farmers choices (e.g.

crop management restriction, soil moisture) could better explain the variability of the sowings for the study area.

Chapter 3 reports the activities conducted to define representative farm typologies in Camargue. Temporal trajectories of winter and summer crops cultivated areas were estimated at farm level on the basis of MODIS satellite data time series in the 2003-2013 periods. The algorithm validation demonstrated that the method was able to produce maps with high overall accuracy (OA 92%) and very low commission errors (3% for summer crops and 7% for winter crops). Omission errors were very low for summer crops (3%) and higher but within an acceptable level for winter crops (31%). Trajectories of annual winter and summer crop repartition in the Camargue's farms were used as an indicator of farm management (e.g. intensive monoculture farm or diversified crop producer) and were analysed through a hierarchical clustering procedure to identify farm management typologies on the basis of their temporal changes. We were able to identify 6 farm types in a sample of 140 farms (50% of the total) covering 75% of the arable land in the study area. A semantic interpretation of the farm types, allowed formulating some hypothesis to describe farming systems. The size of the farms seemed to be an explanatory variable of the intensive or extensive farm management. The results of this study showed that estimations retrieved from time series of coarse spatial resolution MODIS data are adequate to define farm typologies at a regional scale. The monitoring of land use changes with remote sensing represents an innovative approach to analyze farm management. Despite already known approaches, it allows to formulate hypotheses for different possible future scenarios in farm management ("dynamic picture"). The proposed methodology could also represent a scientific contribution to assess or design farming policies. Further researches are needed to integrate in the farm typing methodology new variables able to depict farm management changes in the time domain together with the improvement of estimations uncertainty in the hierarchical clusterization process.

The two main activities presented in this thesis put in evidence the importance of time series spatial and temporal resolution for crop monitoring purposes. Currently, only heterogeneous remote sensed data in terms of spatial and temporal resolutions are available for agricultural monitoring. Therefore, the satellite data involved to perform (long term) time series analyses represents often the better compromise between their resolutions and their archive wideness. Forthcoming sensors (i.e. Sentinel-II A/B) will offer for the first time the chance for the coexistence of high spatial and temporal resolutions. These key features will bring considerable added value in crop monitoring especially for time series analyses approaches. However, (i) cloud obstruction will still represents a major constraint reducing the potential revisiting time (time resolution) and (ii) long time series analyses will not be performed because of a lack of data archives.

In this frame were addressed the activities proposed in chapter 4, where the "SPOT4-Take5" data, simulating the spatio-temporal resolution of Sentinel-II were evaluated to verify the quality and the usefulness of forthcoming data for the monitoring of the main European cultivated crops. In particular, an

innovative remote sensing technique of “data fusion” were applied with the aim to (i) restore the temporal resolution of time series affected by cloud contamination noise and (ii) produce historical (past) archives of data featuring as the forthcoming Sentinel-2 data. Results demonstrated the positive contribution of data fusion technique for the spatio-temporal improvement of satellite time series data. The visual interpretation of SPOT4-Take5 time series seemed to be promising in depicts the peculiarities of crop cultivated areas.

In conclusion, in this thesis work remote sensing has shown to be a reliable solution to study large-scale crop cultivations and it is therefore a cost-effective tool for the retrieval of spatially and temporally distributed information on cropping systems. Remote sensing time series analyses in particular, has proved to represent a useful tool to highlight patterns of intra- and inter-annual dynamics of agro-practices and was also useful to define farm typologies on the base of multi-temporal land use trajectories. Results were fundamental to complete the studies and the characterization of the Camargue study area, in particular by providing information such as sowing dates, that were not available for the considered study area and represents a step forward respect the actual (static) available crop calendar informations. Moreover, the achieved results provide supplementary information layers to summarize and classify the diversity of the farm in the study area and to characterize farming systems. With reference to the SCENARICE project, the achieved results are important to define more accurate base line scenario for crop simulation modelling and to formulate farming system short term scenario assessment and prediction.

Further advancements of these researches work should be conducted to: (i) test and evaluate new methodologies to quantify the level of noise affecting time series (e.g. the Signal to Noise ratio methodology, Duvellier et al., 2015) and (ii) the use of innovative techniques to improve the spatio-temporal resolutions of satellite images (reducing sourcing of noise in the time series) the level of noise due to the MODIS spatial resolution.

References

1. Andersen, E., Elbersen, B., & Godeschalk, F. (2004, March). Farming and the environment in the European Union—using agricultural statistics to provide farm management indicators. In *Rapport présenté à l'Expert Meeting on Farm Management Indicators and the Environment de l' OCDE, Palmerston North, Nouvelle-Zélande, mars*. Disponible à l'adresse: <http://webdomino1.oecd.org/comnet/agr/farmind.nsf>.
2. Andersen, E., Elbersen, B., Godeschalk, F., & Verhoog, D. (2007). Farm management indicators and farm typologies as a basis for assessments in a changing policy environment. *Journal of environmental management*, 82(3), 353-362.
3. Arvor, D., Jonathan, M., Meirelles, M. S. P., Dubreuil, V., & Durieux, L. (2011). Classification of MODIS EVI time series for crop mapping in the state of Mato Grosso, Brazil. *International Journal of Remote Sensing*, 32(22), 7847-7871.
4. Atkinson, P. M., Jeganathan, C., Dash, J., & Atzberger, C. (2012). Inter-comparison of four models for smoothing satellite sensor time-series data to estimate vegetation phenology. *Remote Sensing of Environment*, 123, 400-417.
5. Atzberger, C., & Eilers, P. H. (2011). Evaluating the effectiveness of smoothing algorithms in the absence of ground reference measurements. *International Journal of Remote Sensing*, 32(13), 3689-3709.
6. Atzberger, C., & Eilers, P. H. (2011). A time series for monitoring vegetation activity and phenology at 10-daily time steps covering large parts of South America. *International Journal of Digital Earth*, 4(5), 365-386.
7. Atzberger, C. (2013). Advances in remote sensing of agriculture: Context description, existing operational monitoring systems and major information needs. *Remote Sensing*, 5(2), 949-981.
8. Atzberger, C., Klisch, A., Mattiuzzi, M., & Vuolo, F. (2013). Phenological metrics derived over the European continent from NDVI3G data and MODIS time series. *Remote Sensing*, 6(1), 257-284.
9. Aubry, C., Papy, F., & Capillon, A. (1998). Modelling decision-making processes for annual crop management. *Agricultural systems*, 56(1), 45-65.
10. Azar, R., Stroppiana, D., Boschetti, M., Brivio, P. A., Pepe, A., Paglia, L., ... & Lanari, R. (2012, October). Integration of optical and SAR remotely sensed data for monitoring wildfires in Mediterranean forests. In *SPIE Remote Sensing* (pp. 85312D-85312D). International Society for Optics and Photonics.
11. Azzali, S., & Menenti, M. (2000). Mapping vegetation-soil-climate complexes in southern Africa using temporal Fourier analysis of NOAA-AVHRR NDVI data. *International Journal of Remote Sensing*, 21(5), 973-996.
12. Balzter, H., Gerard, F., George, C., Weedon, G., Grey, W., Combal, B., ... & Los, S. (2007). Coupling of vegetation growing season anomalies and fire activity with hemispheric and regional-scale climate patterns in central and east Siberia. *Journal of Climate*, 20(15), 3713-3729.
13. Baret, F., Guyot, G., & Major, D. J. (1989). Crop biomass evaluation using radiometric measurements. *Photogrammetria*, 43(5), 241-256.
14. Baret, F., & Guyot, G. (1991). Potentials and limits of vegetation indices for LAI and APAR assessment. *Remote sensing of environment*, 35(2), 161-173.
15. Basso, B., Cammarano, D., & De Vita, P. (2004). Remotely sensed vegetation indices: Theory and applications for crop management. *Rivista Italiana di Agrometeorologia*, 1, 36-53.

16. Beck, P. S., Atzberger, C., Høgda, K. A., Johansen, B., & Skidmore, A. K. (2006). Improved monitoring of vegetation dynamics at very high latitudes: A new method using MODIS NDVI. *Remote sensing of Environment*, 100(3), 321-334.
17. Becker-Reshef, I., Justice, C., Sullivan, M., Vermote, E., Tucker, C., Anyamba, A., ... & Doorn, B. (2010). Monitoring global croplands with coarse resolution earth observations: The Global Agriculture Monitoring (GLAM) project. *Remote Sensing*, 2(6), 1589-1609.
18. Blazy, J. M., Ozier-Lafontaine, H., Doré, T., Thomas, A., & Wery, J. (2009). A methodological framework that accounts for farm diversity in the prototyping of crop management systems. Application to banana-based systems in Guadeloupe. *Agricultural systems*, 101(1), 30-41.
19. Borlaug, N. (2007). Feeding a hungry world. *Science*, 318(5849), 359-359.
20. Boschetti, L., Flasse, S. P., & Brivio, P. A. (2004). Analysis of the conflict between omission and commission in low spatial resolution dichotomic thematic products: The Pareto Boundary. *Remote Sensing of Environment*, 91(3), 280-292.
21. Boschetti, M., Stroppiana, D., Brivio, P. A., & Bocchi, S. (2009). Multi-year monitoring of rice crop phenology through time series analysis of MODIS images. *International journal of remote sensing*, 30(18), 4643-4662.
22. Boschetti, M., Stroppiana, D., Confalonieri, R., Brivio, P. A., Crema, A., & Bocchi, S. (2011). Estimation of rice production at regional scale with a light use efficiency model and MODIS time series. *Italian Journal of Remote Sensing*, 43(3), 63-81.
23. Boschetti, M., Nutini, F., Manfron, G., Brivio, P. A., & Nelson, A. (2014). Comparative analysis of normalised difference spectral indices derived from MODIS for detecting surface water in flooded rice cropping systems. *PloS one*, 9(2).
24. Boschetti, M., Nelson, A., Nutini, F., Manfron, G., Busetto, L., Barbieri, M., ... & Bacong, A. P. (2015). Rapid Assessment of Crop Status: An Application of MODIS and SAR Data to Rice Areas in Leyte, Philippines Affected by Typhoon Haiyan. *Remote Sensing*, 7(6), 6535-6557.
25. Boschetti, M., Busetto, L., Nutini, F., Manfron, G., Crema, A., Confalonieri, R., ... & Brivio, P. A. (2015, July). Assimilating seasonality information derived from satellite data time series in crop modelling for rice yield estimation. In *Geoscience and Remote Sensing Symposium (IGARSS), 2015 IEEE International* (pp. 157-160). IEEE.
26. Bowler, I., Clark, G., Crockett, A., Ilbery, B., & Shaw, A. (1996). The development of alternative farm enterprises: a study of family labour farms in the Northern Pennines of England. *Journal of Rural studies*, 12(3), 285-295.
27. Bradley, B. A., & Mustard, J. F. (2008). Comparison of phenology trends by land cover class: a case study in the Great Basin, USA. *Global Change Biology*, 14(2), 334-346.
28. Bisquert, M., Bordogna, G., Bégué, A., Candiani, G., Teisseire, M., & Poncelet, P. (2015). A Simple Fusion Method for Image Time Series Based on the Estimation of Image Temporal Validity. *Remote Sensing*, 7(1), 704-724.
29. Brivio, P. A., Zilioli, E., & Lechi, G. L. (2006). *Principi e metodi di telerilevamento*. CittaStudi.
30. Brown, J. F., Reed, B. C., Hayes, M. J., Wilhite, D. A., & Hubbard, K. (2002, November). A prototype drought monitoring system integrating climate and satellite data. In *PECORA 15/Land Satellite Information IV/ISPRS Commission I/FIEOS 2002 Conference proceedings*.
31. Bullock, D. G. (1992). Crop rotation. *Critical reviews in plant sciences*, 11(4), 309-326.
32. Chen, J. M., Pavlic, G., Brown, L., Cihlar, J., Leblanc, S. G., White, H. P., ... & Swift, E. (2002). Derivation and validation of Canada-wide coarse-resolution leaf area index maps using high-resolution satellite imagery and ground measurements. *Remote Sensing of environment*, 80(1), 165-184.

33. Chen, J., Jönsson, P., Tamura, M., Gu, Z., Matsushita, B., & Eklundh, L. (2004). A simple method for reconstructing a high-quality NDVI time-series data set based on the Savitzky–Golay filter. *Remote sensing of Environment*, 91(3), 332-344.
34. Chen, K. (2002). An approach to linking remotely sensed data and areal census data. *International Journal of Remote Sensing*, 23(1), 37-48.
35. Chiotti, Q. P., & Johnston, T. (1995). Extending the boundaries of climate change research: a discussion on agriculture. *Journal of Rural Studies*, 11(3), 335-350.
36. Chopin, P., Blazy, J. M., & Doré, T. (2015). A new method to assess farming system evolution at the landscape scale. *Agronomy for Sustainable Development*, 35(1), 325-337.
37. Clevers, J. G. P. W. (1988). The derivation of a simplified reflectance model for the estimation of leaf area index. *Remote Sensing of Environment*, 25(1), 53-69.
38. Combal, B. & Bartholomé, E. (2010). Retrieving phenological stages from low resolution earth observation data. In Maselli F., Menenti M., P.A. Brivio (Eds.), 2010. *Remote Sensing Optical Observations of Vegetation Properties*". (pp.115-129). Research Signpost, Trivandrum (India). ISBN: 978-81-308-0421-7.
39. Congalton, R. G. (1991). A review of assessing the accuracy of classifications of remotely sensed data. *Remote sensing of environment*, 37(1), 35-46.
40. Conrad, C., Colditz, R. R., Dech, S., Klein, D., & Vlek, P. L. (2011). Temporal segmentation of MODIS time series for improving crop classification in Central Asian irrigation systems. *International Journal of Remote Sensing*, 32(23), 8763-8778.
41. Curnel, Y., & Oger, R. (2007). Agrophenology indicators from remote sensing: state of the art. In *ISPRS Archives XXXVI-8/W48 Workshop Proceedings: Remote Sensing Support to Crop Yield Forecast and Area Estimates* (pp. 31-38).
42. De Beurs, K. M., & Henebry, G. M. (2010). Spatio-temporal statistical methods for modelling land surface phenology. In *Phenological research* (pp. 177-208). Springer Netherlands.
43. Delbart, N., Le Toan, T., Kergoat, L., & Fedotova, V. (2006). Remote sensing of spring phenology in boreal regions: A free of snow-effect method using NOAA-AVHRR and SPOT-VGT data (1982–2004). *Remote Sensing of Environment*, 101(1), 52-62.
44. Delécolle, R., Maas, S. J., Guérif, M., & Baret, F. (1992). Remote sensing and crop production models: present trends. *ISPRS Journal of Photogrammetry and Remote Sensing*, 47(2), 145-161.
45. Delmotte, S., Barbier, J.M., Mouret, J.C., Christophe, L.P., Wery, J., Chauvelon, P., Sandoz, A., Loper-Ridaura, S. (2015). Participatory integrated assessment of scenarios for organic farming at different scales in Camargue, France. (in press).
46. Demir, B., & Ertürk, S. (2008, July). Empirical mode decomposition pre-process for higher accuracy hyperspectral image classification. In *Geoscience and Remote Sensing Symposium, 2008. IGARSS 2008. IEEE International* (Vol. 2, pp. II-939). IEEE.
47. Diepen, C. V., Wolf, J., Keulen, H. V., & Rappoldt, C. (1989). WOFOST: a simulation model of crop production. *Soil use and management*, 5(1), 16-24.
48. Doraiswamy, P. C., Sinclair, T. R., Hollinger, S., Akhmedov, B., Stern, A., & Prueger, J. (2005). Application of MODIS derived parameters for regional crop yield assessment. *Remote sensing of environment*, 97(2), 192-202.
49. Duchemin, B., Goubier, J., & Courrier, G. (1999). Monitoring phenological key stages and cycle duration of temperate deciduous forest ecosystems with NOAA/AVHRR data. *Remote Sensing of Environment*, 67(1), 68-82.
50. Dury, J., Schaller, N., Garcia, F., Reynaud, A., & Bergez, J. E. (2012). Models to support cropping plan and crop rotation decisions. A review. *Agronomy for sustainable development*, 32(2), 567-580.

51. Duveiller, G., Lopez-Lozano, R., & Cescatti, A. (2015). Exploiting the multi-angularity of the MODIS temporal signal to identify spatially homogeneous vegetation cover: A demonstration for agricultural monitoring applications. *Remote Sensing of Environment*, *166*, 61-77.
52. Eerens, H., Haesen, D., Rembold, F., Urbano, F., Tote, C., & Bydekerke, L. (2014). Image time series processing for agriculture monitoring. *Environmental Modelling & Software*, *53*, 154-162.
53. Eilers, P. H. (2003). A perfect smoother. *Analytical chemistry*, *75*(14), 3631-3636.
54. Field, C. B. (Ed.). (2014). *Climate change 2014: impacts, adaptation, and vulnerability* (Vol. 1). IPCC.
55. Fontana, F., Rixen, C., Jonas, T., Aberegg, G., & Wunderle, S. (2008). Alpine grassland phenology as seen in AVHRR, VEGETATION, and MODIS NDVI time series—a comparison with in situ measurements. *Sensors*, *8*(4), 2833-2853.
56. Food and Agriculture Organization of the United Nations (FAO). *Global Strategy to Improve Agricultural and Rural Statistics*; Report No. 56719-GB; FAO: Rome, Italy, 2011
57. Gao, X., Huete, A. R., Ni, W., & Miura, T. (2000). Optical–biophysical relationships of vegetation spectra without background contamination. *Remote Sensing of Environment*, *74*(3), 609-620.
58. Gebauer, R. H. (1987). Socio-economic classification of farm households—conceptual, methodical and empirical considerations. *European Review of Agricultural Economics*, *14*(3), 261-283.
59. Geng, L., Ma, M., Wang, X., Yu, W., Jia, S., & Wang, H. (2014). Comparison of eight techniques for reconstructing multi-satellite sensor time-series NDVI data sets in the Heihe river basin, China. *Remote Sensing*, *6*(3), 2024-2049.
60. Gilabert, M. A., González-Piqueras, J., Garcia-Haro, F. J., & Meliá, J. (2002). A generalized soil-adjusted vegetation index. *Remote Sensing of Environment*, *82*(2), 303-310.
61. Gitelson, A. A., Kaufman, Y. J., & Merzlyak, M. N. (1996). Use of a green channel in remote sensing of global vegetation from EOS-MODIS. *Remote Sensing of Environment*, *58*(3), 289-298.
62. Gitelson, A. A., Kaufman, Y. J., Stark, R., & Rundquist, D. (2002). Novel algorithms for remote estimation of vegetation fraction. *Remote Sensing of Environment*, *80*(1), 76-87.
63. Godfray, H. C. J., Beddington, J. R., Crute, I. R., Haddad, L., Lawrence, D., Muir, J. F., ... & Toulmin, C. (2010). Food security: the challenge of feeding 9 billion people. *Science*, *327*(5967), 812-818.
64. Goel, N. S., & Qin, W. (1994). Influences of canopy architecture on relationships between various vegetation indices and LAI and FPAR: A computer simulation. *Remote Sensing Reviews*, *10*(4), 309-347.
65. Gras, R. (1989). *Le Fait technique en agronomie: activité agricole, concepts et méthodes d'étude*. Editions Quae.
66. Guerif, M., & Duke, C. L. (2000). Adjustment procedures of a crop model to the site specific characteristics of soil and crop using remote sensing data assimilation. *Agriculture, ecosystems & environment*, *81*(1), 57-69.
67. Hall, M., Frank, E., Holmes, G., Pfahringer, B., Reutemann, P., & Witten, I. H. (2009). The WEKA data mining software: an update. *ACM SIGKDD explorations newsletter*, *11*(1), 10-18.
68. Henebry, G. M., Viña, A., & Gitelson, A. A. (2004). The wide dynamic range vegetation index and its potential utility for gap analysis.
69. Hermance, J. F., Jacob, R. W., Bradley, B., & Mustard, J. F. (2007). Extracting phenological signals from multiyear AVHRR NDVI time series: Framework for applying high-order annual splines with roughness damping. *Geoscience and Remote Sensing, IEEE Transactions on*, *45*(10), 3264-3276.
70. Hermans, C. M. L., Geijzendorffer, I. R., Ewert, F., Metzger, M. J., Vereijken, P. H., Woltjer, G. B., & Verhagen, A. (2010). Exploring the future of European crop production in a liberalised market, with specific consideration of climate change and the regional competitiveness. *Ecological Modelling*, *221*(18), 2177-2187.

71. Heumann, B. W., Seaquist, J. W., Eklundh, L., & Jönsson, P. (2007). AVHRR derived phenological change in the Sahel and Soudan, Africa, 1982–2005. *Remote Sensing of Environment*, 108(4), 385-392.
72. Hird, J. N., & McDermid, G. J. (2009). Noise reduction of NDVI time series: An empirical comparison of selected techniques. *Remote Sensing of Environment*, 113(1), 248-258.
73. Hoffer, R. M. (1978). Biological and physical considerations in applying computer-aided analysis techniques to remote sensor data. *Remote sensing: The quantitative approach*, 5.
74. Holben, B. N. (1986). Characteristics of maximum-value composite images from temporal AVHRR data. *International journal of remote sensing*, 7(11), 1417-1434.
75. Huang, Y., & Lu, L. (2009, May). Monitoring winter wheat phenology using time series of remote sensing data. In *Information and Computing Science, 2009. ICIC'09. Second International Conference on* (Vol. 1, pp. 135-138). IEEE.
76. Huete, A. R. (1988). A soil-adjusted vegetation index (SAVI). *Remote sensing of environment*, 25(3), 295-309.
77. Huete, A. R. (1989). Soil influences in remotely sensed vegetation-canopy spectra. *Theory and applications of optical remote sensing*, 107-141.
78. Huete, A. R., & Liu, H. Q. (1994). An error and sensitivity analysis of the atmospheric-and soil-correcting variants of the NDVI for the MODIS-EOS. *Geoscience and Remote Sensing, IEEE Transactions on*, 32(4), 897-905.
79. Huete, Alfredo, Chris Justice, and Wim Van Leeuwen. "MODIS vegetation index (MOD13)." Algorithm theoretical basis document 3 (1999): 213.
80. Huete, A., Didan, K., Miura, T., Rodriguez, E. P., Gao, X., & Ferreira, L. G. (2002). Overview of the radiometric and biophysical performance of the MODIS vegetation indices. *Remote sensing of environment*, 83(1), 195-213.
81. Iraizoz, B., Gorton, M., & Davidova, S. (2007). Segmenting farms for analysing agricultural trajectories: A case study of the Navarra region in Spain. *Agricultural Systems*, 93(1), 143-169.
82. James, M. E., & Kalluri, S. N. (1994). The Pathfinder AVHRR land data set: an improved coarse resolution data set for terrestrial monitoring. *International Journal of Remote Sensing*, 15(17), 3347-3363.
83. Jensen, J. R., & Lulla, K. (1987). Introductory digital image processing: a remote sensing perspective.
84. Jeong, S. J., Ho, C. H., Gim, H. J., & Brown, M. E. (2011). Phenology shifts at start vs. end of growing season in temperate vegetation over the Northern Hemisphere for the period 1982–2008. *Global Change Biology*, 17(7), 2385-2399.
85. Jiang, Z., Huete, A. R., Chen, J., Chen, Y., Li, J., Yan, G., & Zhang, X. (2006). Analysis of NDVI and scaled difference vegetation index retrievals of vegetation fraction. *Remote sensing of environment*, 101(3), 366-378.
86. Jönsson, P., & Eklundh, L. (2002). Seasonality extraction by function fitting to time-series of satellite sensor data. *Geoscience and Remote Sensing, IEEE Transactions on*, 40(8), 1824-1832.
87. Jönsson, P., & Eklundh, L. (2004). TIMESAT—a program for analyzing time-series of satellite sensor data. *Computers & Geosciences*, 30(8), 833-845.
88. Jordan, C. F. (1969). Derivation of leaf-area index from quality of light on the forest floor. *Ecology*, 663-666.
89. Jurgens, C. (1997). The modified normalized difference vegetation index (mNDVI) a new index to determine frost damages in agriculture based on Landsat TM data. *International Journal of Remote Sensing*, 18(17), 3583-3594.

90. Justice, C. O., Townshend, J. R. G., Holben, B. N., & Tucker, E. C. (1985). Analysis of the phenology of global vegetation using meteorological satellite data. *International Journal of Remote Sensing*, 6(8), 1271-1318.
91. Justice, C. O., Townshend, J. R. G., & Choudhury, B. J. (1989). Comparison of AVHRR and SMMR data for monitoring vegetation phenology on a continental scale. *International Journal of Remote Sensing*, 10(10), 1607-1632.
92. Justice, C. O., Townshend, J. R. G., Vermote, E. F., Masuoka, E., Wolfe, R. E., Saleous, N., ... & Morisette, J. T. (2002). An overview of MODIS Land data processing and product status. *Remote sensing of Environment*, 83(1), 3-15.
93. Kandasamy, S., Baret, F., Verger, A., Neveux, P., & Weiss, M. (2013). A comparison of methods for smoothing and gap filling time series of remote sensing observations—application to MODIS LAI products. *Biogeosciences*, 10(6), 4055-4071.
94. Kaufman, Y. J., & Tanre, D. (1992). Atmospherically resistant vegetation index (ARVI) for EOS-MODIS. *Geoscience and Remote Sensing, IEEE Transactions on*, 30(2), 261-270.
95. Kaufmann, R. K., Zhou, L., Knyazikhin, Y., Shabanov, N. V., Myneni, R. B., & Tucker, C. J. (2000). Effect of orbital drift and sensor changes on the time series of AVHRR vegetation index data. *Geoscience and Remote Sensing, IEEE Transactions on*, 38(6), 2584-2597.
96. Köbrich, C., Rehman, T., & Khan, M. (2003). Typification of farming systems for constructing representative farm models: two illustrations of the application of multi-variate analyses in Chile and Pakistan. *Agricultural systems*, 76(1), 141-157.
97. Kumar, M., & Monteith, J. L. (1981). Remote sensing of crop growth. *Plants and the daylight spectrum*, 133-144.
98. Le Page, M., Toumi, J., Khabba, S., Hagolle, O., Tavernier, A., Kharrou, M. H., ... & Jarlan, L. (2014). A Life-Size and Near Real-Time Test of Irrigation Scheduling with a Sentinel-2 Like Time Series (SPOT4-Take5) in Morocco. *Remote Sensing*, 6(11), 11182-11203.
99. Li, L., Friedl, M. A., Xin, Q., Gray, J., Pan, Y., & Frolking, S. (2014). Mapping Crop cycles in China using MODIS-EVI time series. *Remote Sensing*, 6(3), 2473-2493.
100. Lieth, H. (1974). Purposes of a phenology book. In *Phenology and seasonality modeling* (pp. 3-19). Springer Berlin Heidelberg.
101. Lopez Ridaura, S. (2011). Coping with heterogeneity. Typologies for agricultural research and development, 3rd World Congress of Conservation Agriculture & Farming System Design, Brisbane, Australia. 26-29 sept. 2011.
102. Lu, L., Wang, C., Guo, H., & Li, Q. (2014). Detecting winter wheat phenology with SPOT-VEGETATION data in the North China Plain. *Geocarto International*, 29(3), 244-255.
103. Lunetta, R. S., Knight, J. F., Ediriwickrema, J., Lyon, J. G., & Worthy, L. D. (2006). Land-cover change detection using multi-temporal MODIS NDVI data. *Remote sensing of environment*, 105(2), 142-154.
104. Major, D. J., Baret, F., & Guyot, G. (1990). A ratio vegetation index adjusted for soil brightness. *International Journal of Remote Sensing*, 11(5), 727-740.
105. Manfron, G., Crema, A., Boschetti, M., & Confalonieri, R. (2012, October). Testing automatic procedures to map rice area and detect phenological crop information exploiting time series analysis of remote sensed MODIS data. In *SPIE Remote Sensing* (pp. 85311E-85311E). International Society for Optics and Photonics.
106. Manfron G., (2012). Automatic procedures definition and validation to extract mapping and phenological rice fields' information through time series analysis of remote sensed data. Laurea magistrale in Scienze della Produzione e Protezione delle Piante. LM-69 – Scienze e Tecnologie Agrarie. Università degli Studi di Milano Facoltà di Agraria. Data di discussione: 27 Marzo 2012.

107. Manjunath, K. R., Kundu, N., & Panigrahy, S. (2006, December). Analysis of cropping pattern and crop rotation using multirate, multisensor, and multiscale remote sensing data: case study for the state of West Bengal, India. In *Asia-Pacific Remote Sensing Symposium* (pp. 641100-641100). International Society for Optics and Photonics.
108. Maselli F., Menenti M., P.A. Brivio (Eds.), 2010. *Remote Sensing Optical Observations of Vegetation Properties*. Series in "Recent Research Developments in Remote Sensing", Research Signpost, Trivandrum (India), pp. 274. ISBN: 978-81-308-0421-7.
109. Maton, L., Leenhardt, D., Goulard, M., & Bergez, J. E. (2005). Assessing the irrigation strategies over a wide geographical area from structural data about farming systems. *Agricultural systems*, 86(3), 293-311.
110. Meng, J., Wu, B., Li, Q., Du, X., & Jia, K. (2009). Monitoring crop phenology with MERIS data—a case study of winter wheat in North China plain. *Proceedings of PIERS 2009 in Beijing*, 1225-1228.
111. Moody, A., & Johnson, D. M. (2001). Land-surface phenologies from AVHRR using the discrete Fourier transform. *Remote Sensing of Environment*, 75(3), 305-323.
112. Monteith, J. L. (1972). Solar radiation and productivity in tropical ecosystems. *Journal of applied ecology*, 747-766.
113. Moulin, S., Bondeau, A., & Delecalle, R. (1998). Combining agricultural crop models and satellite observations: from field to regional scales. *International Journal of Remote Sensing*, 19(6), 1021-1036.
114. Mouret, J. C., Hammond, R., Dreyfus, F., Desclaux, D., Marnotte, P., & Mesleard, F. (2004). An integrated study of the development of organic rice cultivation in the Camargue (France)-.
115. Nelson, A., Boschetti, M., Manfron, G., Holecz, F., Collivignarelli, F., Gatti, L., ... & Setiyono, T. (2014). Combining Moderate-Resolution Time-Series RS Data from SAR and Optical Sources for Rice Crop Characterisation: Examples from Bangladesh.
116. Nutini, F., Boschetti, M., Brivio, P. A., Bocchi, S., & Antoninetti, M. (2013). Land-use and land-cover change detection in a semi-arid area of Niger using multi-temporal analysis of Landsat images. *International journal of remote sensing*, 34(13), 4769-4790.
117. Olaizola, A. M., Chertouh, T., & Manrique, E. (2008). Adoption of a new feeding technology in Mediterranean sheep farming systems: Implications and economic evaluation. *Small Ruminant Research*, 79(2), 137-145.
118. Olsson, L., & Eklundh, L. (1994). Fourier series for analysis of temporal sequences of satellite sensor imagery. *International Journal of Remote Sensing*, 15(18), 3735-3741.
119. Osman, J., Inglada, J., & Dejoux, J. F. (2015). Assessment of a Markov logic model of crop rotations for early crop mapping. *Computers and Electronics in Agriculture*, 113, 234-243.
120. Pan, Y., Li, L., Zhang, J., Liang, S., Zhu, X., & Sulla-Menashe, D. (2012). Winter wheat area estimation from MODIS-EVI time series data using the Crop Proportion Phenology Index. *Remote Sensing of Environment*, 119, 232-242.
121. Parc naturel régional de Camargue 2003b. Land use in 2001. http://www.parccamargue.fr/English/popup.php?callback=loadcpage&page_id=483&zoom=5.
122. Parc naturel régional de Camargue 2005. Occupation des sols. Cartographie du territoire du Parc naturel régional de Camargue en 2001 et évolution depuis 1991. Report, 64 p., http://www.parc-camargue.fr/Francais/download.php?categorie_id=58.
123. Parc naturel régional de Camargue 2008. Occupation des sols en Camargue 2006 : document de synthèse. Report, 8 p., http://www.parc-camargue.fr/Francais/download.php?categorie_id=58.
124. Parc Naturel Régional de Camargue, 2013. Evolution de l'occupation du sol en Camargue en 20 ans (1991-2011). Graphistes Associés, Arles, France.

125. Parry, M. L., Rosenzweig, C., Iglesias, A., Livermore, M., & Fischer, G. (2004). Effects of climate change on global food production under SRES emissions and socio-economic scenarios. *Global Environmental Change*, 14(1), 53-67.
126. Pax-Lenney, M., & Woodcock, C. E. (1997). The effect of spatial resolution on the ability to monitor the status of agricultural lands. *Remote Sensing of Environment*, 61(2), 210-220.
127. Pearson, R. L., & Miller, L. D. (1972, October). Remote mapping of standing crop biomass for estimation of the productivity of the shortgrass prairie. In *Remote Sensing of Environment*, VIII (Vol. 1, p. 1355).
128. Pettorelli, N., Vik, J. O., Mysterud, A., Gaillard, J. M., Tucker, C. J., & Stenseth, N. C. (2005). Using the satellite-derived NDVI to assess ecological responses to environmental change. *Trends in ecology & evolution*, 20(9), 503-510.
129. Philippon, N., Jarlan, L., Martiny, N., Camberlin, P., & Mougin, E. (2007). Characterization of the interannual and intraseasonal variability of West African vegetation between 1982 and 2002 by means of NOAA AVHRR NDVI data. *Journal of Climate*, 20(7), 1202-1218.
130. Piao, S., Fang, J., Zhou, L., Ciais, P., & Zhu, B. (2006). Variations in satellite-derived phenology in China's temperate vegetation. *Global Change Biology*, 12(4), 672-685.
131. Pinty, B., & Verstraete, M. M. (1992). GEMI: a non-linear index to monitor global vegetation from satellites. *Vegetatio*, 101(1), 15-20.
132. Poussin, J. C., Imache, A., Beji, R., Le Grusse, P., & Benmihoub, A. (2008). Exploring regional irrigation water demand using typologies of farms and production units: An example from Tunisia. *Agricultural Water Management*, 95(8), 973-983.
133. Pretty, J. (2008). Agricultural sustainability: concepts, principles and evidence. *Philosophical Transactions of the Royal Society of London B: Biological Sciences*, 363(1491), 447-465.
134. Qi, J., Chehbouni, A., Huete, A. R., Kerr, Y. H., & Sorooshian, S. (1994). A modified soil adjusted vegetation index. *Remote sensing of environment*, 48(2), 119-126.
135. Ramsey, R. D., Falconer, A., & Jensen, J. R. (1995). The relationship between NOAA-AVHRR NDVI and ecoregions in Utah. *Remote Sensing of Environment*, 53(3), 188-198.
136. Reed, B. C., Brown, J. F., VanderZee, D., Loveland, T. R., Merchant, J. W., & Ohlen, D. O. (1994). Measuring phenological variability from satellite imagery. *Journal of vegetation science*, 5(5), 703-714.
137. Reidsma, P., Wolf, J., Kanellopoulos, A., Schaap, B. F., Mandryk, M., Verhagen, J., & van Ittersum, M. K. (2015). Climate change impact and adaptation research requires integrated assessment and farming systems analysis: a case study in the Netherlands. *Environmental Research Letters*, 10(4), 045004.
138. Richardson, A. J., & Weigand, C. L. (1977). Distinguishing vegetation from soil background information. *Photogrammetric Engineering and Remote Sensing*, 43(12).
139. Righi, E., Dogliotti, S., Stefanini, F. M., & Pacini, G. C. (2011). Capturing farm diversity at regional level to up-scale farm level impact assessment of sustainable development options. *Agriculture, ecosystems & environment*, 142(1), 63-74.
140. Rondeaux, G., Steven, M., & Baret, F. (1996). Optimization of soil-adjusted vegetation indices. *Remote sensing of environment*, 55(2), 95-107.
141. Rosenberg, A., & Turvey, C. G. (1991). Identifying management profiles of Ontario swine producers through cluster analysis. *Review of Agricultural Economics*, 201-213.
142. Roughgarden, J., Running, S. W., & Matson, P. A. (1991). What does remote sensing do for ecology?. *Ecology*, 1918-1922.

143. Roujean, J. L., & Breon, F. M. (1995). Estimating PAR absorbed by vegetation from bidirectional reflectance measurements. *Remote Sensing of Environment*, 51(3), 375-384.
144. Rounsevell, M. D. A., Annetts, J. E., Audsley, E., Mayr, T., & Reginster, I. (2003). Modelling the spatial distribution of agricultural land use at the regional scale. *Agriculture, Ecosystems & Environment*, 95(2), 465-479.
145. Rouse Jr, J., Haas, R. H., Schell, J. A., & Deering, D. W. (1974). Monitoring vegetation systems in the Great Plains with ERTS. *NASA special publication*, 351, 309.
146. Saini, A. D., Dhadwal, V. K., & Nanda, R. (1988). Pattern of changes in yield of Kalyansona and Sonalika varieties of wheat in sowing date experiments at different locations. In *Field crop Abstracts* (Vol. 42, p. 6777).
147. Sakamoto, T., Yokozawa, M., Toritani, H., Shibayama, M., Ishitsuka, N., & Ohno, H. (2005). A crop phenology detection method using time-series MODIS data. *Remote sensing of environment*, 96(3), 366-374.
148. Savitzky, A., & Golay, M. J. (1964). Smoothing and differentiation of data by simplified least squares procedures. *Analytical chemistry*, 36(8), 1627-1639.
149. Schnelle, F. (1955). *Pflanzen-Phänologie*, Akademische Verlagsgesellschaft.
150. Shabanov, N. V., Zhou, L., Knyazikhin, Y., Myneni, R. B., & Tucker, C. J. (2002). Analysis of interannual changes in northern vegetation activity observed in AVHRR data from 1981 to 1994. *Geoscience and Remote Sensing, IEEE Transactions on*, 40(1), 115-130.
151. Shalaby, A., & Tateishi, R. (2007). Remote sensing and GIS for mapping and monitoring land cover and land-use changes in the Northwestern coastal zone of Egypt. *Applied Geography*, 27(1), 28-41.
152. Shen, Y., Wu, L., Di, L., Yu, G., Tang, H., Yu, G., & Shao, Y. (2013). Hidden Markov models for real-time estimation of corn progress stages using MODIS and meteorological data. *Remote Sensing*, 5(4), 1734-1753.
153. Shihua, L., Jingtao, X., Ping, N., Jing, Z., Hongshu, W., & Jingxian, W. (2014). Monitoring paddy rice phenology using time series MODIS data over Jiangxi Province, China. *International Journal of Agricultural and Biological Engineering*, 7(6), 28-36.
154. Smith, P. M., Kalluri, S. N., Prince, S. D., & DeFries, R. (1997). The NOAA/NASA Pathfinder AVHRR 8-km land data set. *Photogrammetric Engineering and remote sensing*, 63(1), 27-32.
155. Solano, R., Didan, K., Jacobson, A., & Huete, A. (2010). MODIS vegetation index user's guide (MOD13 series). *Vegetation index and phenology lab*.
156. Sun, H., Xu, A., Lin, H., Zhang, L., & Mei, Y. (2012). Winter wheat mapping using temporal signatures of MODIS vegetation index data. *International journal of remote sensing*, 33(16), 5026-5042.
157. Swets, D. L., Reed, B. C., Rowland, J. D., & Marko, S. E. (1999, May). A weighted least-squares approach to temporal NDVI smoothing. In *Proceedings of the 1999 ASPRS Annual Conference: From Image to Information, Portland, Oregon* (pp. 17-21).
158. Taffetani, F., Rismondo, M., & Lancioni, A. (2011). Environmental Evaluation and Monitoring of Agro-Ecosystems Biodiversity. *Ecosystems Biodiversity*, 333-370.
159. Tanré, D., Holben, B. N., & Kaufman, Y. J. (1992). Atmospheric correction against algorithm for NOAA-AVHRR products: theory and application. *Geoscience and Remote Sensing, IEEE Transactions on*, 30(2), 231-248.
160. Tateishi, R., & Ebata, M. (2004). Analysis of phenological change patterns using 1982–2000 Advanced Very High Resolution Radiometer (AVHRR) data. *International Journal of Remote Sensing*, 25(12), 2287-2300.
161. Tilman, D., Cassman, K. G., Matson, P. A., Naylor, R., & Polasky, S. (2002). Agricultural sustainability and intensive production practices. *Nature*, 418(6898), 671-677.

162. Tilman, D., Balzer, C., Hill, J., & Befort, B. L. (2011). Global food demand and the sustainable intensification of agriculture. *Proceedings of the National Academy of Sciences*, *108*(50), 20260-20264.
163. Tornos, L., Huesca, M., Dominguez, J. A., Moyano, M. C., Cicuendez, V., Recuero, L., & Palacios-Orueta, A. (2015). Assessment of MODIS spectral indices for determining rice paddy agricultural practices and hydroperiod. *ISPRS Journal of Photogrammetry and Remote Sensing*, *101*, 110-124.
164. Tucker, C. J. (1979). Red and photographic infrared linear combinations for monitoring vegetation. *Remote sensing of Environment*, *8*(2), 127-150.
165. Tucker, C. J., Pinzon, J. E., Brown, M. E., Slayback, D. A., Pak, E. W., Mahoney, R., ... & El Saleous, N. (2005). An extended AVHRR 8-km NDVI dataset compatible with MODIS and SPOT vegetation NDVI data. *International Journal of Remote Sensing*, *26*(20), 4485-4498.
166. Ünsalan, C., & Boyer, K. L. (2004). Linearized vegetation indices based on a formal statistical framework. *Geoscience and Remote Sensing, IEEE Transactions on*, *42*(7), 1575-1585.
167. Van Deventer, A. P., Ward, A. D., Gowda, P. H., & Lyon, J. G. (1997). Using Thematic Mapper data to identify contrasting soil plains and tillage practices. *Photogrammetric Engineering and Remote Sensing*, *63*, 87-93.
168. Van Dijk, A., Callis, S. L., Sakamoto, C. M., & Decker, W. L. (1987). Smoothing vegetation index profiles: An alternative method for reducing radiometric disturbance in NOAA/AVHRR data. *Photogrammetric Engineering and Remote Sensing*, *53*(8), 1059-1067.
169. Van Leeuwen, W. J., Huete, A. R., & Laing, T. W. (1999). MODIS vegetation index compositing approach: A prototype with AVHRR data. *Remote Sensing of Environment*, *69*(3), 264-280.
170. Vermote, E., & Kaufman, Y. J. (1995). Absolute calibration of AVHRR visible and near-infrared channels using ocean and cloud views. *International Journal of Remote Sensing*, *16*(13), 2317-2340.
171. Vermote, E. F., & Vermeulen, A. (1999). Atmospheric correction algorithm: spectral reflectances (MOD09). *ATBD version*, *4*.
172. Verstraete, M. M., & Pinty, B. (1996). Designing optimal spectral indexes for remote sensing applications. *Geoscience and Remote Sensing, IEEE Transactions on*, *34*(5), 1254-1265.
173. Viovy, N., Arino, O., & Belward, A. S. (1992). The Best Index Slope Extraction (BISE): A method for reducing noise in NDVI time-series. *International Journal of Remote Sensing*, *13*(8), 1585-1590.
174. Waldhoff, G., Curdt, C., Hoffmeister, D., & Bareth, G. (2012). Analysis of multitemporal and multisensor remote sensing data for crop rotation mapping. *ISPRS International Archives of the Photogrammetry, Remote Sensing and Spatial Information Sciences*, *1-7*, 177-182.
175. Wardlow, B. D., Egbert, S. L., & Kastens, J. H. (2007). Analysis of time-series MODIS 250 m vegetation index data for crop classification in the US Central Great Plains. *Remote Sensing of Environment*, *108*(3), 290-310.
176. Weng, Q. (2002). Land use change analysis in the Zhujiang Delta of China using satellite remote sensing, GIS and stochastic modelling. *Journal of environmental management*, *64*(3), 273-284.
177. Whittaker, E. T. (1922). On a new method of graduation. *Proceedings of the Edinburgh Mathematical Society*, *41*, 63-75.
178. Wijnands, F. W. T. (1999). Crop rotation in organic farming: theory and practice. *Designing and Testing Crop Rotations for Organic Farming (eds. Olesen JE et al.)*, 21-35.
179. Wulder, M., & Franklin, S. E. (Eds.). (2012). *Remote sensing of forest environments: concepts and case studies*. Springer Science & Business Media.
180. Xiao, X., Boles, S., Frolking, S., Salas, W., Moore Iii, B., Li, C., ... & Zhao, R. (2002). Observation of flooding and rice transplanting of paddy rice fields at the site to landscape scales in China using VEGETATION sensor data. *International Journal of Remote Sensing*, *23*(15), 3009-3022.

181. Xiao, X., Boles, S., Liu, J., Zhuang, D., Frohling, S., Li, C., ... & Moore, B. (2005). Mapping paddy rice agriculture in southern China using multi-temporal MODIS images. *Remote Sensing of Environment*, 95(4), 480-492.
182. Xin, J., Yu, Z., van Leeuwen, L., & Driessen, P. M. (2002). Mapping crop key phenological stages in the North China Plain using NOAA time series images. *International Journal of Applied Earth Observation and Geoinformation*, 4(2), 109-117.
183. You, X., Meng, J., Zhang, M., & Dong, T. (2013). Remote sensing based detection of crop phenology for agricultural zones in China using a new threshold method. *Remote Sensing*, 5(7), 3190-3211.
184. Yu, F., Price, K. P., Ellis, J., & Shi, P. (2003). Response of seasonal vegetation development to climatic variations in eastern central Asia. *Remote Sensing of Environment*, 87(1), 42-54.
185. Yu, G., Di, L., Yang, Z., Shen, Y., Chen, Z., & Zhang, B. (2012, August). Corn growth stage estimation using time series vegetation index. In *Agro-Geoinformatics (Agro-Geoinformatics), 2012 First International Conference on* (pp. 1-6). IEEE.
186. Zhang, X., Friedl, M. A., Schaaf, C. B., Strahler, A. H., Hodges, J. C., Gao, F., ... & Huete, A. (2003). Monitoring vegetation phenology using MODIS. *Remote sensing of environment*, 84(3), 471-475.
187. Zhang, X., Friedl, M. A., Schaaf, C. B., & Strahler, A. H. (2004). Climate controls on vegetation phenological patterns in northern mid-and high latitudes inferred from MODIS data. *Global Change Biology*, 10(7), 1133-1145.
188. Zhao, Y. S. (2003). Remote Sensing Application Analysis Theory and Method.
189. Zhao, Y., Gong, P., Yu, L., Hu, L., Li, X., Li, C., ... & Cheng, Q. (2014). Towards a common validation sample set for global land-cover mapping. *International Journal of Remote Sensing*, 35(13), 4795-4814.
190. Zhou, L., Kaufmann, R. K., Tian, Y., Myneni, R. B., & Tucker, C. J. (2003). Relation between interannual variations in satellite measures of northern forest greenness and climate between 1982 and 1999. *Journal of Geophysical Research: Atmospheres (1984–2012)*, 108(D1), ACL-3.
191. Zhu, W., Pan, Y., He, H., Wang, L., Mou, M., & Liu, J. (2012). A changing-weight filter method for reconstructing a high-quality NDVI time series to preserve the integrity of vegetation phenology. *Geoscience and Remote Sensing, IEEE Transactions on*, 50(4), 1085-1094.

Personal bibliography

Book chapter

Andrew Nelson, Mirco Boschetti, Giacinto Manfron, Franceco Holecz, Francesco Collivignarelli, Luca Gatti, Massimo Barbieri, Lorena Villano, Parvesh Chandna and Tri Setiyono (2014). Combining Moderate-Resolution Time-Series RS Data from SAR and Optical Sources for Rice Crop Characterisation: Examples from Bangladesh, Land Applications of Radar Remote Sensing, Dr. Damien Closson (Ed.), ISBN: 978-953-51-1589-2, InTech, DOI: 10.5772/57443. Available from: <http://www.intechopen.com/books/land-applications-of-radar-remote-sensing/combining-moderate-resolution-time-series-rs-data-from-sar-and-optical-sources-for-rice-crop-charact>.

Peer review paper

Boschetti, M., Nutini, F., Manfron, G., Brivio, P. A., & Nelson, A. (2014). Comparative analysis of normalised difference spectral indices derived from MODIS for detecting surface water in flooded rice cropping systems. *PLoS one*, 9(2).

Boschetti, M., Nelson, A., Nutini, F., Manfron, G., Busetto, L., Barbieri, M., ... & Bacong, A. P. (2015). Rapid Assessment of Crop Status: An Application of MODIS and SAR Data to Rice Areas in Leyte, Philippines Affected by Typhoon Haiyan. *Remote Sensing*, 7(6), 6535-6557.

Paleari, L., Cappelli, G., Bregaglio, S., Acutis, M., Donatelli, M., Sacchi, G. A., ... & Confalonieri, R. (2015). District specific, in silico evaluation of rice ideotypes improved for resistance/tolerance traits to biotic and abiotic stressors under climate change scenarios. *Climatic Change*, 132(4), 661-675.

International conferences

Boschetti, M., Holecz, F., Manfron, G., Collivignarelli, F., & Nelson, A. (2013, April). Remote sensing-based Information for crop monitoring: contribution of SAR and Moderate resolution optical data on Asian rice production. In EGU General Assembly Conference Abstracts (Vol. 15, p. 13507).

Boschetti, M.; Busetto, L.; Nutini, F.; Manfron, G.; Crema, A.; Confalonieri, R.; Bregaglio, S.; Pagani, V.; Guarneri, T.; Brivio, P.A., "Assimilating seasonality information derived from satellite data time series in crop modelling for rice yield estimation," in Geoscience and Remote Sensing Symposium (IGARSS), 2015 IEEE International , vol., no., pp.157-160, 26-31 July 2015. doi: 10.1109/IGARSS.2015.7325723

Candiani G., Bordogna G., Manfron G., Boschetti M., Pepe M. (2014). Simulation of Sentinel-2 time series of vegetation indexes for agricultural monitoring from the fusion of remote sensing dataset with heterogeneous spatio-temporal resolution. SENTINEL-2 for Science workshop. Frascati 20-22 May. Poster Presentation

Candiani G., Manfron G., Pepe M., Courault D., Boschetti M. (2014) From multi-temporal mapping to time series analysis with high spatial resolution data: evaluation of SPOT4 Take5 data to simulate Sentinel-2 contribution – Earsel 2014 Berlin poster presentation

Holecz F., Barbieri M., Collivignarelli F., Nelson A., Setiyono T.D., Boschetti M., Manfron G., Brivio P.A. (2013). An operational remote sensing based service for rice production estimation at national scale. ESA living planet symposium, Edinburgh 9-13 September 2013. ISBN 978-92-9221-286-5 ISSN 1609-042X. Accepted as oral presentation.

Jean-Marc Barbier, Stefano Bocchi, Sylvestre Delmotte, Andrea Porro, Francesca Orlando, Mirco Boschetti, Pietro Alessandro Brivio, Giacinto Manfron, Simone Bregaglio, Giovanni Capelli, Roberto Confalonieri, Françoise Ruget, Vincent Courderc, Laure Hossard, Jean-Claude Mouret, Santiago Lopez- Ridaura. (2015). Combining systems analysis tools for the integrated assessment of scenarios in rice production systems at different scales. 5th International Symposium for Farming Systems Design 7-10 September 2015, Montpellier, France

Manfron G., Boschetti M., Confalonieri R., Pagani V., Nutini F., Filipponi F., Crema A. and Brivio P.A., (2013), Application of an automatic rice mapping system to extract crop phenological information from time series of MODIS satellite images: first results on Senegal case study. 33rd EARSeL Symposium June 3-8, 2013 Matera, Italy. Accepted as oral presentation, session 3, Remote Sensing for Developing Countries, 03 Jun 2013.

National conferences

Candiani G., Manfron G., Boschetti M., Busetto L., Nutini F., Crema A., Pepe M., e Bordogna G. (2014). Fusione di immagini telerilevate provenienti da dataset eterogenei: ricostruzione di serie temporali ad alta risoluzione spazio-temporale. 18° Conf. Naz. ASITA, Firenze 14-16 Ottobre 2014.

Manfron G., Boschetti M., Holectz F., Collivignarelli F., Barbieri M. and Nelson A. (2013). Utilizzo congiunto di dati SAR e ottici per il monitoraggio di agro-ecosistemi risicoli in ambiente tropicale: primi risultati in Bangladesh. 17° Conf. Naz. ASITA, Desenzano sul Garda 5-7 Novembre 2013. Presentazione orale.

Manfron G., Delmotte S., Boschetti M., Brivio P.A. (2015). Analisi di serie temporali di dati satellitari per la caratterizzazione della variabilità di pratiche agricole del frumento duro nel Parco Regionale della Camargue, Francia. 19° Conf. Naz. ASITA, Lecco 29 Settembre-1 Ottobre 2015.

Technical Report

E-AGRI, D33.3. Simone Bregaglio, Valentina Pagani, Giacinto Manfron, Mirco Boschetti and Roberto Confalonieri. *Evaluation Report On Integration Of RS Data*. 10/01/2014